

The copyright of this thesis vests in the author. No quotation from it or information derived from it is to be published without full acknowledgement of the source. The thesis is to be used for private study or non-commercial research purposes only.

Published by the University of Cape Town (UCT) in terms of the non-exclusive license granted to UCT by the author.

**Molecular characterisation of *XvVTC2*, a gene coding
for a GDP-L-Galactose phosphorylase from *Xerophyta*
*viscosa***

Andries Petrus Bresler



**A thesis submitted in fulfilment of the requirements for the degree of Master
of Science in the Department of Molecular and Cell Biology, Faculty of
Science, University of Cape Town, South Africa**

April 2010

*If you can keep your head when all about you
Are losing theirs and blaming it on you,
If you can trust yourself when all men doubt you
But make allowance for their doubting too,
If you can wait and not be tired by waiting,
Or being lied about, don't deal in lies,
Or being hated, don't give way to hating,
And yet don't look too good, nor talk too wise:*

*If you can dream – and not make dreams your master,
If you can think – and not make thoughts your aim;
If you can meet with Triumph and Disaster
And treat those two impostors just the same;
If you can bear to hear the truth you've spoken
Twisted by knaves to make a trap for fools,
Or watch the things you gave your life to, broken,
And stoop and build 'em up with worn-out tools:*

*If you can make one heap of all your winnings
And risk it all on one turn of pitch-and-toss,
And lose, and start again at your beginnings
And never breath a word about your loss;
If you can force your heart and nerve and sinew
To serve your turn long after they are gone,
And so hold on when there is nothing in you
Except the Will which says to them: "Hold on!"*

*If you can talk with crowds and keep your virtue,
Or walk with kings – nor lose the common touch,
If neither foes nor loving friends can hurt you;
If all men count with you, but none too much,
If you can fill the unforgiving minute
With sixty seconds' worth of distance run,
Yours is the Earth and everything that's in it,
And – which is more – you'll be a Man, my son!*

Rudyard Kipling

Acknowledgments

I would like to thank Pannar seed (Pty) Ltd and the National Research Foundation for providing funding for my studies.

Thank you very much to my supervisor Dr. Suhail Rafudeen. I really appreciate all the help during this project, without you this project would not have been possible. Thank you for all the guidance, support and motivation over the last two years. Thanks to my co-supervisor Prof. Jill Farrant, your insight has been really valuable. Many thanks to Prof. Jennifer Thomson; you have been an inspiration in your enthusiasm on the improvement of crops and thereby the lives of many.

I would like to thank Marion Bezuidenhout for her help in looking after the plants as well as her assistance in the particle bombardment. I would also like to thank Faezah Davids for her organising the raising of the polyclonal antibodies as well as assistance in the western blotting. Many thanks to Prof. Wolf Brandt for helping me with the HPLC.

Thanks a lot to my colleagues from the Plant Stress Research Group at UCT. Thanks; Alexis, Shakiera, Monique, Mubeen, Ali, Kershini, Tamaryn, Revel, Tshego, Tafara, Ryman, Betty and Richard. I really enjoyed your company and the conversations may we remain friends for many years to come.

Last but not least; thank you very much to my family. Dad, mom and little bro thanks for supporting and sharing my dream from the start. Even though you might not have always understood what I was doing, I really appreciate all the guidance and motivation.

Declaration

This work has not been not been presented at any other university for examination or for any other purposes. Furthermore, I know the meaning of plagiarism and declare that all of the work in the document, save for that which is properly acknowledged, is my own.

Andries Petrus Bresler

April 2010

University of Cape Town

Table of Contents

Acknowledgments	iii
Declaration.....	iv
Table of Contents	v
List of Figures.....	viii
List of Appendices.....	x
Abbreviations	xi
Abstract.....	xiii
Chapter 1: Introduction and Literature review	1
1.1 General Introduction	2
1.1.1 Role of Ascorbate in plants.....	4
1.1.2 <i>De-Novo</i> synthesis of Ascorbate	8
1.2 Resurrection Plants	16
1.3 Aim	20
2 Chapter 2: Cloning and Bioinformatics analysis.....	22
2.1 Introduction.....	23
2.2 Materials and Methods.....	23
2.2.1 cDNA and gDNA cloning.....	23
2.2.2 Promoter analysis.....	25
2.2.3 Bioinformatics.....	26
2.3 Results and Discussion	26
2.3.1 cDNA and gDNA cloning.....	26
2.3.2 Promoter analysis.....	30
2.3.3 Bioinformatics analysis.....	31

2.4	Conclusions.....	36
3	Chapter 3: Protein expression	37
3.1	Introduction.....	38
3.2	Materials and methods	39
3.2.1	Primer design and cloning	39
3.2.2	Recombinant protein expression.....	40
3.3	Results and Discussion	42
3.3.1	Primer design and cloning	42
3.3.2	Recombinant protein expression.....	43
3.4	Conclusions.....	46
4	Chapter 4: Protein function and Localisation.....	47
4.1	Introduction.....	48
4.2	Materials and methods	49
4.2.1	In-vitro assay of GDP-D-Glucose phosphorylase activity.....	49
4.2.2	YFP localisation.....	49
4.2.3	Western blot analysis	50
4.3	Results and Discussion	52
4.3.1	<i>In-vitro</i> assay.....	52
4.3.2	YFP localisation.....	56
4.3.3	Western blot analysis	59
4.4	Conclusions.....	62
5	Chapter 5: Water deficit Stress treatment and Quantitative Real-Time PCR analysis.....	64
5.1	Introduction.....	65
5.2	Materials and methods	65
5.2.1	Plant stress treatment	65
5.2.2	Quantitative Real-Time PCR analysis	66
5.3	Results and Discussion	68

5.3.1	Plant stress treatment	68
5.3.2	Quantitative Real-Time PCR analysis	71
5.4	Conclusions.....	76
6	Chapter 6: Overview and Conclusions	77
	Appendix 1 – Oligos.....	81
	Appendix 2 – PCR Conditions.....	82
	Appendix 3 – Transformation protocol	84
	Appendix 4 – Splinkerette flow diagram.....	85
	Appendix 5 cDNA sequence	86
	Appendix 6 – SDS Poly-acrylamide gel recipes	89
	Appendix 6 – SDS Poly-acrylamide gel recipes	89
	Appendix 7 – eFP expression profiles of <i>VTC2</i> in <i>A. thaliana</i>	90
	Appendix 8 – Real-time PCR runs	97
	Appendix 9 – Phosphorylation site prediction graphs	98
	References:.....	100

List of Figures

Figure 1.1: The Smirnov-Wheeler pathway of Ascorbate biosynthesis adapted from (Linster et al., 2007).....	11
Figure 1.2: The L-Gulose pathway of ASC biosynthesis as proposed by Wolucka and van Montagu, 2003.	12
Figure 1.3: The extended VTC2 cycle as proposed by (Wolucka and Montagu, 2007), which links ascorbate biosynthesis to photosynthesis and cell wall biosynthesis. Adapted from (Linster and Clarke, 2008).	14
Figure 2.1: Ethidium bromide stained 1% w/v agarose gel showing <i>XvVTC2</i> amplified PCR products from <i>X. viscosa</i> cDNA.	27
Figure 2.2: Ethidium bromide stained 1% w/v agarose gel showing amplified colony PCR products.	28
Figure 2.3: Ethidium bromide stained 1% w/v agarose gels showing <i>XvVTC2</i> amplified PCR products from genomic DNA	29
Figure 2.4: Recombinant plasmid maps of the cloning vectors pTZ57R/T and pJET1.2/blunt (Fermentas) containing the <i>XvVTC2</i> cDNA and gDNA fragments (blue) respectively.	30
Figure 2.5: The structure of the <i>XvVTC2</i> gene showing the sequenced gene, including the untranslated regions, exons and introns.	31
Figure 2.6: A phylogenetic tree showing the evolutionary relationship between homologs of VTC2 related proteins from various organisms..	31
Figure 2.7: Prediction of phosphorylation sites of the <i>XvVTC2</i> protein by the Netphos 2.0 server (Blom et al., 1999).	32
Figure 2.8: An alignment of amino acid sequences of five VTC2 homologs from various plants.	34
Figure 3.1: Ethidium bromide stained 1% w/v agarose gel showing <i>XvVTC2</i> amplified PCR products from cDNA.....	42
Figure 3.2: Recombinant plasmid map of the expression vector pET32b (Novagen) containing the <i>XvVTC2</i> gene.....	43
Figure 3.3: Coomassie Blue stained 12% SDS-PAGE analysis of <i>XvVTC2</i> recombinant protein expression.	43

Figure 3.4: His-tag specific Western Blot to detect expressed recombinant XvVTC2 protein.	45
Figure 4.1: Reverse phase HPLC chromatograms showing phosphorylase activity of recombinant XvVTC2 protein.	54
Figure 4.2: Ethidium bromide stained 1% w/v agarose gel showing in A) XvVTC2 amplified PCR products from a cDNA clone, B) digested XvVTC2 + pEYFP plasmid....	56
Figure 4.3: Recombinant plasmid map of 35S pEYFP NosT containing the XvVTC2 gene.	57
Figure 4.4: A series of images showing the expression of yellow fluorescent protein in transformed onion (<i>Allium cepa</i>) epidermal cells.	57
Figure 4.5: A series of images showing the expression of XvVTC2: pEYFP fusion protein in transformed onion (<i>Allium cepa</i>) epidermal cells.	58
Figure 4.6: Ponceau S stained membrane (A) and western blot (B) of <i>X. viscosa</i> soluble leaf proteins extracted from plants during a dehydration experiment.	60
Figure 5.1: A graph showing the mean \pm SE (n=3) of the relative water content of <i>X. viscosa</i> plants.	69
Figure 5.2: Images showing the drying and re-hydration of <i>Xerophyta viscosa</i> in a long day, 16h light and 23°C, growth room.	70
Figure 5.3: A graph showing the mean \pm SE (n=3) relative change mRNA expression level of XvVTC2, compared to 18s ribosomal RNA of <i>X. viscosa</i> plants under dehydration stress calculated by the comparative quantification method (Rotorgene 6000 software).	71
Figure 5.4: A graph showing the mean \pm SE (n=3) relative change mRNA expression level of XvVTC2, compared to 18s ribosomal RNA of <i>X. viscosa</i> plants under dehydration stress calculated by the Pfaffl REST method (Pfaffl, 2001).	72

List of Appendices

- Appendix 1:** Oligos
- Appendix 2:** PCR Conditions
- Appendix 3:** Transformation protocol
- Appendix 4:** Splinkerette Diagram
- Appendix 5:** cDNA sequence
- Appendix 6:** SDS poly-acrylamide gel recipes.
- Appendix 7:** eFP expression profiles of *VTC2* in *A. thaliana*
- Appendix 8:** Real-time PCR runs.
- Appendix 9:** Phosphorylation site prediction graphs

Abbreviations

ABA	abscisic acid
APX	ascorbate peroxidase
ASC	ascorbate (vitamin c)
AWC	absolute water content
bp	base pair(s)
CAT	catalase
cDNA	copy DNA
DEPC	diethylpyrocarbonate
DHA	dehydroascorbate
DHAR	dehydroascorbate reductase
DNA	deoxyribonucleic acid
DNase	deoxyribonuclease
DNTPs	di-nucleotide-triphosphates
EDTA	ethylenediaminetetra-acetic acid
ELISA	enzyme-linked immunosorbent assay
gDNA	genomic DNA
GSH	glutathione
GPX	glutathione peroxidase
IPTG	isopropyl- β -D-thiogalactopyranoside
kb	kilobase(s)
kDa	kilodalton(s)
LB	Luria-Bertani
MDHAR	monodehydroascorbate reductase
mM	millimolar
MI	<i>myo</i> -inositol
mRNA	messenger RNA
Ni-NTA	nickel-nitrilotriacetic acid
ORF	open reading frame
PBS	phosphate-buffered saline
PCR	polymerase chain reaction
PMSF	phenylmethylsulfonyl fluoride

PrxR	peroxiredoxin
RNA	ribonucleic acid
RNase	ribonuclease
RWC	relative water content
sdH ₂ O	sterile distilled water
SDS	sodium dodecyl sulphate
SDS-PAGE	SDS polyacrylamide gel electrophoresis
SOD	superoxide dismutase
RFO	raffinose family oligosaccharides
ROS	reactive oxygen species
TBE	tris borate EDTA
TE	tris-EDTA
TEMED	N,N,N',N' - tetramethylethylene diamine
Tris	tris(hydroxymethyl)aminomethane
u	unit(s) of enzymatic activity
UTR	untranslated region
VTC	genes involved in the ASC biosynthesis pathway
<i>vtc</i>	ascorbate defective mutant genes in the ASC biosynthesis pathway
w/v	weight per volume
WC	water content
X-Gal	5-bromo-4-chloro-3-indolyl- β -D-galactoside

Abstract

Climate change is predicted to have a negative impact on world food security in the next 40 years. Resurrection plants can withstand highly variable and harsh climatic conditions. This makes them ideal candidates to elucidate possible mechanisms which can be used to adapt crop plants to tolerate variable climatic conditions associated with climate change. The recent characterisation of the role of *VTC2*, a gene coding for a GDP-L-galactose phosphorylase and also the final step to be elucidated in the ascorbate (Vitamin C) biosynthesis pathway of plants, has re-ignited interest in the study of regulation of the pathway. Ascorbate is an antioxidant which is known to be produced in response to conditions that lead to oxidative stress. In this project the *Xerophyta viscosa* homolog (*XvVTC2*) of *VTC2* is characterised. In the characterisation of *XvVTC2* the gene was isolated, cloned, sequenced, analysed bioinformatically, the recombinant protein expressed, functional assays and localisation studies done and the expression analysed at the protein and mRNA level. The *XvVTC2* cDNA length is 1278bp and the gDNA length is 2510bp. The *VTC2* characteristic Histidine triad (HIT) motif was identified and *in silico* analyses predicted nucleotide binding, N-myristoylation and nuclear localisation sites. There was a high level of sequence similarity between *XvVTC2* and other *VTC2* homologs. The recombinant *XvVTC2* protein of 68kDa was expressed in *Escherichia coli* BL21(DE3) using the pET32b expression vector. *In vitro* assays showed that *XvVTC2* has GDP-D-glucose phosphorylase activity. Yellow fluorescent protein (YFP) localisation studies showed that the *XvVTC2*:YFP fusion proteins are localised to the nucleus and cytoplasm. Western blot analysis showed that the protein is differentially expressed in response to desiccation and rehydration. Quantitative real-time PCR analysis showed that the mRNA level of *XvVTC2* increases at least a thousand fold in response to desiccation and remains high during the course of rehydration. The *in vitro* assay, localisation and sequencing results correspond to that found with other *VTC2* homologs. The high mRNA transcript level of *XvVTC2* in response to desiccation indicates its importance in *X. viscosa* stress tolerance. This project provides the basis for further studies in which the regulatory mechanism, function and significance of the *XvVTC2* response to desiccation in *X. viscosa* can be elucidated. This might provide a future target for increasing the tolerance of crop plants to environmental stresses such as drought.

Chapter 1: Introduction and Literature review

University of Cape Town

1.1 General Introduction

Africa is considered to be the continent that is most at risk from climate change, with more frequent drought and higher temperatures expected in the near future (FAO, 2008 aa; 2008 bb). It is predicted that by 2050 climate change in Africa will significantly affect agriculture and in some areas could lead to the complete abandonment of cropping in some areas (Thornton et al., 2009). This in turn will affect food security due to crop production shortfalls and could result in social and political upheaval.

To reduce the impact of droughts on crop yields, plants need to be developed that can withstand and adapt to conditions of low water abundance. It is therefore necessary to understand how plants detect and respond to the onset of drought. In this context it is important to understand that environmental conditions are dynamic and differences in the environment occur daily as well as seasonally and that the daily and seasonally activated detection and response mechanisms might overlap. In perennial plants, a basal level of stress response elements is needed in order to cope with the day to day changes in the environment as well as mechanisms to signal and respond to more severe (seasonal) stress conditions. Reactive oxygen species (ROS) serve as such molecules within plants, and this is highlighted in a recent review by Miller et al., (2008) in which the dual role of ROS as important signalling molecules as well as its toxic effects under stress conditions were explored.

ROS are found in the environment and are created metabolically by the plant during photosynthesis and respiration, *inter alia* (Smirnoff, 1996, 1998). Under stress conditions such as water deficit and high light, ROS production can exceed the plant's capacity for the neutralisation and can cause damage to plants. Cells are damaged by ROS due to oxidation of proteins, lipids and DNA within the cell and can also trigger programmed cell death (Sasaki-Sekimoto et al., 2005). Thus, plants have to constantly keep ROS at a level where it is not harmful under normal (non-stress) conditions.

Other than the potential harm that ROS might cause, its role in signalling has been gaining increased attention (Foyer and Noctor, 2005 aa). Under high concentrations of ROS physicochemical damage in plants is caused by the triggering of programmed cell

death cascades. However, under most conditions ROS are not present in high concentrations and have an important function in oxidative signalling (Dat et al., 2000; Foyer and Noctor, 2005 aa; 2005 bb). In this regard ROS have been shown to play an important function in a plant's ability to sense and respond to the surrounding environment and pathogens (Delledonne et al., 2004; Miller et al., 2007). The proposed evolutionary mechanism is that; because ROS are produced under stress conditions they are an indicator of stress, and signal for stress responses to be activated (Mittler et al., 2004). During evolution variations in this signalling pathway might have originated leading to signalling of other processes such as plant growth, hormonal signalling, defence and development. The ROS signalling mechanism is initiated by developmental or environmental signals leading to altered ROS levels in certain cells or cell compartments. These altered ROS levels are then sensed by enzymes and receptors, which initiate corresponding developmental, defence or metabolic pathways (Mittler et al., 2004).

The control of the levels of ROS is achieved by an array of enzymatic and non-enzymatic antioxidants. The major enzymatic antioxidants include superoxide dismutase (SOD), ascorbate peroxidase (APX), catalase (CAT), glutathione peroxidase (GPX) and peroxiredoxin (PrxR). The major non-enzymatic antioxidants are, ascorbate (ASC), glutathione (GSH) and to a lesser extent tocopherol, flavonoids, alkaloids, and carotenoids. These antioxidants scavenge ROS in order to maintain homeostasis (Apel and Hirt, 2004; Mittler et al., 2004; Miller et al., 2008). The concentration and localisation of these antioxidants play a vital role in the signalling by ROS in the plant.

In a review by Mittler et al. (2004) it was stated that the role of the enzymatic components as well as ASC and GSH is to equip cells with highly efficient machinery to detoxify ROS, O_2^- and H_2O_2 . Key factors driving the efficiency of this machinery are the redundancy and flexibility of these various components (Mittler et al., 2004). The redundancy can be illustrated when some of the genes encoding for these enzymes are knocked out, for example: when APX1 is knocked out there is an increase in expression of a type 2 PrxR and ferritin (Mittler et al., 2004). The flexibility of these components is realised when looking at various stress conditions under which they are expressed. An example of this is SOD, more specifically FSD2, which is expressed in response to heat,

cold, salt and high light stresses (Mittler et al., 2004). These examples just illustrate some of the conditions under which these antioxidants have been shown to be of importance. To discuss the roles of all the antioxidants in plants is beyond the scope of this thesis. As the subject matter of this thesis is to characterise a gene involved in the de-novo synthesis of ASC, more detail will be shed on the role of ASC in plants.

1.1.1 Role of Ascorbate in plants

Ascorbate is an abundant and important antioxidant in plants. Beyond being a housekeeping antioxidant, ASC has been shown to be involved in a myriad of processes including; an enzyme cofactor, involvement in redox signalling, a role in pathogen response, growth, programmed cell death and recently as an alternative electron donor in photosystem II. (Conklin and Barth, 2004; Foyer and Noctor, 2005 a; Cordoba-Pedregosa et al., 2007; Colville and Smirnoff, 2008; Toth et al., 2009)

When ASC reacts with a ROS it becomes oxidised and forms the monodehydroascorbate radical and needs to be reduced before it can serve in its antioxidant function again. This recycling of ASC from its oxidised to reduced form is achieved by the enzymes monodehydroascorbate reductase (MDHAR) and dehydroascorbate reductase (DHAR). In the recycling process MDHAR reduces monodehydroascorbate to ASC or disproportionates of ASC and dehydroascorbate (DHA). The DHA can then undergo hydrolysis to 2,3-diketogulonic acid in which case it is lost or can be reduced to ASC by DHAR. Thus the enzymes MDHAR and DHAR play important roles in the maintenance of the levels of reduced ASC in plants (Chen and Gallie, 2004).

In cell growth it has been shown that ASC plays a variety of roles. In a study by Córdoba-Pedregosa et al., (1996) it was shown that ASC stimulates the growth of onion (*Allium cepa*) roots. It was suggested that a process which plays a role in this growth is that in the apoplast of roots O_2 and Cu^{2+} are reduced to hydrogen peroxide (H_2O_2) and Cu^+ respectively under the control of ASC in a reaction known as the Fenton reaction (Fry, 1998). The H_2O_2 and Cu^+ molecules react to form a short lived $\cdot OH$ radical. The $\cdot OH$ radical can cause oxidative scission of polysaccharide chains, such as xyloglucan found in cell walls. The short lived $\cdot OH$ radical affects oxidative scission which leads to the loosening of cell walls. The loosening of cell walls is important in cell expansion,

fruit ripening and organ abscission. Because the $\cdot\text{OH}$ radical is short lived and produced site specifically, oxidative damage is not caused to the cell. A more recent study by Córdoba-Pedregosa et al., (2007) has shown that onion roots treated with ASC and its immediate precursor L-galactono- γ -lactone show an increase in biomass, H_2O_2 and changes in the ASC related enzymes in cytosolic and apoplastic compartments. The H_2O_2 as well ASC are localised to the meristematic and elongation regions of the root. Thus there is an ever increasing amount of evidence to suggest that ASC plays an important role in growth regulation in the roots of plants.

Ascorbate along with H_2O_2 plays roles in stomatal function. In transgenic tobacco and wheat plants overexpressing the ASC recycling enzyme dehydroascorbate reductase (DHAR) an increased amount of reduced ASC and altered stomatal movement and guard cell signalling was observed (Chen et al., 2003; Chen and Gallie, 2004). Leaves with increased ASC levels showed more open stomata and lower levels of H_2O_2 . Naturally, along with the higher number of open stomata, increased stomatal conductance and increased transpiration rates were shown. The plants suffered from greater water loss under drought conditions, which was restored when the DHAR expression was suppressed. The conclusions drawn from this study was that under natural conditions DHAR is expressed at a rate limiting level. Furthermore, DHAR serves to maintain a basal level of ASC in guard cells which is insufficient to scavenge the high rate H_2O_2 that is produced in the afternoon (under high light conditions), due to high photosynthetic rates. Once this basal threshold is met, the stomata close to protect the plant against excessive water loss (Chen and Gallie, 2004).

The role of ASC as a cofactor for various enzymes has been well documented. In one example, the violaxanthin cycle, ASC acts as a cofactor for the enzyme violaxanthin de-epoxidase as reviewed in Jahns et al. (2009). This enzyme is involved in the formation of zeaxanthin from violaxanthin. The violaxanthin cycle regulates the formation of the xanthophylls, violaxanthin and zeaxanthin, which are important for plants to adapt to differing light conditions. Under low light conditions violaxanthin accumulates and has a light harvesting role. Under high light conditions the violaxanthin is converted to zeaxanthin which leads to the dissipation of light and plays a photoprotective role. The switch between violaxanthin and zeaxanthin is reversible and violaxanthin can be

converted to zeaxanthin in 10-30 minutes, the reverse reaction however takes 5-10 times longer (Horemans et al., 2000; Jahns et al., 2009). Thus in its role as cofactor to violaxanthin de-epoxidase, ASC plays an indirect role in the protection of the plant against photo-oxidative stress.

A. thaliana mutant plants (*vtc2*) deficient in ASC are unable to acclimate to high light when transferred from low light. The leaves of these plants show bleaching of mature leaves, increased signs of lipid peroxidation and photoinhibition. Mutant plants (*npq1*) that are deficient in zeaxanthin production differ only slightly in terms of the abovementioned characteristics from wild type plants when transferred to high light. However double mutants for *vtc2* and *npq1* show the light stress symptoms even earlier and more severe than observed in the *vtc2* mutant (Muller-Moule' et al., 2003). This indicates that the light dissipation capacity (provided to a large degree by zeaxanthin) along with antioxidant capacity (provided to large degree by ascorbate) of the plant are vital to the acclimatisation to high light conditions. The results from these studies clearly indicate that ascorbate is important as an enzyme cofactor and antioxidant for the acclimatisation of plants to high light conditions.

Ascorbate has been implicated in the response of plants to pathogens. A microarray analysis conducted by (Pastori et al., 2003) has indicated that in an ASC deficient mutant (*vtc1*) 171 genes are differentially expressed. Several genes involved in pathogen resistance showed an increase in expression levels in the mutant plant when compared to the wildtype (Col-0). The genes that showed a significant increase in expression levels were the pathogenicity related (PR) proteins, PR1 and 2, a putative disease resistance protein (DRP), β -glucanase and chitinase. The authors found it striking that the expression levels of Phe ammonia-lyase (PAL) genes were not different in the mutant and wildtype plants. The significance of this is that PAL activity is required for the production of antimicrobial phyto-alexins and salicylic acid, with salicylic acid inducing the production of PR proteins. Thus the production of PR proteins in this case is not induced by PAL activity but rather by the ASC deficiency, leading the authors to suggest that factors influencing the ASC content of the cell can play a role in disease susceptibility (Pastori et al., 2003).

Barth et al., (2004) found that the salicylic acid levels were increased in *vtc1* mutants, which leads to an increased response to pathogens and increased disease resistance. Thus it can be inferred that ASC deficiency induces an increase in salicylic acid levels via a PAL independent mechanism, which leads to an increase in resistance to pathogens. It is suggested that the mechanism at work could be reliant on abscisic acid (ABA) signalling, as Pastori et al., (2003) also showed a 60% increase in the concentration of ABA in the ASC deficient mutants (Colville and Smirnoff, 2008).

In the abovementioned study, some of the genes that are differentially expressed in the *vtc1* mutant plant might not have been due to the lack of ascorbate but due to the lack of the enzyme produced by the gene (*vtc1*) which may affect other processes in the cell. This is based on the fact that products and substrates affected by the VTC1 enzyme are involved in cell wall metabolism. The authors do acknowledge this and suggest that a mutant for an enzyme committed only to ASC biosynthesis be used in future studies (Pastori et al., 2003). Recently it has been shown that the *vtc1* mutant does exhibit a stronger response to pathogens when compared to other *vtc* mutants (*vtc2-1*, *vtc2-2* and *vtc4*) which suggests that the cell wall composition also plays a role in the triggering of pathogen response genes (Colville and Smirnoff, 2008).

In the aforementioned examples it is clear that ascorbate plays a significant role in many signalling pathways within the plant. Many of these pathways bear some relation to the production of ROS. Drought (water-deficit/dehydration) stress is the major abiotic stress under study in this thesis, and like some of the other stresses mentioned; water-deficit also increases the production of ROS in the plant. Thus it is also expected that ASC would play a role in water-deficit stress and defence response pathways during drought conditions.

In a review by Jubany-Marí et al., (2010) it is reported that the drought tolerant Mediterranean shrub *Cistus albidus* has an approximately 3.5 fold increase in ASC level in response to drought. Furthermore, drought resistant plants under field grown conditions show in general an increase in ASC levels and a decrease in DHA levels and the opposite has been found for drought sensitive plants. It is proposed that the oxidative status of plants under drought stress is in large controlled by the redox status of the ASC pool.

Furthermore, the redox status is especially important for the activity of enzymes that are redox regulated such as those that contain cysteine residues in their active centre. The authors do however acknowledge that further work needs to be done to determine the precise role of ASC in terms of cellular localisation, redox status and oxidative signalling under drought conditions.

In the drought sensitive plant *Triticum aestivum*, Bartoli et al., (1999) showed that the ASC content of the leaves decreased under moderate water-deficit conditions. This work corresponds to that of Jubany-Marí et al., (2010). An interesting observation from this study is that the levels of other antioxidants including β -carotene and α -tocopherol increased, which is another example of the redundancy of the antioxidant defence system. The reduction in reduced ASC content is possibly because the rate at which the oxidised form is recycled to the reduced form is lower than the rate at which the ASC is oxidised. Thus it seems that the reduced ASC pool in *T. aestivum* is not large enough or turned over fast enough to buffer against the oxidative stress due to drought.

Another stress factor which should be taken into account during drought stress is the role of heat stress. This component is taken into account in the review by Jubani-Marí (2010 a). The correlation between ASC and heat stress is also exemplified in the work by Pastori et. al., (2003), where it is shown that heat-shock proteins are upregulated in the ASC deficient *A. thaliana* mutant *vtc1*. This shows that when ASC content is low or depleted stress response elements are activated.

1.1.2 *De-Novo* synthesis of Ascorbate

Despite the importance of ASC, a complete pathway for the *de-novo* synthesis of ASC has only recently been elucidated in plants. The immediate precursor to ASC, L-galactone1,4-lactone, however was first suggested by Isherwood and Mapson in 1962 based on the analogous pathway in animals where L-gulonono-1,4-lactone is oxidised to ASC. Though it was confirmed that L-galactone 1,4-lactone was indeed the precursor, but the pathway was not an inversion pathway as found in animals (Wheeler et al., 1998). Many studies were done in which several of the intermediates in the pathway were identified, and some of the early studies are well reviewed by Smirnoff, (1996). However a complete pathway, from D-Glucose to ASC, was only proposed by Wheeler et al.,

(1998) and is now known as the L-galactose or Smirnov-Wheeler pathway (Figure 1.1). The gene (*VTC2*) responsible for the first committed step to ASC in this pathway was characterised recently by Linster et al. and Laing et al. in 2007.

The Smirnov-Wheeler pathway has two major components. The first component, comprised of six steps, is not specific to ASC biosynthesis and is focused on the conversion of D-glucose to GDP-L-galactose. In this component glucose is converted to glucose-6-phosphate by hexokinase. The glucose-6-phosphate is subsequently converted to fructose-6-phosphate by phosphoglucose isomerase. The enzymes in these first two steps are well characterised for their roles in glycolysis.

In the third step fructose-6-phosphate is converted to mannose-6-phosphate by a phosphomannose isomerase (PMI), of which two paralogs exist in *A. thaliana* based on sequence analysis (Linster and Clarke, 2008). However, there was some contention over whether this enzyme is functional or is expressed in plants. This is because the expression of one of these PMI paralogs, *din9*, has only been detected after *A. thaliana* plants have been dark treated for 24 hours and the other's expression is unknown. Furthermore, an *E. coli* ortholog of PMI is used as a selectable marker for the transformation of citrus (Ballester et al., 2008). The assumption in this case being, that plants that do not contain the PMI are not able to convert mannose-6-phosphate to fructose-6-phosphate in the reversible reaction. The mannose-6-phosphate then acts as a potent growth inhibitor. This leads one to believe the plant does not possess or express its own machinery to convert the mannose-6-phosphate to fructose-6-phosphate as needed in the Smirnov-Wheeler pathway. However, PMI activity has been demonstrated in *A. thaliana* leaf extracts and thus suggests the presence of an active form of PMI (Dowdle et al., 2007). Recent work by Maruta et al., (2008) has confirmed that there is an active PMI paralog (PMI1) in *A. thaliana* which is correlated to ASC biosynthesis. Interestingly it was also found that the other PMI paralog (PMI2 formerly *din9*) does not play a role in ASC biosynthesis.

The fourth step in the ASC biosynthesis pathway is the conversion of mannose-6-phosphate to mannose-1-phosphate by a phosphomannomutase (PMM) enzyme. The function and presence of PMM has been well documented in animals, fungi and plants. The physiological characterisation of several plant PMM paralogs has only recently been

conducted (Qian et al., 2007). This characterisation of the paralogs provided evidence for the role of PMM in ASC biosynthesis. When the PMM transcript level in tobacco (*Nicotiana benthamiana*) is reduced, via viral mediated gene silencing, a notable reduction in ASC is observed. These results as well as functional assays, showing substrate specificity, provide convincing evidence that PMM in plants does convert mannose-6-phosphate to mannose-1-phosphate. The evidence for the role of PMM in ASC biosynthesis is further strengthened by a study that shows a PMM *A. thaliana* mutant (*pmm-12*) is deficient in ASC (Hoeberichts et al., 2008).

The fifth step in the pathway involves the conversion of mannose-1-phosphate to GDP-mannose in the presence of GTP. This conversion is mediated by a GDP-mannose pyrophosphorylase enzyme. The gene coding for the enzyme is called *VTC1*, formerly *SOZI*, and was first identified in an ozone sensitive, ASC deficient *A. thaliana* mutant (Conklin et al., 1996). The mutant plants display approximately 30% of wild type ASC levels indicating its importance in ASC biosynthesis. In characterising *VTC1*, it was shown that the reduced ASC levels are not because of an increase in the level of ASC oxidation or a lower rate of reduction of oxidised ASC (Conklin et al., 1997). Furthermore, the *vtc1* mutation does not affect the ability of a plant to convert L-galactono-1,4-lactone to ASC in the final step of the L-galactose pathway. Carbon labelling (C^{14}) experiments suggest that reduction in ASC levels is because of a defect in the biosynthesis (Conklin et al., 1997). In the light of the proposed L-galactose pathway the gene was further characterised by biochemical, molecular and genetic techniques to establish its function as well as the role of GDP-mannose in ASC biosynthesis (Conklin et al., 1999).

The GDP-mannose produced by *VTC1* as well as GDP-L-galactose produced by GDP-mannose epimerase (GME) are activated nucleotide sugars, and are precursors to cell wall polysaccharides and glycoproteins (Linster and Clarke, 2008). GME uses GDP-mannose as substrate and produces GDP-L-gulose and GDP-L-galactose in a reaction that reaches an equilibrium between the products (Wheeler et al., 1998; Wolucka and van Montagu, 2003; Major et al., 2005). The production of GDP-L-gulose in this reaction prompted Wolucka and van Montagu, (2003) to suggest an alternative pathway of ASC biosynthesis via the intermediates L-gulose and L-gulono-1,4-lactone (Figure 1.2).

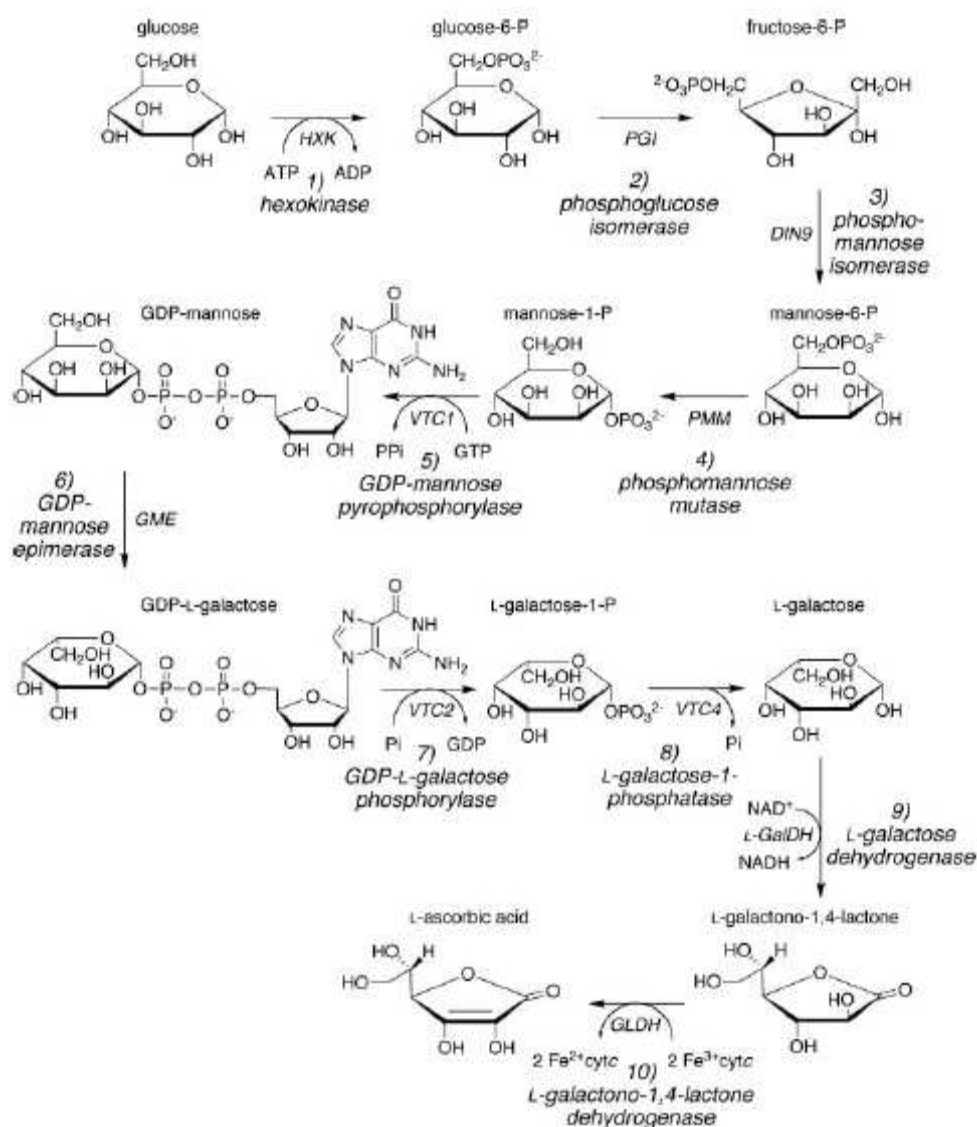


Figure 1.1: The Smirnov-Wheeler pathway of Ascorbate biosynthesis adapted from (Linster et al., 2007). The pathway shows the conversion of D-Glucose to L-ascorbic acid. The first six steps of the pathway involve the conversion of D-Glucose to GDP-L-galactose, substrates used in glycosylation and cell wall biosynthesis. The first committed step to ascorbate biosynthesis is step seven, where GDP-L-galactose is converted to L-galactose-1-phosphate and GDP in the presence of inorganic phosphate. In step eight L-galactose-1-phosphate is converted to L-galactose. In steps nine and ten the L-galactose and L-galactono-1,4-lactone are oxidised, by the NAD⁺ and ferric cytochrome c-dependant enzymes, L-galactose dehydrogenase and L-galactono-1,4-lactone dehydrogenase respectively, to form L-Ascorbic acid.

The reasoning and evidence provided by Wolucka and van Montagu, (2003) does suggest that ASC biosynthesis in plants can occur via the L-gulose pathway. This is evident in that L-gulose and L-gulono-1,4-lactone is converted to ASC in *A. thaliana* cell suspension cultures. Furthermore there is evidence of L-gulono-1,4-lactone dehydrogenase activity in plant cell extracts as well six L-gulono-1,4-lactone

dehydrogenase genes in the *A. thaliana* genome (Wolucka and van Montagu, 2003; Wolucka and Montagu, 2007). However, whether ASC biosynthesis does occur via this pathway and the extent of its role under natural conditions is debatable. Enzymes associated with the subsequent steps in the L-gulose pathway have not been characterised and mutant plants deficient in these proposed enzymes are not available to show ascorbate deficiency. The authors of these studies do recognise the L-galactose pathway in ASC biosynthesis but, with good reason, propose that ASC biosynthesis may possess intricacies which should be explored. However, evidence in favour of the L-galactose pathway as the major pathway in ASC biosynthesis is ever increasing (Linster and Clarke, 2008). This evidence has come in the recent characterisation of GDP-L-galactose phosphorylases en route to ASC biosynthesis.

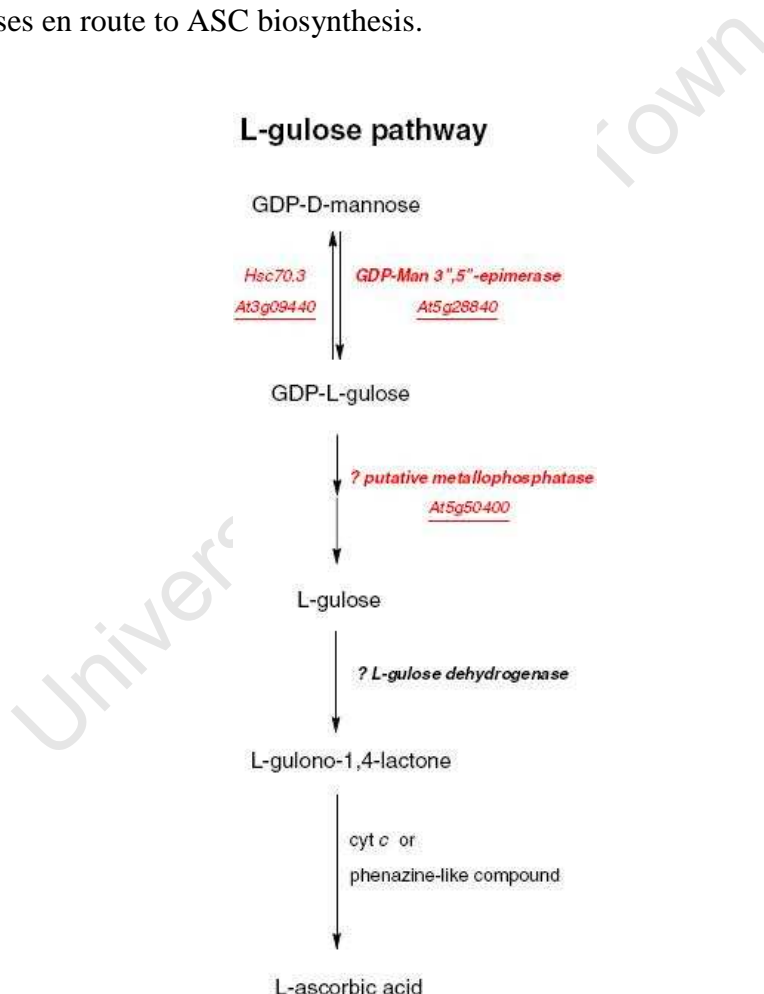


Figure 1.2: The L-Gulose pathway of ASC biosynthesis as proposed by Wolucka and van Montagu, 2003. The diagram illustrates the conversion of GDP-D-mannose to L-ascorbic acid via the intermediates GDP-L-gulose, L-gulose and L-gulono-1,4-lactone. Adapted from (Wolucka and Montagu, 2007)

The second component of the L-galactose ASC biosynthesis pathway is committed to the production of ASC. The first step of this second component involves the conversion of GDP-L-galactose to L-galactose-1-phosphate and GDP in a reversible reaction (Dowdle et al., 2007; Laing et al., 2007; Linster et al., 2007; Linster et al., 2008). The precise biochemical mechanism by which this conversion takes place has been debated. Here the enzyme will be referred to as a phosphorylase and the reasoning will be discussed in later chapters. The reaction is performed by a GDP-L-Galactose phosphorylase in the presence of inorganic phosphate. There are two paralogs, *VTC2* and *VTC5*, of this gene in *A. thaliana*. These proteins possess the same phosphorylase activity and are highly specific for GDP-L-galactose as well as GDP-D-Glucose (Linster et al., 2007; Linster et al., 2008). *A. thaliana* double mutants of *VTC2* and *VTC5* show an arrest in growth immediately after germination followed by a bleaching of the cotyledons. Normal growth can then be restored by supplementing the plants with ASC or L-galactose (Dowdle et al., 2007). These experiments indicate that in *A. thaliana* and in probably most plants that a GDP-L-Galactose phosphorylase is needed for ASC biosynthesis. Furthermore it suggests that there is no other pathway, which is sufficiently active in germination and probably under most conditions, other than the L-galactose pathway leading to ASC biosynthesis.

The ability of these phosphorylase enzymes to use GDP-D-Glucose in addition to GDP-L-Galactose as a substrate in a reversible reaction has led to the proposal of a *VTC2* cycle (Figure 1.3) (Wolucka and Montagu, 2007). In the proposed cycle, components of the ASC biosynthesis pathway are recycled and the ASC biosynthesis pathway is linked to photosynthesis and cell wall biosynthesis. The basis of this hypothesis is fuelled by two facts. Firstly, D-glucose-1-phosphate, which is produced in photosynthesis, can be converted to GDP-D-glucose which is used for cell wall biosynthesis by the *VTC2* enzyme. This argument is strengthened by a three times greater efficiency in converting D-glucose-1-phosphate to GDP-D-glucose, compared to L-galactose-1-phosphate to GDP-L-galactose, by the *VTC2* enzyme (Linster et al., 2007). Secondly, upon the formation of GDP-D-glucose it can be converted to GDP-D-mannose which feeds back into the ASC biosynthesis pathway. However, this reaction is hypothetical and would require a GDP-mannose-2'-epimerase which is yet to be identified or characterised. The epimerase activity needed for this reaction has been shown to exist in plants, but without the identification of a specific enzyme (Wolucka and Montagu, 2007). Thus the proposal

of a VTC2 cycle has merit, but characterisation of a GDP-mannose-2'-epimerase and evidence directly implicating VTC2 in cell wall biosynthesis is still needed.

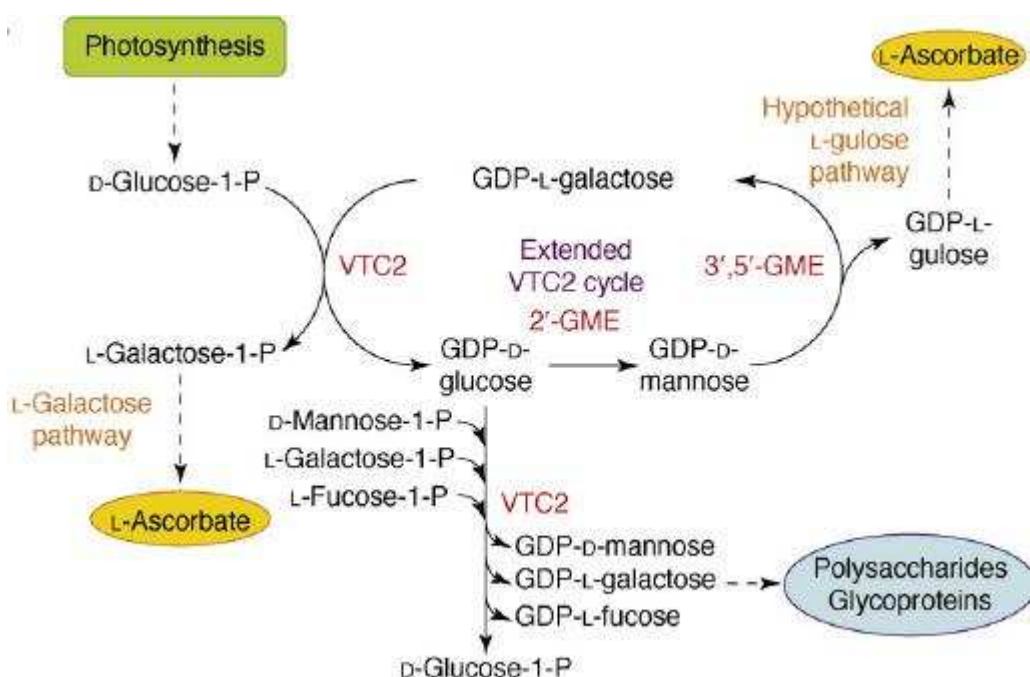


Figure 1.3: The extended VTC2 cycle as proposed by (Wolucka and Montagu, 2007), which links ascorbate biosynthesis to photosynthesis and cell wall biosynthesis. Adapted from (Linster and Clarke, 2008).

In the eighth step of the L-galactose pathway L-galactose-1-phosphate is converted to L-galactose by an L-galactose-1-phosphatase, which is coded for by the *VTC4* gene in *A. thaliana* (Conklin et al., 2006). *A. thaliana vtc4* mutants as well as complete knock-out mutant plants exhibit less than 50% wildtype ASC levels. Although important in ASC biosynthesis it also suggests that there might be other paralogs of *VTC4* that convert L-galactose-1-phosphate to L-galactose as ASC biosynthesis is not completely halted or that ASC biosynthesis can also occur via a different pathway (Conklin et al., 2006). Recent studies indicate that this enzyme is a bi-functional enzyme which is involved in the myoinositol as well as ASC biosynthetic pathways (Torabinejad et al., 2009). The enzyme has been shown to be able to convert D-myo-inositol-3-phosphate to myoinositol. This is of significance, because in animals myoinositol is converted to ASC via D-glucuronic acid. Furthermore, when a myoinositol oxygenase gene (*miox4*), which forms D-glucuronic acid from myoinositol, is overexpressed in *A. thaliana* there is an increase in ASC levels (Lorence et al., 2004). However, results contrasting the findings of Lorence

et al., (2004) have recently been published by Endres and Tenhaken (2009), where it is shown that *miox4* controls the level of myoinositol in *A. thaliana* but does not increase ASC levels. These results suggest that the role of *VTC4* in the myoinositol pathway does not feed into a different ASC biosynthesis pathway and is limited to the myoinositol biosynthesis pathway.

The penultimate step of the L-galactose pathway involves the oxidation of L-galactose to form L-galactono-1,4-lactone. This reaction is mediated by an L-galactose dehydrogenase (Gatzek et al., 2002). The role of this enzyme in the pathway has been tested via antisense suppression in *A. thaliana* plants that showed 30% of wild type activity. Under high light conditions, when the gene is suppressed, the plants show a reduction in ASC accumulation and an increase in L-galactose. Interestingly, when this gene is overexpressed there is no increase in ASC formation. However, when L-galactose is exogenously applied, the ASC pool size increases (Gatzek et al., 2002). This evidence suggests that this enzyme is required for ASC biosynthesis but does not regulate the flux through the pathway. The ASC pool size is rather controlled by the availability of L-galactose as a substrate for this enzyme.

The final step of the L-galactose pathway is mediated by a mitochondrial flavin-containing L-galactono-1,4-lactone dehydrogenase (L-galLDH) (Smirnov et al., 2001; Linster and Clarke, 2008). L-galactono-1,4-lactone is converted to ASC in this reaction and involves cytochrome c as electron acceptor. Unlike the animal pathway, in this final step H_2O_2 is not produced, which prevents the electron transport chain in the mitochondria from becoming unnecessarily oxidised (Millar et al., 2003). Recent studies indicate that, similar to the L-galactose dehydrogenase, the flux of the pathway is not controlled at this step. The synthesis of ASC is rather dependant on the size of the L-galactono-1,4-lactone pool, because an increase in expression level of the enzyme does not translate to an increase in ASC level (Imai et al., 2009 a). These results do not take into account the actual regulation of the protein in different light conditions. There is some contrasting evidence about the light regulation of this protein under differing light conditions. Pignocchi et al., (2003) showed that the enzyme is not light regulated in tobacco, and more recent work by Yabuta et al., (2007) showed that it is light regulated in *A. thaliana*. The more recent publication suggests specifically that the photosynthetic

electron transport of chloroplasts is correlated to the expression of the L-galLDH enzyme. Other research also suggests that this step in the pathway is light regulated and changes in respiration affect the activity of this enzyme (Millar et al., 2003; Bartoli et al., 2006). Light regulation of this enzyme is to be expected as the need for quenching of ROS is greater when the plant is metabolically active.

The complete characterisation of the *de novo* synthesis pathway of ASC has provided the basis for the identification possible points where the pathway can be manipulated to increase the ASC content of plants. The literature reviewed above suggests that there is one major pathway, the L-galactose / Smirnoff-Wheeler pathway, to ASC biosynthesis. There are a few steps in the biosynthesis pathway that play roles in the regulation of the flux through the pathway. These include the steps controlled by PMI1, GME, VTC2/VTC5 and L-galLDH (Yabuta et al., 2007; Maruta et al., 2008). These steps would thus be candidates for future studies in enhancing the ASC content of plants.

The majority of the evidence for the L-galactose pathway is derived from studies in *A. thaliana*. It is worth keeping in mind, that variations in the control of the pathway or other pathways may exist in other plants. As ASC is produced in response to water deficit stress, amongst other stresses, it would be of interest to explore the adaptations of plants resistant to drought and desiccation and the role of ASC under these conditions.

1.2 Resurrection Plants

Plants can be found in all biospheres and have evolved mechanisms which allow them to grow in some of the most inhospitable places on the planet. Certain plants, called resurrection plants, have adapted the ability to withstand severe loss of water and can recover rapidly upon watering. Many of these angiosperms occur in Southern Africa and can withstand virtually complete desiccation. The majority of these plants are pioneer species and have adapted to harsh environments, such as rock surfaces or shallow soils, which provide little protection against severe water deficit stress (Gaff, 1971, 1977). Therefore, these plants serve as ideal model organisms to study how plants can effectively survive water deficit stress, which could potentially lead to the development of drought tolerant crops (Mundree et al., 2002).

Resurrection plants have to overcome a number of obstacles in order to survive in the desiccated state. These obstacles include, minimising the mechanical damage caused by turgor loss, maintaining the integrity of membranes and macromolecules as well as minimising the accumulation, and subsequent damage, of free radicals such as ROS (Farrant et al., 2007; Moore et al., 2009). One of the main factors that can cause damage during drying is light. The excitation energy used by chlorophyll can not be dissipated by photosynthesis, and can subsequently lead to ROS damage (Sherwin and Farrant, 1998).

Resurrection plants can be divided into two groups, those that maintain most of their chlorophyll (homoichlorophyllous) and those that lose most their chlorophyll (poikilochlorophyllous) upon drying (Bewley, 1995; Sherwin and Farrant, 1996). As protection against light the homoichlorophyllous plant *Craterostigma wilmsii*, reduces the leaf surface area exposed to light by tightly curling its leaves, so that only the abaxial surface of the outer whorl of the older leaves are exposed. These leaves become red in colour and have a hairy reflective surface. (Sherwin and Farrant, 1998). In the poikilochlorophyllous plant *Xerophyta viscosa*, leaves fold in half, along the midrib, and only the abaxial surface is exposed to light. The leaves initially turn yellow, as chlorophyll is lost, and become dark purple when dry. The abaxial surface also accumulates a sticky substance which is thought to aid in a reduction of absorbed light (Sherwin and Farrant, 1998). Both these plants accumulate anthocyanins during drying which are photoprotective pigments that serve as a sunscreen. Due to the loss of photosynthetic apparatus it takes longer for poikilochlorophyllous plants to recover from desiccation than homoichlorophyllous plants. This is attributed to the time needed for re-assembly of the photosynthetic machinery (Sherwin and Farrant, 1996; Sherwin and Farrant, 1998).

These unique plants have also adapted ways to reduce the mechanical damage associated with turgor loss (reviewed in Farrant 2000, 2007 and Viret et al. 2004(a)). These adaptations include changes to the cell wall in terms of its rigidity and the withdrawal of the cell membrane from the cell wall. In the poikilochlorophyllous plant *Xerophyta* spp, large water filled vacuoles are replaced by smaller vacuoles containing non aqueous substances in response desiccation. This prevents the withdrawal of the cell membrane and the collapse of the cell wall. In *C. wilmsii* there are also smaller vacuoles present but

in order to prevent withdrawal of the cell membrane, the cell wall is folded extensively. This folding (and unfolding on rehydration) is a regulated process involving structural changes to xyloglucan components (Vicré et al., 2004 b). The homoichlorophyllous plant *Myrothamnus flabellifolia* uses a combination of vacuolar water replacement and cell wall folding (Moore et al., 2006; Moore et al., 2008 a).

The non-aqueous metabolites that accumulate in the vacuoles in these plants have not been characterised for many species and specific components are likely to vary on a species basis. In the resurrection fern a combination of glycerol and monohexadecanoglycerol have been proposed to replace water in vacuoles (Farrant et al., 2009). In the cytoplasm, there is accumulation of predominantly sugars, such sucrose and raffinose family oligosaccharides and proteins that serve to stabilise membranes and protect the subcellular *milieu* during drying (reviewed in (Berjak, 2006; Farrant et al., 2007). It is proposed that the sugars and proteins form in a glassy state, which stabilise and protects the cell in the desiccated state (Crowe et al., 1998; Bryant et al., 2001; Hoekstra et al., 2001). The accumulation of sucrose and raffinose family oligosaccharides has been shown in *X. viscosa* in response to desiccation (Peters et al., 2007). Other than the accumulation of sugars in the cells, the cell wall components of resurrection plants change in response to desiccation (reviewed in Moore et al., 2008b; 2009).

In response to water deficit, be it drought or desiccation, plants show a change in cell wall structure. In general the cell walls become more loosened, elastic and flexible. However, desiccation sensitive plants only show this loosening of the cell walls in growth areas and other non-growth areas show a tightening of the cell wall (Moore et al., 2008 b). In trees there is a species dependant variation in terms of cell wall elasticity associated with increased drought resistance. Trees that show increased cell wall elasticity in response to water deficit have little to no osmotic adjustment. On the other hand, trees that show an increase in the rigidity of the cell walls undergo osmotic adjustment in response to water deficit stress (Clifford et al., 1998). Thus, the response to water deficit and factors increasing drought resistance in terms of the cell wall is varied among non-resurrection plants.

In some resurrection plants there are marked changes in composition as well as the structure of the cell wall upon drying. In *C. wilmsii* there are differences in the hemicellulosic wall fraction between the desiccated and hydrated state. In dry plants there is a decrease in glucose content and the xyloglucan is also substituted more with galactose (Vicré et al., 2004 b). This allows for the cleavage and partial degradation of the xyloglucan which allows the cell wall to become more flexible in response to desiccation. The accumulation of sucrose is proposed to aid in the stabilisation of the polymers and act as buffer to the lost water (Moore et al., 2008 b). These features put together provide the cell wall architecture for the plant to be able to withstand desiccation and recover rapidly upon watering (Moore et al., 2006; Moore et al., 2007; Moore et al., 2008 b).

An important part of a resurrection plant's ability to withstand desiccation relies on the efficient quenching and a reduction in the production ROS. In *M. flabellifolia* there are vast changes in the pigment content and antioxidant status of the plant which also correlates with the revival of the plant (Kranter et al., 2002). Upon desiccation the antioxidants GSH and ASC show a shift towards their oxidised forms. There is an initial increase in total glutathione (GSH + oxidised glutathione GSSG) in response to desiccation, thereafter the glutathione content decreases. This could be because the plant needs to build up the necessary antioxidant defence to withstand a potentially long desiccation period, before its metabolism virtually shuts down. A different observation is apparent for total ascorbate (ASC + DHA), which under normal conditions is present at 25x molar excess compared to glutathione. There is no initial increase in total ascorbate and total ascorbate level decreases as desiccation is prolonged and is eventually depleted. Upon rehydration from mild and severe desiccation there is an increase in the ASC level, which is required to buffer the oxidative stress due to the resumption of normal metabolic activity (Kranter et al., 2002).

The roles that ASC plays in ROS quenching, the violaxanthin cycle and in the regeneration of α -tocopherol could explain why ASC could become depleted in prolonged desiccation. Georgieva et al., (2009) also found an increase in zeaxanthin in the poikilochlorophyllous *Haberlea rhodopensis* in response to desiccation. In *M. flabellifolia* there is also a decrease in levels of α -tocopherol and β -carotene as desiccation progresses. In this plant if desiccation persists for long periods of time, more

than 8 months, the antioxidant system breaks down and upon rehydration the plant abscises its leaves. The plant however still manages to recover and produce new leaves (Kranter et al., 2002).

Other than the abovementioned example, several other studies have also highlighted the importance of antioxidants in the ability of resurrection plants to withstand desiccation. In *X. humilis*, *M. flabellifolia* and *C. wilmsii* the activity of antioxidant enzymes increase in response to desiccation (Farrant, 2000). The poikilochlorophyllous, *X. humilis*, shows an increase in the activity of APX, SOD and glutathione reductase. In the homoichlorophyllous *C. wilmsii* and *M. flabellifolia* the most marked increase in activity is that of APX, with SOD and glutathione reductase showing relatively smaller increases in activity in *M. flabellifolia* (Farrant, 2000). In *X. viscosa* a 1-Cys peroxiredoxin, *XvPer1*, is expressed in response to desiccation in the leaves (Mowla et al., 2002). This enzyme is usually expressed in the seeds of other angiosperms and homologs of this enzyme have known antioxidant activity (Mowla et al., 2002).

The examples discussed in this section indicate the importance of antioxidants and the antioxidant status in the desiccation tolerance of resurrection plants. It has been shown that ASC has a multifunctional role in the defence against damage during desiccation for example the scavenging of ROS and being a cofactor in the violaxanthin cycle. The mechanisms, by which the detection and response to desiccation take place, and more specifically the role of ASC, are key areas that need further investigation in resurrection plants.

1.3 Aim

The biosynthesis of ASC is of particular interest as there is a marked increase in activity of processes requiring ASC in response to desiccation. The steps at which the biosynthesis of ASC is controlled would be of importance as these steps control the flux of ASC in the system. The isolation of the homolog of one of these controlling enzymes, VTC2, in a dehydration stress cDNA library from *X. viscosa* provided partial and preliminary evidence of the importance of this pathway. Thus, this study serves to characterise the *XvVTC2* gene in terms of sequence and *in silico* analysis. The expression in response to dehydration stress will be characterised at the mRNA and protein level.

The cellular localisation of the protein will be characterised and the enzyme activity of the recombinant XvVTC2 protein will be measured. The ultimate aim of the study is to propose possible mechanisms by which *XvVTC2* can play a role in the ability of *X. viscosa* to withstand desiccation.

2 Chapter 2: Cloning and Bioinformatics analysis

University of Cape Town

2.1 Introduction

Due to the significant amount of open databases on gene sequences, structure and function, an *in-silico* or bioinformatics analysis can be done once the sequence is known. This creates a platform from where the gene function can be predicted from the sequence (Snustad and Simmons, 2003)..

To identify the genes involved in desiccation tolerance of the resurrection plant *X. viscosa* a cDNA library was constructed by B. Baker in the Plant Stress Laboratory at the University of Cape Town (Pers. comm. 2008). The aim of this study was to identify genes that are upregulated in response to water deficit conditions in *X. viscosa*. One of the genes that was isolated under dehydration stress conditions was the *X. viscosa* *VTC2* homologue and it was named *XvVTC2*. The coding region of the gene was partially sequenced by T. Mokgethi and B. Baker but errors were apparent in the sequencing and the full length copy DNA (cDNA) sequence was not obtained. This chapter deals with the cloning, sequencing and bioinformatics analysis of the *XvVTC2* gene

2.2 Materials and Methods

2.2.1 cDNA and gDNA cloning

From partial sequences provided by B. Baker (Pers comm., 2008), primers were designed to amplify the full length cDNA of the *XvVTC2* gene. The primers were designed using DNAMAN version 5.2.10 (Lynnon Biosoft). The primers were designed in the 5' and 3' untranslated regions (UTRs) of the gene. One forward primer VTC2seqF and two reverse primers VTC2seqR1 and VTC2seqR2 were designed respectively (Appendix 1). The primers were synthesised by the UCT Molecular Cell Biology DNA synthesis unit using a Beckman 1000M DNA synthesizer.

For amplification of the *XvVTC2* gene from cDNA the parameters are outlined in Appendix 2 under standard PCR conditions: The polymerase that was used was Supertherm Taq polymerase (Southern Cross biotechnology). Both reverse primers mentioned above were used respectively with the VTC2seqF primer. The cDNA that was used was kindly provided by Ali Kiyaei (Honours student, Plant Stress Laboratory University of Cape Town 2008) and was synthesized from RNA extracted during a

dehydration timecourse of *X. viscosa*. The DNA was synthesized using the ImPrompII Reverse transcriptase (Promega, USA) using oligo dT₍₁₈₎ and random hexamers at a ratio of 1:10

For amplification of the full length genomic DNA (gDNA) sequence of *XvVTC2* the VTC2seqF and VTC2seqR1 primers were used. The amendments from the standard PCR conditions (Appendix 2) are; Phusion polymerase (Finnzymes) 1 unit, gDNA template 347ng, and an increase in extension time from 2 minutes to 3 minutes. The gDNA used was kindly provided by Kershini Iyer (Research Assistant, Plant Stress Laboratory University of Cape Town 2009)

The amplification products from cDNA and gDNA template were run on 1% and 0.8%, 0.5x TBE agarose gels respectively stained with 10 μ g.ml⁻¹ ethidium bromide. The specific bands on the gels showing the amplified products were excised under long wavelength UV. The respective cDNA and gDNA products were purified using Biobasic EZ-10 gel cleanup spin column kit according to the manufacturer's protocol. The purified DNA was quantified by absorbance at 260nm using a Nanodrop spectrophotometer.

The purified PCR products, from reactions using the respective reverse primers for the cDNA template, were cloned into the Instaclone pTZ57R/T cloning vector (Fermentas). The ligation reactions were done according to the manufacturer's recommendation in the Instaclone cloning kit (Fermentas). The molar ratio of insert to vector used for this reaction was 5: 1. *E. coli* DH5 α competent cells were used for transformation. The transformation protocol is outlined in Appendix 3. Clones containing the gene of interest, for the cDNA ligation reaction, were screened for by colony PCR. The reaction conditions were the same as those outlined as in Appendix 2, except the polymerase used was Taq (New England Biolabs, USA).

For the ligation reactions of the amplified product from the gDNA template, the pJet 1.2/blunt cloning vector (Fermentas) was used. Ligation reactions were set up as per the clonejet® (Fermentas) instruction manual. The insert to vector molar ratio was 3:1 for the purified product. The transformation procedure is outlined in Appendix 3. To screen for clones containing the gDNA insert, a plasmid mini prep was done. Several colonies were

selected from the transformed plates, containing 100 μ g.ml⁻¹ ampicillin, and 5ml overnight LB cultures (100 μ g.ml⁻¹ ampicillin), were inoculated. The method used to extract the plasmid DNA was adapted from the Qiagen plasmid midi kit, with the use of isopropanol to precipitate the DNA, rather than using the spin column. The purified plasmid DNA was screened using the modified standard PCR conditions (Appendix 2) for the gDNA fragment mentioned above. In this case vector specific primers, included in the Clonejet[®] kit, were used to screen for clones containing the gene of interest.

Upon positive screening of the plasmid DNA using PCR, three positive clones were selected and sequenced for both the cDNA and gDNA clones. The plasmid DNA was sent to the UCT DNA sequencing service, from where the samples were relayed to Macrogen Inc. (1001 World Meridian Center 60-24, Gasan-dong Geumchun-gu Seoul Korea 153-021) for sequencing. The primers used for the sequencing reaction of the cDNA fragment were the M13 sequencing primers. For the sequencing of the gDNA clones the T7 forward and pJet reverse primers were used to sequence the 5' and 3' ends respectively. To sequence the internal regions of the gDNA fragment, the VTC2rtR, VTC2splnk2 and VTC2int primers were used (Appendix 1).

2.2.2 Promoter analysis

The splinkerette method was used to find the promoter of the *XvVTC2* gene. The method was adapted and modified from Devon *et al* (1995) and Stover (2001). A flow diagram illustrating the method can be found in Appendix 4. The *XbaI* adapters were prepared as described by Stover (2001). The enzyme used for digestion of 3 μ g genomic DNA was *XbaI* (Roche, USA) as per manufacturers' instructions. Digestion took place for seven hours at 37°C. After digestion the enzyme was heat inactivated at 80°C for 20 minutes. Thereafter the buffer constituents were adapted to represent T4 ligase buffer (New England Biolabs, USA). The adapters and digested gDNA were ligated 4°C overnight. Thereafter the T4 ligase was heat inactivated at 65°C for 10 minutes. The product (1 μ l) was then amplified by PCR using Phusion (Finnzymes) high fidelity polymerase and the external primers VTC2splnk_R1 and splnkA (Appendix 1). The splnkA primer is complimentary to the splintop adapter sequence. A second round of amplification was performed using 1 μ l of the product from the first round amplification and the primers VTC2splnk_R2 and splnkB (Appendix 1). The splnkB primer complementary region is

downstream from the splnkA complimentary region within the splnktop adapter region. The PCR product was run on a 1.5% 1x TAE agarose gel, the fragment of interest excised, purified and cloned into the pJET1.2/blunt cloning vector as described in the CloneJet cloning kit (Fermentas). The ligation product was transformed into *E. coli* DH5 α competent cells and plated on LB plates containing 100 μ g.ml⁻¹ ampicillin. Colonies were selected and grown in overnight culture, the plasmid extracted via the modified Qiagen method described above. A clone was sent for sequencing using the same facilities described above.

2.2.3 Bioinformatics

The DNA sequence obtained was translated to protein sequence using DNAMAN version 5.2.10 (Lynnon Biosoft). A PSI-BLAST analysis was run to find similar proteins in a variety of organisms (Altschul et al., 1997). Several sequences were downloaded and the evolutionary distances mapped on a phylogenetic tree. The tree was assembled using DNAMAN version 5.2.10 (Lynnon Biosoft) and the maximum likelihood option with 5000 bootstrap trials and the Jones, Taylor & Thornton model. A multiple sequence alignment of several plant homologs of XvVTC2 was also performed.

Phosphorylation sites in the protein were predicted using NetPhos 2.0 server (Blom et al., 1999). N-Myristoylation sites were predicted using Prosite which is available on the Expasy proteomics server (Sigrist et al., 2002; de Castro et al., 2006; Hulo et al., 2007). The C-terminus nucleotide binding region was predicted using the PFP tool (Hawkins et al., 2006). Nuclear localization signals were predicted by using PSORT (Muller-Moule', 2008).

2.3 Results and Discussion

2.3.1 cDNA and gDNA cloning

The protein coding region of the *XvVTC2* gene is 1278bp in length. When compared to that of *A. thaliana*, there is a 102bp difference which is 1380bp in length. The DNA coding sequence of rice (*Oryza sativa*) *VTC2* homolog is shorter than the *A. thaliana* homolog, but still longer than the *X. viscosa* homolog. The length of the coding region can not be used as an indication of whether the protein is functionally different and might

just be a function of evolution. The bioinformatics in the second part of this chapter will provide an indication of whether the functional regions of the protein are different.

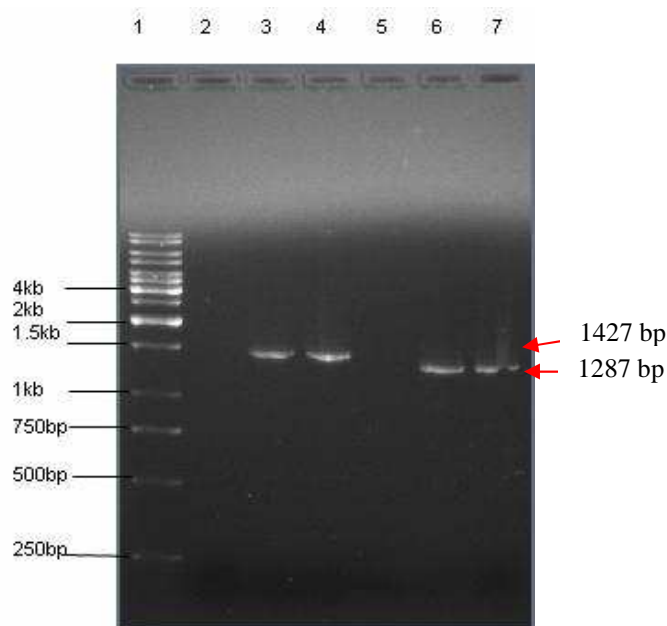


Figure 2.1: Ethidium bromide stained 1% w/v agarose gel showing *XvVTC2* amplified PCR products from *X. viscosa* cDNA. Lane 1, Fermentas 1kb ladder, Lane 2, no template control using the VTC2seqF and VTC2seqR1 primers. Lanes 3 and 4 are PCR products obtained using the VTC2seqF and VTC2seqR1 primers and cDNA as a template. Lane 5, no template control using the VTC2seqF and VTC2seqR2 primers. Lanes 6 and 7 are PCR products obtained using the VTC2seqF and VTC2seqR2 primers and cDNA as a template.

The two different reverse primers used showed slight differences in the size of the fragment amplified (Figure 2.1). This was expected as the first reverse primer, VTC2seqR1, was designed further downstream of the second reverse primer, VTC2seqR2. The product sizes were 1427bp and 1287bp using VTC2seqR1 and VTC2seqR2 respectively. The slightly longer 3' untranslated region (UTR) obtained when using the VTC2seqR1 primer allowed for more accurate sequencing of 3' end of the coding region of the gene (Appendix 5). The PCR conditions were optimal as no non-specific amplification is observed from cDNA using either of the reverse primers.

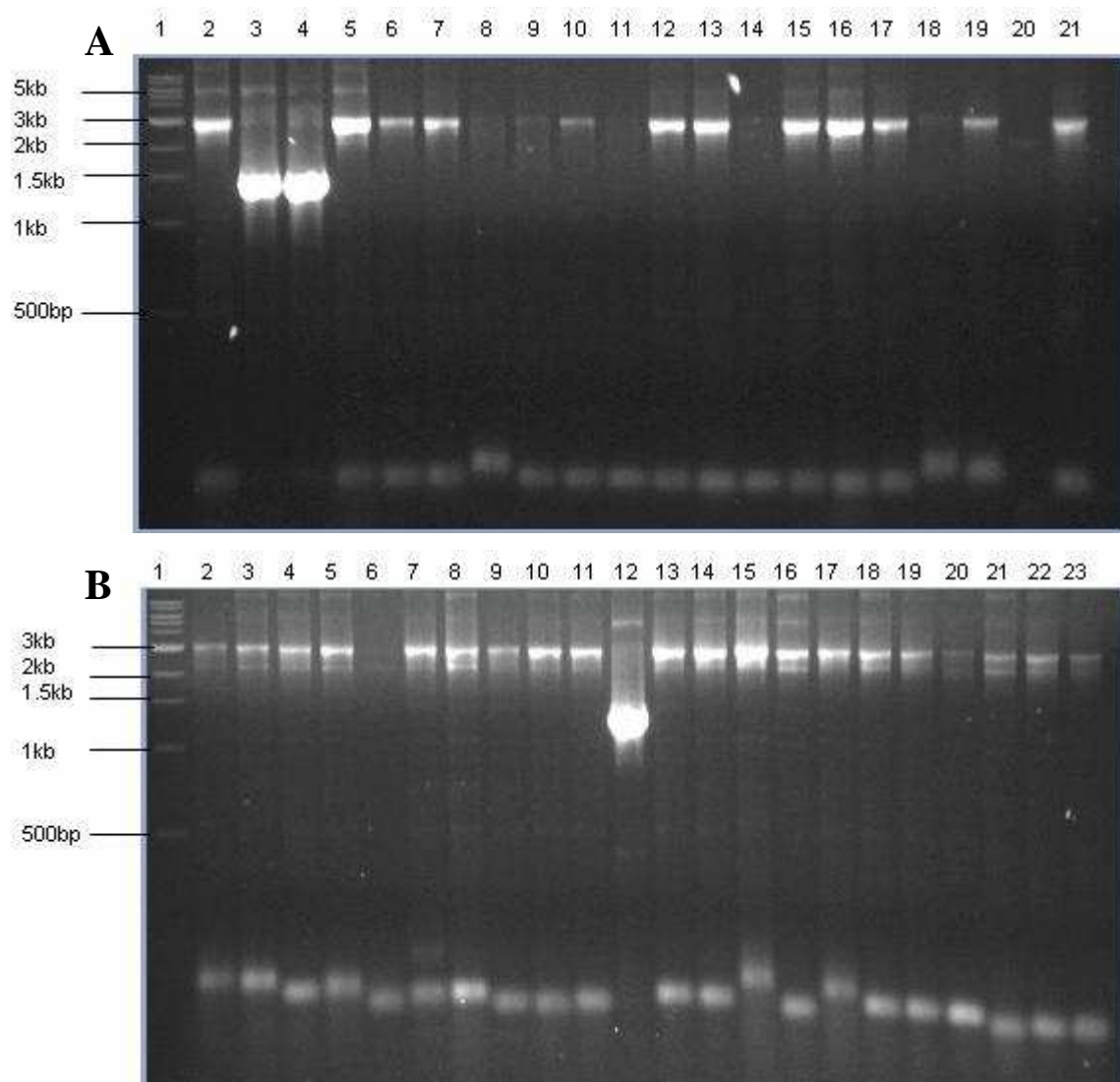


Figure 2.2: Ethidium bromide stained 1% w/v agarose gel showing amplified colony PCR products. The *E. coli* DH5 α cells contained Instaclone vector after it was ligated to *XvVTC2* cDNA PCR product. In A - Lane 1, New England Biolabs 1kb ladder, Lanes 2, 5- 21, products from colony PCR, where the *XvVTC2* gene was not detected. Lanes 3 and 4, positive clones where *XvVTC2* was detected using the primers VTC2seqF and VTC2seqR1. In B – Lane 1, New England Biolabs 1kb ladder, Lanes 2 - 11 and 13 - 23, products from colony PCR, where the *XvVTC2* gene was not detected. Lane 12, a positive clone where *XvVTC2* was detected using the primers VTC2seqF and VTC2seqR2. The clones where the *XvVTC2* fragment was detected were sequenced.

Cloning of the amplified product from cDNA into the Instaclone pTZ57R/T vector proved problematic. Only three colonies from the 42 tested proving positive for containing the *XvVTC2* cDNA fragment (Figure 2.2), representing a cloning efficiency of 7.1%. The three positive clones were sequenced which, after alignment and extraction of the consensus sequence, reduces the possibility of obtaining a sequence containing errors.

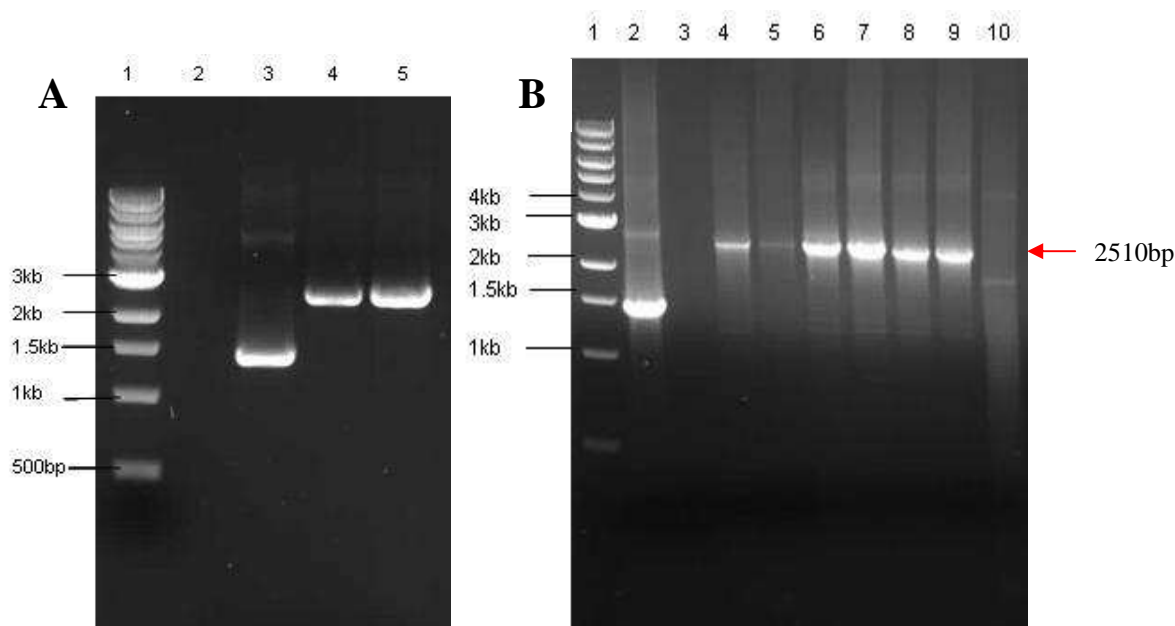


Figure 2.3: Ethidium bromide stained 1% w/v agarose gels showing *XvVTC2* amplified PCR products from genomic DNA (A) and clones containing the genomic DNA fragment (B). In A, lane 1, New England Biolabs 1kb ladder, Lane 2, no template control, lane 3, positive control of a cDNA clone. Lanes 4 and 5, PCR products obtained from genomic DNA (2510bp). In B, lane 1, New England Biolabs 1kb ladder, Lane 2, positive control of cDNA clone, lane 3, no template control. Lanes 4 – 10, PCR products obtained from plasmids isolated from various colonies that grew under positive selection on LB ampicillin ($100\mu\text{g}.\text{ml}^{-1}$) plates. The products in lanes 4 – 9 are of the expected size for the *XvVTC2* genomic fragment. The primers used for all the reactions were VTC2seqF and VTC2seqR1.

The gDNA fragment of *XvVTC2* is 2510 bp in length, compared to the cDNA fragment which is 1427 bp (Figure 2.3). Because genomic DNA region contains non-coding regions (introns) as well as the coding regions (exons) (Snustad and Simmons, 2003) the size difference is indicative of large portions of non-coding regions in the gene. The absence of non-specific amplified fragments from the PCR shows that the reaction conditions were optimal (Figure 2.3).

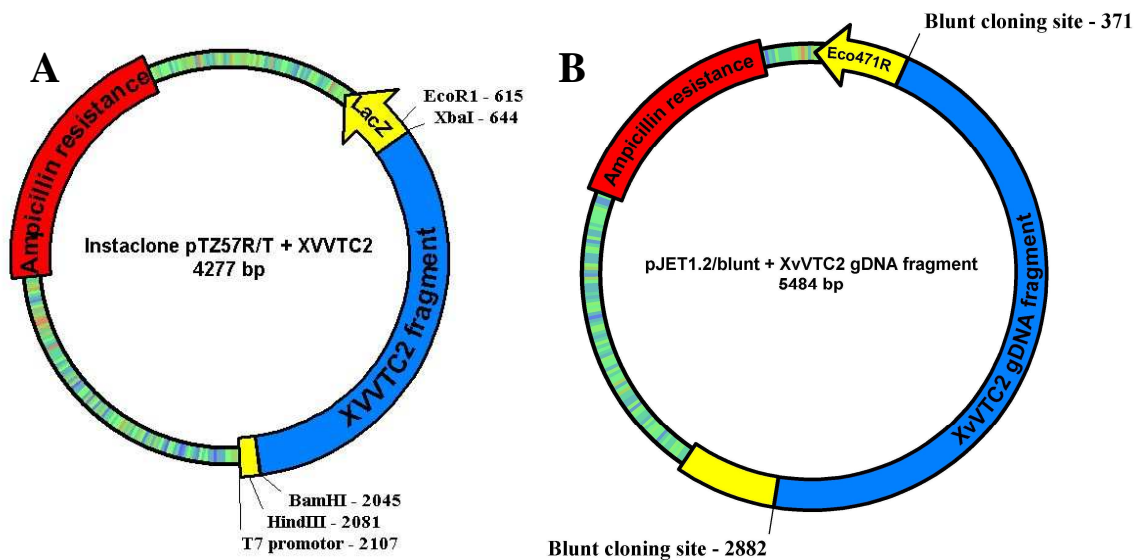


Figure 2.4: Recombinant plasmid maps of the cloning vectors pTZ57R/T and pJET1.2/blunt (Fermentas) containing the *XvVTC2* cDNA and gDNA fragments (blue) respectively. In A, the T7 promotor (2107) which drives the expression of the *LacZ* gene (yellow) is used for visual blue and white colony selection when cultured on plates containing X-Gal and IPTG. The restriction sites *HindIII* (2081) and *BamHI* (2045) indicate the first and last restriction sites in the downstream multiple cloning site from the *XvVTC2* fragment. The restriction sites *XbaI* (644) and *EcoRI* (615) indicate the first and last restriction sites in the upstream multiple cloning site from the *XvVTC2* fragment. In B, the *Eco471R* gene (yellow) is used for positive screening. The *XvVTC2* gene is inserted in the *Eco471R* gene, which allows colonies containing the plasmid to survive. The restriction blunt cloning sites are indicated on each side of the *XvVTC2* fragment. The ampicillin resistance gene, used for antibiotic selection, is indicated in red for both vectors.

2.3.2 Promoter analysis

A 448bp fragment upstream from the start codon was isolated and sequenced (Figure 2.5). This fragment is expected to contain approximately half of the regulatory region, as plant promoters are approximately a thousand base pairs in length (Chrispeels and Sadava, 2003). The fragment contained a TATA box 50bp upstream from the start codon. The upstream region was characterised using the PlantCare database (Lescot et al., 2002). As expected several light regulating elements were found (data not shown). Other elements included several stress response elements, including water deficit and salt stress. ABA and JA response elements were also found. However the regulatory elements found in this region are all very short and high have a high probability of arising by chance. Thus further characterisation of the upstream region is in progress and functional characterisation of the promoter is planned. The sequence and other precise elements found are not presented, due to intellectual property protection (Promoter will be used for commercial purposes).

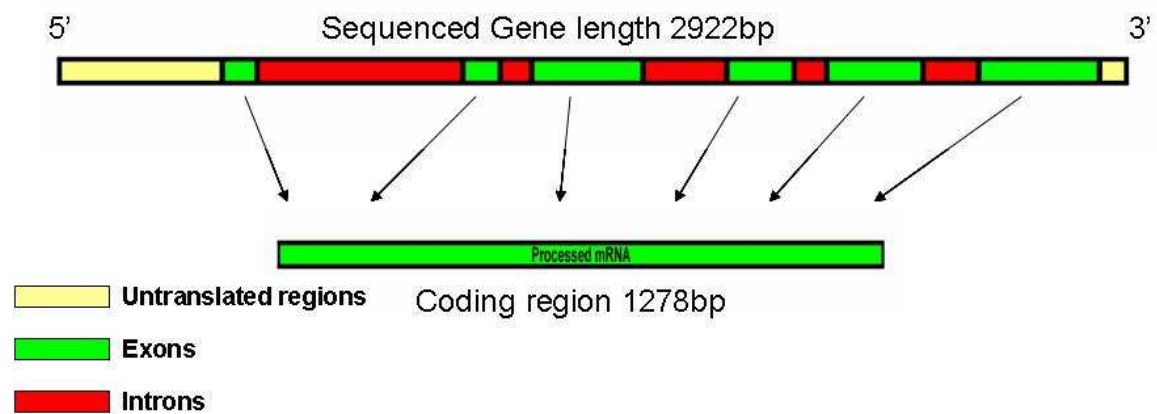


Figure 2.5: The structure of the *XvVTC2* gene showing the sequenced gene, including the untranslated regions, exons and introns. The 5' untranslated region (yellow) represented is a 448bp upstream region isolated using the splinkerette method of chromosome walking. The full length genomic sequence contains six exons (green) and five introns (red). The exons are spliced to produce a 1278bp mRNA which codes for the *XvVTC2* (GDP-L-galactose phosphorylase) protein. The sequence of the 3' untranslated region (yellow) was obtained when the gene was isolated using a poly-T primer during cDNA library construction.

2.3.3 Bioinformatics analysis

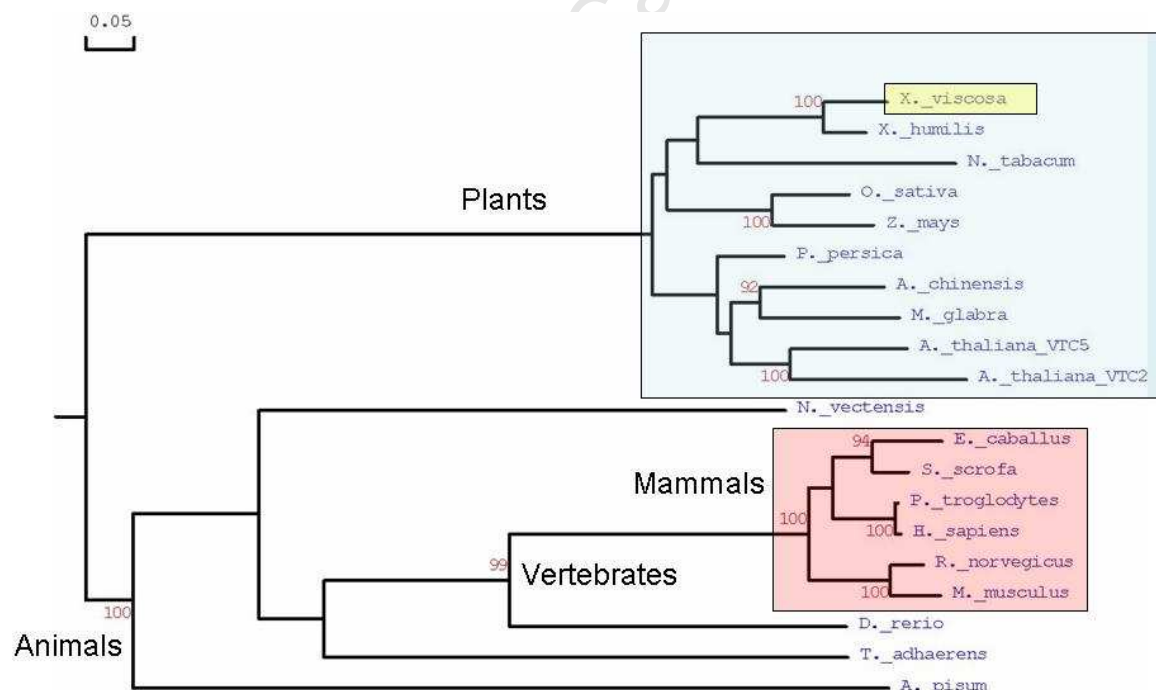


Figure 2.6: A phylogenetic tree showing the evolutionary relationship between homologs of VTC2 related proteins from various organisms. The tree was constructed using maximum likelihood with 5000 bootstrap trials using the Jones, Taylor & Thornton model. At the first level the tree shows the splitting of plants and animals. In the plants *X. viscosa* is indicated in yellow. On the animal side, the tree follows the expected evolutionary trend, with the mammals (red) showing the most recent divergence.

The phylogenetic analysis showed the divergence of the proteins most related to XvVTC2 from various organisms (Figure 2.6). The closest homolog to XvVTC2 is a VTC2 homolog isolated from *Xerophyta humilis*. Interestingly this homolog was also obtained from a cDNA library of a plant subjected to desiccation stress. As expected the homologs from plants are the most closely related and those in animals more distant. In general, the monocotyledons and dicotyledons analysed to date form two different clades. However, tobacco (*Nicotiana tabacum*) a dicotyledon is grouped with the monocotyledons (*Z. mays*, *O. sativa*, *X. humilis* and *X. viscosa*). The reason for this grouping is unknown and at this stage it would be speculation to clarify the matter. It could possibly be an indication that the protein is overall and functionally highly conserved in plants, as long as the functional domains are conserved, the other sites are not very large and have little selection pressure. Thus it would be possible for mutations to revert. Another possibility could be convergent evolution, where a similar characteristic (mutation) might occur via separate routes.

In *A. thaliana*, the closest homolog to VTC2 is VTC5 and this is an indication of a recent duplication event rather than a protein arising with a similar structure but a different function. Among the other homologs, the expected animals show close relationship e.g. the horse (*Equus caballus*) and pig (*Sus scrofa*), the chimpanzee (*Pan troglodytes*) and humans (*Homo sapiens*) and the rat (*Rattus norvegicus*) and mouse (*Mus musculus*).

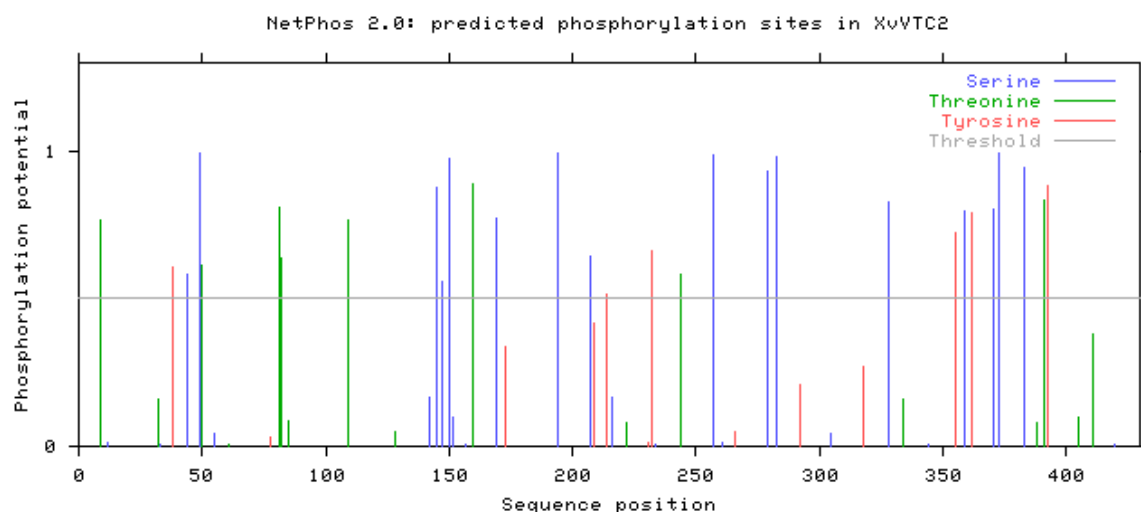


Figure 2.7: Prediction of phosphorylation sites of the XvVTC2 protein by the Netphos 2.0 server (Blom et al., 1999). The threshold for predicted phosphorylation potential is at 0.5 and only where values are higher than the threshold, phosphorylation is predicted to happen. The vertical lines indicate serine (blue), threonine (green) and tyrosine (red) residues in their sequence position (x-axis) and the predicted phosphorylation potential of the residue (y-axis).

The phosphorylation of proteins is important in controlling protein activity. This has implications in cellular signalling and may influence the manner in which a protein interacts with a substrate (Blom et al., 1999). The program (Netphos 2.0) used to predict the phosphorylation sites in XvVTC2 has a reported sensitivity of 69 – 96% (Blom et al., 1999). Thus the predicted phosphorylation sites that have a phosphorylation potential close to 1 have a very high probability of being actual phosphorylation sites on the XvVTC2 protein (Figure 2.7). How the phosphorylation of the protein at these sites influence the function of the protein is a matter for future study. For such a study *X. viscosa* mutants containing mutations in these phosphorylation sites will have to be created and the effect be studied *in vivo*.

The number of phosphorylation sites predicted above the threshold in XvVTC2 is 30, in the rice VTC2 homolog there are 26 and in the *A. thaliana* homolog there are 17. Whether the difference in the number of predicted phosphorylation sites holds any significance is questionable. It is however interesting to note that the regions and order in which phosphorylation sites occur across the different VTC2 homologs show a trend (Appendix 9). This suggests that site specific phosphorylation activity is conserved in certain regions of the protein. The difference in the number of phosphorylation sites at a given region might suggest that these proteins are regulated within the plants in their niche environment by different intra- or extracellular signals. The relative abundance of phosphorylation sites in a given region might through evolution have been selected as a redundancy measure to ensure phosphorylation takes place in a given region. This might increase the stability of the protein under the niche of the given plant.

X. viscosa	...MKTIRVPTIVSNFMD...GCGRNCLGGCCLP... ..	32
N. tabacum	...MKTIRVPTIVSNYQEDVPESNNV...VGCGRNCLGGCCLPV... ..	39
O. sativa	MEMKTIIRVPTIVSNYQEDAAATAGERPRAGCGRDCIGDCCLPD... ..	45
A. thaliana	...MKTIRVPTIVSNYQKD...DGAEDPVGCGRNCLGACCLNGTFWKPESSFL	48
A. chinensis	...MKTIRVPTIVSNFQKDEAE.DGARSGGCGRNCLQKCCIQG... ..	41
Consensus	l i rvpt vsn d gogr cl cc	
X. viscosa	SKLPLYAKPDSPGPAS..TGDLPD...FHTHTILGKWEEDRMKGLFRYDVT	81
N. tabacum	SRPLPLYAKNDNDNEPIENNIDTLPGEDCQISFINDLILGLWEERMSQGLFRYDVT	94
O. sativa	SKLPLYAKASPKKPSS..QEDASND...EFVNITLGLWEEDRMARGLFRYDVT	94
A. thaliana	IMPLPLYACRNLVKS.GEKLVISHEAIEPPVAFLESLVLGEWEEDRFORGLFRYDVT	102
A. chinensis	AKLPLYAKRVKEVVGKGLLAVDDEEAPVAFLDSTILGEWEEDRVORGLFRYDVT	96
Consensus	lplya k f l lg we r glfrydvt	
X. viscosa	TCETKVIPIGKHGFIAQLNEGRHLKKRPTEFRVDRVLQCFDPDKFNFTKVGQEEVI	136
N. tabacum	TCETKVIPIGRYGFIAQLNEGRHLKKRPTEFRIDCVLQCFDENKFNFTKVGQDEVI	149
O. sativa	ACETKVIPIGNIGFVAQLNEGRHLKKRPTEFRVDRVLQCFDAAKFNFTKVGQEEVI	149
A. thaliana	ACETKVIPIGKYGFVAQLNEGRHLKKRPTEFRVDRVLQSFDSKFNFTKVGQEEVI	157
A. chinensis	ACETKVIPIGEYGFIAQLNEGRHLKKRPTEFRVDRVLQCFDES KFNFTKVGQEEVI	151
Consensus	c tkvipg gf aqlnegrhlkkrpTEfr d vlq fd kfnftkvqg e l	
X. viscosa	FRFEPSTDKSNFSESAPIDSND.TPNVVAINVS.....PIEYGHVLLIPRVF	183
N. tabacum	FRFEPSTDYKARYFSGVGVVGI.SPSIVAINVS.....PIEYGHVLLIPRVL	196
O. sativa	FCFENGDDSFVVESSPISVADRAPNVVAINVS.....PIEYGHVLLIPRVL	197
A. thaliana	FCFEGEDAQVQFFPCMPIDPEN.SPSVAINVKTIVQACPIEYGHVLLIPRVL	211
A. chinensis	FCFEASDDNEVQFFPNAPVDVEN.SPSVAINVS.....PIEYGHVLLIPRII	198
Consensus	f fe p vainv pieyghvllipr	
X. viscosa	DCIPQRIDRMSFEIAVRMAEAGSPYFRIGYNSLGAFATINHLHFQAYYISVPFF	238
N. tabacum	DYLPQRIDRDSFTVALHEAREIADPFVRGYNSLGAFATINHLHFQAYYISVPFF	251
O. sativa	DRIPQRIDQESFLLIALHVAEBAASPYFRIGYNSLGAFATINHLHFQAYYITVPFF	252
A. thaliana	DCIPQRIDHKSLLIAVHVAEBAANPYFRIGYNSLGAFATINHLHFQAYYIAMPFF	266
A. chinensis	ECIPQRIDRESFLLIALHVAEAGNYPYFRIGYNSLGAFATINHLHFQAYYIAPFF	253
Consensus	pqrld s a a e p fr gynslgafatinhlhfqayyl pfp	
X. viscosa	VEKETTRIMVARRQDENSEVSHLLDYPVRGLVFEGQRPS..RGLSDVADACI	291
N. tabacum	VEKAPMRIRMRGKGLGDAGVIVSKLLNYPVRGFSFEGGNGSTVRDLSDAVNSCI	306
O. sativa	VEKAATKRIFLAEGTMNSVKVSKIMNYPVRGLVFEGGNSLS..DIANVSSACI	305
A. thaliana	IEKAPTAKITTTVS....GVKISELLSYPVRSILFEGGSSMQ..ELSDTVSDCCV	315
A. chinensis	IEKAPTAKITTLNG....GVKISDILNYPVRGLVFEGGNSLE..LISNAVSDSSI	302
Consensus	ek i v s l ypvr feg l v	
X. viscosa	YLQENNIENVLISDILGRIFLPQCYAEKQALGVSRRELLDTQVNPVAVWEISGH	346
N. tabacum	SLQNNNIENVLIAQCGKKIFLPQCYAEKQALGVVDQELLDTQVNPVAVWEISGH	361
O. sativa	WLQDNNVFNVLISDCGKKIFLPQCYAEKQALGEVSDRELLDTQVNPVAVWEISGH	360
A. thaliana	CLQNNNIENVLISDCGRQIFLPMQCYAEKQALGEVSPVILETQVNPVAVWEISGH	370
A. chinensis	CLQNNNIENVLISDSKCIIFLPQCYAEKQALGEVSSDILLDTQVNPVAVWEISGH	357
Consensus	lq n p n li g ifl pqcyaeqalg v l tqvnpavweisgh	
X. viscosa	MVLKRRKDYEEASEEYAWRLAEVSLSEERFEVVKASIFEATGLITEY.....	393
N. tabacum	MVLKRRKDYNDASEEYAWRLAEVSLSEERFEVVKGYISEADLQEA.....	408
O. sativa	IVLKRRSDYEEASEASAWRLAEVSLSEERFEVVKAYIFDAAGLVQS.....	407
A. thaliana	MVLKRRKDYEGASEDNARLLAEASLSEERFEVVTALAFAEAGCSNQ.....EED	420
A. chinensis	MVLKRRKDYEEASEGNARLLAEVSLSEERFEVVKALIFEAISCADDRSGSTAEN	412
Consensus	vlkr dy ase aw ll e slseerf ev a	
X. viscosaEDGGVEREEETALQPLTP...MAVHFPESCLVL	424
N. tabacumEDKSINPELDPEKEIPDSPGPGQVASHMPQDCVLV	442
O. sativaDEEEVSEDEDAT....YTPVSIAPPVAEGCLVL	437
A. thaliana	LEGTIVHQONSSGNVNQKSNR..THGGPITNGTAAECVLV	458
A. chinensis	LLEPDDNPQSRKVANDALNKGSHRGMVPG..KQECVLV	449
Consensus	clv	

Figure 2.8: An alignment of amino acid sequences of five VTC2 homologs from various plants. Dark blue shading indicates complete conservation of amino acid, pink shading indicates near complete conservation of an amino acid and light blue shading indicates the conservation of amino acid with similar properties across all five plants respectively. The HIT-motif is indicated by the red line and N-myristoylation sites by the green lines. The conserved regions indicated by the orange lines is proposed to be part of a nucleotide binding region and the residues indicated by the pink lines represent nuclear localisation signals. The accession numbers are; *N. tabacum* (ACD92981.1), *O. sativa* (NP_001066338.1), *A. thaliana* (AAM34266.1|AF508793_1), and *A. chinensis* (ABP65665.1).

N-myristoylation is an important mechanism involved in controlling protein activity. The process is specific to the N-terminal glycine of proteins and can change the conformation of proteins (Boutin, 1997). In XvVTC2 a number of N-myristoylation sites were predicted by Prosite. The recognition sequences for N-myristoylation sites are short and the probability of the sites arising by chance and potentially having no effect is great. However, two of the sites predicted in XvVTC2 are of interest as they are conserved across all the plants used in the alignment (Figure 2.8 – green lines). The first of these sites is situated towards the N-terminus of the protein. Thus if the residues before the site are cleaved by post-translation modification then this site could be a target for N-terminal myristoylation. The other site is situated next to the Hit-motif active site and is probably conserved because of its proximity to the active site for structural purposes and not necessarily myristoylation.

The Hit-motif was identified by aligning XvVTC2 with VTC2 homologs from other plants (Figure 2.8 – red line). The characteristic sequence, HLHFQ, is conserved across all the homologs aligned. This result concurs with those obtained by Linster *et al* (2007) and Laing *et al* (2007) in their characterisation of *A. thaliana* and *A. chinensis* VTC2 homologs respectively.

Two nucleotide binding regions have been identified (Figure 2.8 – orange lines). Both of these regions are highly conserved across all the homologs aligned. Nucleotide binding regions are expected to occur in the protein as the protein uses a nucleotide sugar (GDP-L-galactose) as a substrate (Linster *et al.*, 2007). The first region was identified by aligning a proposed nucleotide binding region from an ADP-glucose phosphorylase from *A. thaliana* (McCoy *et al.*, 2006). This phosphorylase also contains a Hit-motif. The nucleotide binding recognition sequence used aligned to the XvVTC2 total protein sequence. A significant similarity was detected with the region indicated by the first orange line (Figure 2.8). This similarity along with the high level of conservation makes it worth noting as a possible nucleotide binding region.

The second nucleotide binding region was predicted using the protein function predictor tool (PFP) (Hawkins *et al.*, 2006). The high probability obtained in the prediction along with the high level of conservation of this section of the protein sequence indicates that

this region might also be involved in nucleotide binding. The structure of the protein at these sites will have to be determined by X-ray crystallography and only then can the nucleotide binding sites be verified.

Two nuclear localisation signals were identified by PSORT (Figure 2.8 – under pink lines). The first of these signals was identified by Muller-Moulé (2008) in *A. thaliana*. Here a second signal is identified in XvVTC2 and is also found in the *N. tabacum* homolog but not any of the other VTC2 homologs used in the alignment. This is probably of little significance as the nuclear localisation recognition sequence is short and has a high probability of arising by chance. The localisation of XvVTC2 is discussed in Chapter 4.

2.4 Conclusions

This chapter dealt with the isolation, cloning and sequence analysis of XvVTC2. The XvVTC2 sequence has shown to be very similar to those of other VTC2 homologs, both in length and structural motifs. The promoter sequence contained environmental stress, light and hormone regulated elements. However the promoter sequence obtained was not complete and the regulatory recognition sequences are very short. An anomaly was observed in sequence similarity where the dicotyledenous, *N. tabacum*, sequence showed a closer degree of similarity to XvVTC2 than that of other monocotyledons. Several bioinformatically determined phosphorylation, N-myristoylation, nucleotide binding and nuclear localisation sites were identified. The function of these sites in the protein still needs to be determined experimentally. The nuclear localisation of VTC2 has been shown (Muller-Moulé, 2008), but the definite role of the nuclear localisation signal need to be determined experimentally.

The results from this chapter provided the platform for further experiments and questions that have arisen from this include; the size, activity and localisation of the protein as well as the expression of the gene and protein product in response to desiccation.

3 Chapter 3: Protein expression

University of Cape Town

3.1 Introduction

In order to study the function and properties of a protein it is important to obtain a relatively large volume of purified protein. This is achieved by cloning the gene coding for the protein of interest into an expression vector containing an inducible promoter and overexpressing the recombinant protein in a suitable host cell. The use of bacteria such as *Escherichia coli* as protein expression hosts is well established (Snustad and Simmons, 2003).

The expression of a recombinant protein in *E. coli* is often problematic and requires optimisation at various stages. The factors to keep in mind are protein solubility, size of the protein, protein toxicity, type of growth media, culture aeration, culture temperature, culture volume and the use of rare codons to name but a few and the factors have been extensively reviewed (Baneyx, 1999; Dyson et al., 2004; EMD Biosciences, 2005).

This chapter deals with the expression of the XvVTC2 protein in *E. coli* BL21(DE3) cells using pET32b (Novagen) as an expression vector. The pET32b vector allows for the expression of a recombinant protein that contains a thioredoxin (Trx) tag and His-tags at the N-terminus and C-terminus respectively. The vector uses the T7-lac promoter which, when used in conjunction with an expression host containing a chromosomally integrated T7 RNA polymerase gene (λ DE3 lysogen) under the control of the lacUV5 promoter allows for the induction of expression by IPTG (Dyson et al., 2004). The *E. coli* BL21(DE3) is such a strain and is the most widely used host strain for target gene expression, and allows for stable expression of most target proteins (EMD Biosciences, 2005). The Trx tag increases the solubility, as the tag itself is highly soluble, and the His-tags can be used for detection and purification of the recombinant protein (Dyson et al., 2004; EMD Biosciences, 2005). The protein expression aspect of the project required extensive optimisation in order to determine the correct conditions for the expression and purification of the XvVTC2 recombinant protein. The conditions that proved successful will only be mentioned and discussed.

3.2 Materials and methods

3.2.1 Primer design and cloning

The full length *XvVTC2* DNA sequence was analysed using DNAMAN version 5.2.10 (Lynnon Biosoft) and the largest open reading frame (ORF) was identified. The restriction sites used for cloning were *Bam*HI and *Sac*I and were included in the forward and reverse primers respectively and were designed for the correct pET32b reading frame. The primers used were vtc2expF and vtc2expR respectively (Appendix 1). The stop codon was not included on the reverse primer in order for the gene to read through and allow for the C-terminus Histidine tag to be added to the protein.

The designed primers were used to amplify *XvVTC2* from cDNA, the protocol is outlined in Appendix 2. The PCR product was gel purified using the Wizard Gel Purification kit (Promega). The pET32b vector and purified PCR product were double digested respectively using *Bam*HI and *Sac*I (New England Biolabs, USA) restriction enzymes. The reaction conditions used are standard conditions as prescribed by the manufacturer using 9µg vector and 243ng PCR product in the respective reactions. The vector was de-phosphorylated by adding Fast-AP alkaline phosphatase (Fermentas) as per the manufacturer's instructions. The digested PCR fragment was purified using the EZ-10 spin column PCR cleanup kit (Bio-Basic). The digested pET32b vector was purified using the Wizard Gel Purification kit (Promega).

The PCR product and vector were ligated using T4 DNA ligase (New England Biolabs), with molar ratio of 5:1 for insert to vector, and incubation time of 4 hours at 4°C. The ligation products were transformed into *E. coli* DH5α competent cells. The transformed cells were plated on LB plates containing 100µg.ml⁻¹ ampicillin. Positive clones were screened for by colony PCR using the protein expression primers and the method outlined in Appendix 2. Selected clones were grown in overnight LB cultures containing 100µg.ml⁻¹ ampicillin and the plasmid DNA subsequently extracted via the modified Qiagen method described in Chapter 2. The plasmid DNA was digested with *Bam*HI and *Sac*I enzymes, as described above, to check whether the fragment was released. The frame of the gene of interest in the vector was confirmed by sequencing using the same facilities as described in Chapter 2.

3.2.2 Recombinant protein expression

The plasmid containing the *XvVTC2* fragment was transformed into *E. coli* BL21 (DE3) and *E. coli* BL21 Rosetta gami (DE3) pLysS cells (Novagen). The same transformation procedure was used as was described in Chapter 2, except that 2µg of vector DNA was used in the transformation. The plates used to culture the Rosetta gami (DE3) pLysS cells also contained 34µg.ml⁻¹ chloramphenicol. Positive clones were selected using colony PCR using the protein expression primers and the method outlined in Appendix 2.

The culture medium for recombinant protein expression was Overnight express Instant TB medium (Novagen). The media was prepared as per the manufacturer's instructions, using a microwave to dissolve the media, and divided into six 20 ml culture volumes in 100 ml Erlenmeyer culture flasks. Three PCR positive colonies were selected from transformed *E. coli* BL21 (DE3) and *E. coli* BL21 Rosetta gami (DE3) pLysS plates and used to inoculate the six respective culture flasks. The cultures were grown whilst shaking at 30°C for 26 hours. The cells were harvested by centrifugation at 4°C.

The same lysis buffer as described by (Linster et al., 2007; Linster et al., 2008) was used for resuspension of the cells. The cells were lysed by sonication using the Virsonic sonicator. The sonication was done for 10 minutes with 30 second bursts on power setting 3. The samples were centrifuged at 10 000 rpm for 5 minutes at 4°C using a Beckman Ja20 rotor (Beckman Coulter, USA). The cleared lysate was removed and stored at -20°C.

The recombinant protein was purified using the Sigma His-select nickel affinity gel as per the manufacturer's instructions. After purification the buffer was exchanged to 10mM HEPES pH 7.5, 100mM NaCl, 1mM DTT using a 35kDA Amicon Ultra Centrifugal Filter Unit (Millipore, Ireland) (Linster et al., 2007). Glycerol was added and the purified protein was stored in at -80°C until further analysis. All other fractions collected during purification were also stored.

To visualise the purified recombinant protein, the protein samples were run on SDS-polyacrylamide gels. The resolving gels were 12% polyacrylamide (19:1 acrylamide: bis-acrylamide) and the stacking gels were 5% polyacrylamide (19:1 acrylamide: bis-acrylamide) and were prepared as per the layout in Appendix 6. The gels were run at 30mA for two hours. Each well was loaded with 20µl of the samples respectively, which

for the first elution of the XvVTC2 His-purified protein was 18.75µg total protein loaded. The gels were stained for one hour using the Crystalgen DyeHard Coomassie brilliant blue stain (Crystalgen Inc., USA) and were de-stained with water.

A His-tag specific western blot was performed to confirm that the protein expressed was a recombinant XvVTC2 protein. The transfer and alkaline phosphatase chromagenic detection methods that were used were adapted from the QIAexpress Ni-NTA Fast Start Handbook and the QIAexpress Detection and assay Handbook. The tank blotting transfer was performed using a Bio-Rad western blot transfer apparatus. The tank was placed in an ice box and the transfer was at 300mA for 2 hours. The membrane used was the Whatman Protran Nitrocellulose transfer membrane with a pore size of 0.2µm (Whatman, UK). A prestained protein ladder, Fermentas spectra ladder (Sm1841), was run on the gel thus transfer could be confirmed by the ladder on the membrane.

The primary antibody used was a Rabbit Anti-His antibody that was diluted to 1: 2000 in blocking buffer. The secondary antibody was an anti-rabbit alkaline phosphatase conjugate antibody which was diluted 1: 5000 in blocking buffer. The membrane was stained in the dark using the NBT/ BCIP (Roche, USA) solution. The solution was prepared at half the strength of the manufacturer's recommendation.

3.3 Results and Discussion

3.3.1 Primer design and cloning

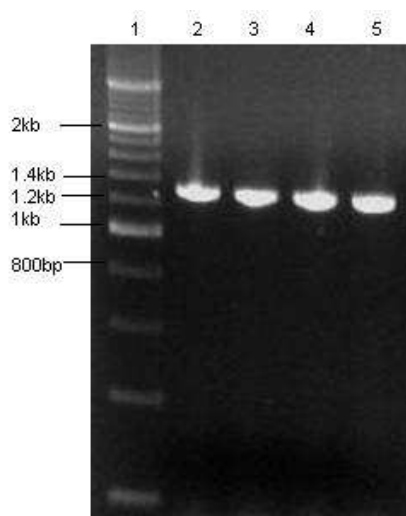


Figure 3.1: Ethidium bromide stained 1% w/v agarose gel showing *XvVTC2* amplified PCR products from cDNA (cDNA kindly provided by Ali Kiyaei (Honours student, Plant Stress Laboratory University of Cape Town)). Lane 1, Fermentas 200 bp ladder. Lanes 2 – 5, PCR products obtained using the VTC2expF and VTC2expR primers.

The *XvVTC2* fragment amplified from cDNA using the protein expression primers, VTC2expF and VTC2expR; corresponded to the expected size (1278bp), as obtained from sequencing (Figure 3.1). Initially the *XvVTC2* fragment was cloned into pET22b and pET41b expression vectors. However stable recombinant protein expression could not be obtained using these vectors (data not shown). The pET32b vector was therefore chosen as it contained a thioredoxin (Trx) tag which has been shown to enhance the expression of large insoluble proteins (Dyson et al., 2004).

After cloning into pET32b, the identity and frame of the fragment was confirmed by sequencing. This ensured that the protein was expressed in the correct frame with the tags attached. As further validation that the *XvVTC2* ORF was in the correct frame in pET32b, the plasmid was digested using *Bam*HI and *Sac*I restriction enzymes (New England Biolabs, USA). This showed that the fragment was released and thus the restriction sites reconstituted correctly on ligation (data not shown). The plasmid map of pET32b containing *XvVTC2* is shown in Figure 3.2

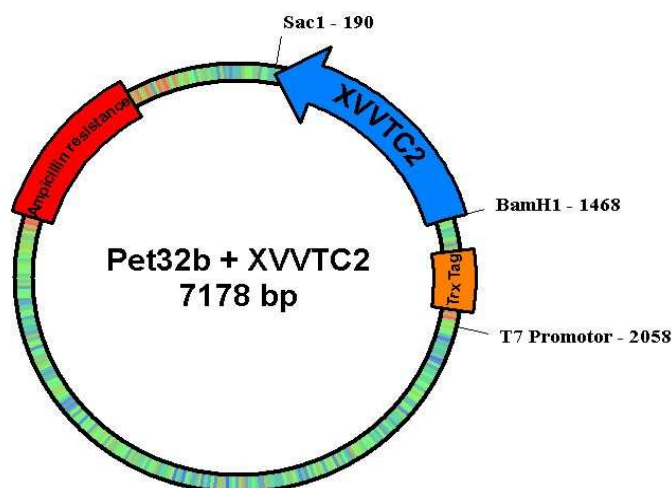


Figure 3.2: Recombinant plasmid map of the expression vector pET32b (Novagen) containing the *XvVTC2* gene. The map shows the T7 promoter which controls the expression of the recombinant protein and is IPTG inducible. The Trx-tag is shown in orange and gives the expressed recombinant *XvVTC2*+Pet32b protein increased solubility. The restriction sites *BamHI* (1468) and *SacI* (190) are indicated as they were used to clone the *XvVTC2* (blue) gene into the pET32b vector. The ampicillin resistance gene, used for antibiotic selection, is indicated in red.

3.3.2 Recombinant protein expression

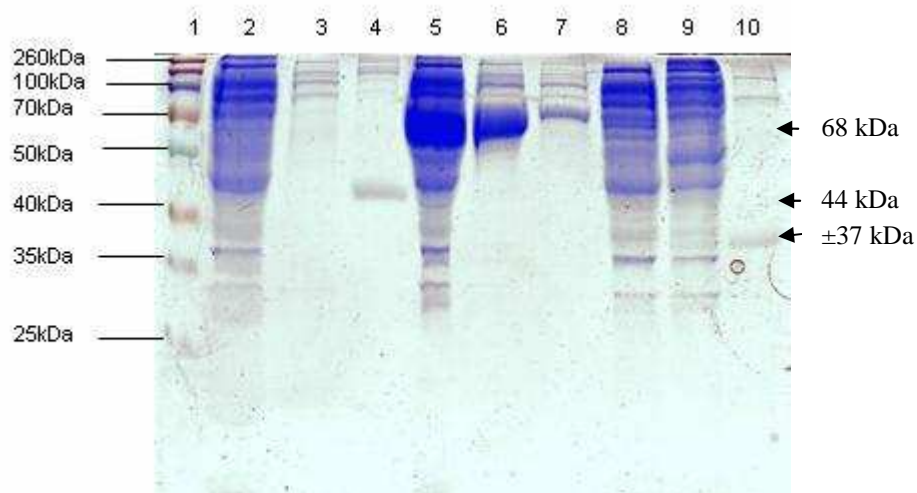


Figure 3.3: Coomassie Blue stained 12% SDS-PAGE analysis of *XvVTC2* recombinant protein expression. Lane 1, Fermentas spectra ladder (Sm1841). Lane 2, negative control (soluble protein fraction from *E. coli* BL21(DE3) cells containing pET32b only); lane 3, His-purified fraction of *E. coli* BL21(DE3) cells containing pET32b only (showing no band at 70kDa). Lane 4, positive control of a His-tagged *XvPP2C* recombinant protein. Lane 5, crude extract of the soluble protein fraction from *E. coli* BL21(DE3) cells containing pET32b+*XvVTC2*; lane 6, first elution of the His-purified fraction of pET32b+*XvVTC2*, lane 7, second elution of pET32b+*XvVTC2*. Lane 8, flow through of the His-purification of pET32b+*XvVTC2*. Lane 9, crude extract of the soluble protein from *E. coli* BL21(DE3) cells containing pET22b+*XvVTC2*; lane 10, first elution of the His-purified fraction of pET22b+*XvVTC2*.

Based on *in silico* analysis the expected size of the recombinant protein is approximately 68 kDa and corresponds to the expressed protein (Figure 3.3 lanes 5 - 7). The XvVTC2 protein on its own is calculated to be 48.2 kDa, and the tags add 19.8kDa to the protein. From DNA sequence data the XvVTC2 protein was expected to be slightly smaller than the *A. thaliana* homolog, which is 51 kDa without recombinant tags and shown to migrate to 53 kDa when expressed as a recombinant protein by Linster *et al* (2008). As expected the recombinant XvVTC2 protein migrated to 68 kDa. The products from the pET22b+XvVTC2 expression construct (Figure 3.3 lanes 9 - 10) will be discussed below.

From published results it seems that expression of VTC2 protein homologs are difficult and require optimisation for optimal expression. The conditions shown by Linster *et al.* (2007) and Laing *et al* (2007) show expression overnight at low temperatures of 18°C and 20°C respectively. The protein also seems susceptible to degradation; Linster *et al.* (2008) included relatively high PMSF and leupeptin protease inhibitor concentrations in the extraction buffer while Laing *et al.* (2007) used protease inhibitor tablets to prevent degradation. The addition of protease inhibitors, to the same concentrations as described by Linster *et al* (2008), as well as the reduction of the growth temperature lead to the successful expression and extraction of soluble XvVTC2 recombinant protein.

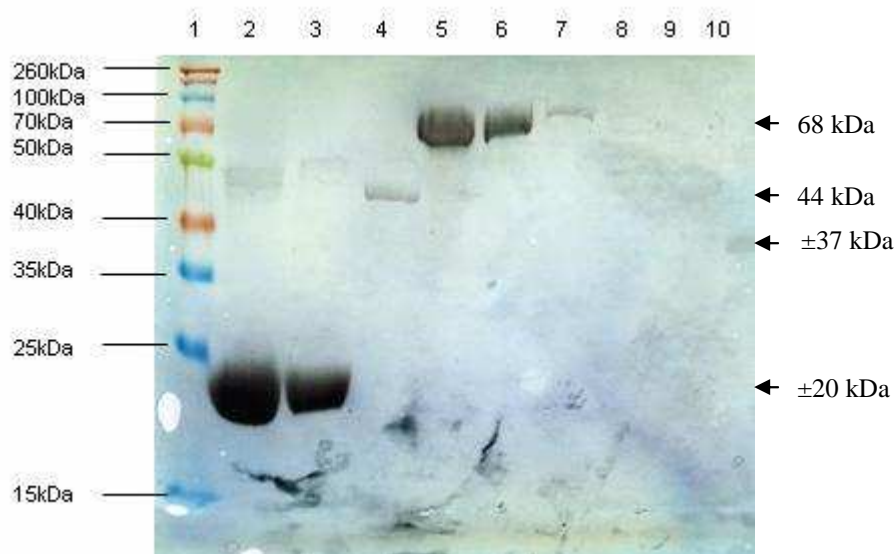


Figure 3.4: His-tag specific Western Blot to detect expressed recombinant XvVTC2 protein. Lane 1, Fermentas spectra ladder (Sm1841); lane 2, negative control (crude sample of the soluble fraction of protein extracted from *E.coli* BL21 (DE3) cells containing only the pET32b plasmid); lane 3, His-purified fraction of the negative control; lane 4, positive control (His-tagged XvPP2C recombinant protein); lane 5, crude extract of the soluble fraction protein extracted from *E. coli* BL21 (DE3) cells containing pET32b+XvVTC2; lane 6, first elution of the His-purified fraction of the soluble fraction protein extracted from *E. coli* BL21 (DE3) cells containing pET32b+XvVTC2; lane 7, second elution of the soluble fraction protein extracted from *E. coli* BL21 (DE3) cells containing pET32b+XvVTC2;. Lane 8, flow through of the His-purification of the soluble fraction protein extracted from *E. coli* BL21 (DE3) cells containing pET32b+XvVTC2;. Lane 9, crude extract of the soluble fraction protein extracted from *E. coli* BL21 (DE3) cells containing pET22b+XvVTC2; lane 10, first elution of the His-purified fraction of the soluble fraction protein extracted from *E. coli* BL21 (DE3) cells containing pET22b+XvVTC2.

The confirmation that the protein expressed is in fact a His-tagged recombinant protein was shown by performing a His-tag specific western blot. The negative control, which was soluble protein extracted from cells containing the pET32b plasmid without the insert, showed a protein smaller than 25 kDa and most likely around the expected 20 kDa mark. As no fragment is cloned into vector this protein contains only the S-, Trx- and His-tags (EMD Biosciences, 2005). The positive control His- tagged XvPP2C recombinant protein was obtained from T. Ellick (Pers. Comm. 2008) and was expected to be 44 kDa in size. The soluble protein extracted from the cells containing the pET32b+XvVTC2 fragment, showed a product of approximately 68 kDa in size (Figure 3.4 lanes 5 - 7). The crude extract from the soluble fraction showed the highest concentration of XvVTC2 protein. The His-purified fractions showed lower concentrations of XvVTC2 protein than

the crude fraction but these protein fractions were of higher purity and fewer contaminants were observed (Figure 3.3 lanes 6 - 7).

The flow through of the recombinant XvVTC2 His-purification showed no detection of His-tagged protein indicating no protein was lost during the wash step of the purification (Figure 3.4, lane 8). A soluble crude extract from *E. coli* BL21(DE3) cells containing pET22b+XvVTC2 construct showed no detection of a His-tagged protein (Figure 3.4, lane 9). However, a His-purified fraction of the same extract showed a His-tagged protein at approximately 37 kDa (Figure 3.4 lane 10). This is not the expected size of the XvVTC2 recombinant protein of 52 kDa when expressed using the pET22b vector. The extraction buffer used for the XvVTC2 recombinant protein expressed in pET22b did not contain the protease inhibitors, PMSF and leupeptin. Thus the protein might have been degraded and only a protein fragment containing the C-terminal His-tag remained. However sufficient soluble recombinant protein was obtained when using pET32b as an expression vector.

3.4 Conclusions

The DNA product used for cloning and the recombinant protein product obtained after expression were of the expected respective sizes. The results confirm that pET32b-XvVTC2 recombinant protein was successfully expressed in *E. coli* (BL21) DE3 cells. Optimisation of the conditions for expression and extraction proved to be important as shown in other studies in which VTC2 proteins were expressed. For future studies attempts should be made to express XvVTC2 in a vector containing fewer tags for kinetic studies. However the presence GDL-D-Glucose phosphorylase activity of the protein is not affected by the tags attached to the protein, as is discussed and shown in Chapter 4.

4 Chapter 4: Protein function and Localisation

University of Cape Town

4.1 Introduction

This chapter deals with the characterisation of the XvVTC2 in terms of its biochemical function, cellular localisation and protein expression in response to desiccation.

To establish and confirm the function of a protein, assays are required. The *X. viscosa* VTC2 homolog is expected to have the same role in the ASC biosynthesis pathway as is found in *A. thaliana* and *A. chinensis* (Laing et al., 2007; Linster et al., 2007). VTC2 has substrate specificity for GDP-L-galactose as well as GDP-D-glucose. The reaction takes place as follows; GDP-L-galactose/GDP-D-glucose + VTC2 (GDP-L-galactose phosphorylase) + Pi \longrightarrow L-galactose-1-phosphate / D-glucose-1-phosphate + GDP. Because GDP-L-galactose is not readily available, in this assay GDP-D-glucose was used as a substrate and the formation of GDP measured at various time points to determine recombinant enzyme activity.

The use of fluorescent fusion proteins has allowed for the study of protein localisation (Chalfie et al., 1994). Several colour variations of the original green fluorescent protein (GFP), are available to allow for studying of more than one protein in a cell as well as their interaction (Day and Schaufele, 2008; Mohanty et al., 2009). In this experiment a yellow variant of GFP is used as a fusion protein to study the localisation of the XvVTC2 protein.

The use of western blotting to establish the expression of proteins is well established technique and widely used. However obtaining specific antibodies to novel proteins can be problematic and requires time and optimisation. Here a western blot analysis of XvVTC2 protein expression in response to desiccation in *X. viscosa* is presented.

4.2 Materials and methods

4.2.1 In-vitro assay of GDP-D-Glucose phosphorylase activity

The purified pET32b-XvVTC2 recombinant protein was used for the assays. The N- and C-terminal tags of the protein were not removed. The enzyme reaction was done as per (Linster et al., 2007) using $26\mu\text{g.ml}^{-1}$ protein, 1mM GDP-D-glucose (Sigma) and 5mM inorganic phosphate. Samples were taken at 30 and 60 min after the addition of enzyme to measure GDP formation. A control reaction was done containing no enzyme. A 1mM GDP standard was also prepared in the same buffer and used as a control

The samples were analysed by a reverse phase HPLC using a Shimadzu liquid chromatograph LC-10AD and Shimadzu photodiode UV-VIS detector SPD-M6A. A Phenomenex Type: Synergi max-RP 80A, 250 x 4.6mm 4μ column was used. The buffers used were A - 0.1% TFA in milli-Q water and B – 100% methanol. A gradient of 0 – 100% methanol was used at a flow rate of 0.7ml.min^{-1} . The buffer exchange setup was as follows: start 0% buffer B, 6minutes 0% buffer B, 46 minutes 100% buffer B, 56 minutes 100% buffer B, 66 minutes 0% buffer B. The wavelength used for detection of the nucleotides was 254nm. The raw data was exported and plotted using Microsoft Excel 2003.

4.2.2 YFP localisation

XvVTC2 was PCR amplified from one of the cDNA clones used for sequencing (Chapter 2), using Phusion[®] high fidelity polymerase (Finnzymes, Finland). The primers used to amplify the fragment were the VTC2expF and VTC2yfpR primers (Appendix 1). The PCR conditions used were the same as those used for the expression cloning (Appendix 2). The fragment was cloned into a 35s-pEYFP-NosT vector (Clontech, USA), to incorporate the fluorescent protein at the C-terminus of XvVTC2 protein. For directional cloning the *Bam*HI and *Kpn*I sites of the vector were used. After amplification the same purification, ligation and transformation procedures as described in Chapter 3 were used. A pEYFP vector containing no insert was used as a negative autofluorescence control.

Onion (*Allium cepa*) epidermal cells were used for the transformation by particle bombardment. Gold particles ($0.6\mu\text{m}$) were prepared and sterilised as described by

Sanford *et al* (1993). Six micrograms of purified DNA was mixed with three microgram aliquots of purified gold whilst vortexing. One volume and 0.4 volumes of 2.5mM CaCl₂ and 0.1M spermidine were added respectively. Two volumes of ethanol was added for the precipitation of the DNA onto the microcarriers. Microcarriers were placed in their holders and these were placed in petri dishes. Approximately 10µl DNA coated gold was added to the centre of the microcarriers and allowed to dry for 20 minutes. This was repeated six times for the experimental as well as control samples.

Onions were peeled and cut into square pieces approximately 1.5 x 1.5 cm. The epidermal cells were transformed by particle bombardment as outlined in Scott et al (1999). A PDS-1000/He Biolistic Bombardment Delivery System (Bio-Rad Laboratories, Germany) and 650psi rupture discs were used for the transformation. After bombardment the onion pieces were placed in Petri dishes containing a 500µl dH₂O to avoid drying out and were incubated for 24 hours at 27°C in the dark.

A glass slide wet mount of the bombarded epidermal layer was prepared for confocal microscopy. The epidermal layer was peeled from the bombarded onion segment and placed in a 0.07M phosphate buffer (pH8.5) containing 0.01% Aniline blue and 20µg.ml⁻¹ Hoechst 33258 stain and placed in the dark for 20 minutes (Majewska-Sawka et al., 2002; Thakur et al., 2003). The cells were viewed using a Zeiss LSM510 Meta confocal microscope using an argon laser at 514nm for the yellow channel (Carl Zeiss Inc, Germany). The blue channel was obtained using the epi-fluorescence setting and the bright field using white light. The imaging software used was the LSM software accompanying the microscope.

4.2.3 Western blot analysis

The recombinant XvVTC2 protein was used to raise polyclonal antibodies in New Zealand white rabbits. The procedure used for the antibody production was approved by the University of Cape Town Animal Research ethics committee (Reference number: REC REF 009/013). The procedure used was modified from Rybicki (1979). The modifications entailed four injections of 500µg XvVTC2 protein per injection to be administered over a four week period. Thereafter four bleeds were obtained over a six week period.

To determine the titre of the antibody from the antisera from the respective bleeds an enzyme linked immuno-sorbent assay (ELISA) was done. The procedure used was obtained from Faezah Davids (Research assistant, Molecular cell biology department, University of Cape Town 2009). In brief, Nunc Maxisorp Immuno™ 96 well plates (Nunc, Denmark) were coated with 500ng recombinant XvVTC2 protein as antigen. The plate was washed several times using TBS-Tween after coating and blocked using 3% BSA in TBS-Tween. The plate was washed again several times using TBS-Tween. Then the plate was incubated using the following dilutions of antisera; 10^{-2} , 10^{-4} , 10^{-6} and 10^{-8} in TBS-Tween. Thereafter the plate was washed again and incubated with an anti rabbit alkaline phosphatase conjugate (Sigma, Germany) secondary antibody at a 1/5000 dilution in TBS-Tween. The plate was washed again several times using TBS-Tween. For equilibration the plate was washed with 10% Diethanolmine, 0.5mM MgCl_2 pH 9.6. Thereafter the p-Nitrophenyl phosphate at 1mg.ml^{-1} in 10% Diethanolmine, 0.5mM MgCl_2 pH 9.6 substrate was added. The colour reaction was allowed to develop for 20 minutes and absorbance readings were taken at 405nm using a Titertek Multiskan® Plus MK II (Flow laboratories, UK) plate reader. The selected antisera were purified as per D. Chopera (2005) using polyethylene glycol 6000 (PEG 6000).

The protein used for the western blotting was total soluble protein extracted using Tri-reagent (Bio Basic, Canada). The protein was extracted from the remaining organic phase after RNA extraction, described in Chapter 5. Briefly, after RNA extraction 300 μl cold ethanol was added to the respective protein extracts. The tubes were inverted several times, incubated at room temperature for 5 minutes and centrifuged at 4000 rpm for 10 minutes in a Spectrafuge 16m (Labnet International, USA) microcentrifuge. The supernatant was transferred to fresh microfuge tube containing 1.5ml isopropanol and incubated for 10 minutes at room temperature. Thereafter the tubes were centrifuged at 12000rpm for 10 minutes at 4°C in a Spectrafuge 16m (Labnet International, USA) microcentrifuge. The supernatant discarded and the pellet was three times with 0.1M ammonium acetate prepared in methanol and washed once with cold acetone. The pellet was air dried for approximately 10 minutes and resuspended in urea lysis buffer containing 0.125M DTT. The protein concentration was quantified using a modified

Bradford assay which is not affected by urea (Bradford, 1976; Ramagli and Rodriguez, 1985).

The western blotting transfer procedure was the same as described in Chapter 3. The detection procedure was adapted from Qiagen (2002) using the chemiluminescent method. The primary antibody was the polyclonal rabbit anti XvVTC2 antibody and was used in a 1/1000 dilution. The secondary antibody was goat anti-rabbit HRP conjugate (Sigma, Germany) in a 1/5000 dilution. The detection substrate was the Supersignal – Westpico detection system (Pierce, USA) and was used as per the manufacturer's instructions. The imaging system used was the G:Box-Chemi (Syngene, USA).

4.3 Results and Discussion

4.3.1 *In-vitro* assay

The HPLC analysis show different elution times for GDP and GDP-D-glucose as expected. The peak GDP elution was at 18.187 min (Figure 4.1 A) and the peak GDP-D-glucose elution was at 17.333 min (Figure 4.1B). In the presence of XvVTC2, GDP formation is observed and the amount of GDP formed increases and the GDP-D-glucose decreases with prolonged incubation (Figure 4.1 C & D). This is a clear indication that GDP-D-glucose is utilised as a substrate by XvVTC2 and GDP formed as a product. It is then justified to infer that D-glucose-1-phosphate is the other product formed in this reaction as XvVTC2 forms GDP and D-glucose-1-phosphate as products from GDP-D-glucose in the presence of inorganic phosphate.

The graphs show that in the reaction not all the substrate was used. This could be attributed to a low enzyme concentration; however the same concentration or even less has been reported for other studies. The enzyme was stored at -80°C for several weeks before the reaction was performed and may have partially degraded. The tags attached to the protein might have interfered with the function, but even so clear activity can be observed from the graphs. Another possible explanation could be that the reaction had reached equilibrium. This would however need to be confirmed by incubating the reaction for longer to see if there is any change in the concentrations of the substrate or product beyond 60 minutes.

In a different reaction a reaction buffer containing GDP-D-glucose was stored for several weeks at -20°C and had undergone several freeze/thaw cycles before performing the reaction. Upon HPLC analysis the GDP-D-glucose seemed degraded as two peaks were obtained for the no enzyme control (data not shown). The first peak that was observed appeared earlier than the GDP-D-glucose peak and it was assumed that it was GMP. In the reaction where the enzyme was added to this buffer containing the degraded GDP-D-glucose as substrate only one peak was obtained which corresponded to GDP (data not shown).

These results indicate that XvVTC2 is acting as a phosphorylase, by which inorganic phosphate is used to phosphorylate GMP forming GDP. This agrees with what has been reported in other studies (Dowdle et al., 2007; Linster et al., 2007; Linster et al., 2008; Linster and Clarke, 2008). Furthermore, it shows that the enzyme does not need a sugar moiety attached to the substrate for its phosphorylation function. However this does need to be confirmed by running a GMP standard and using GMP as a substrate only.

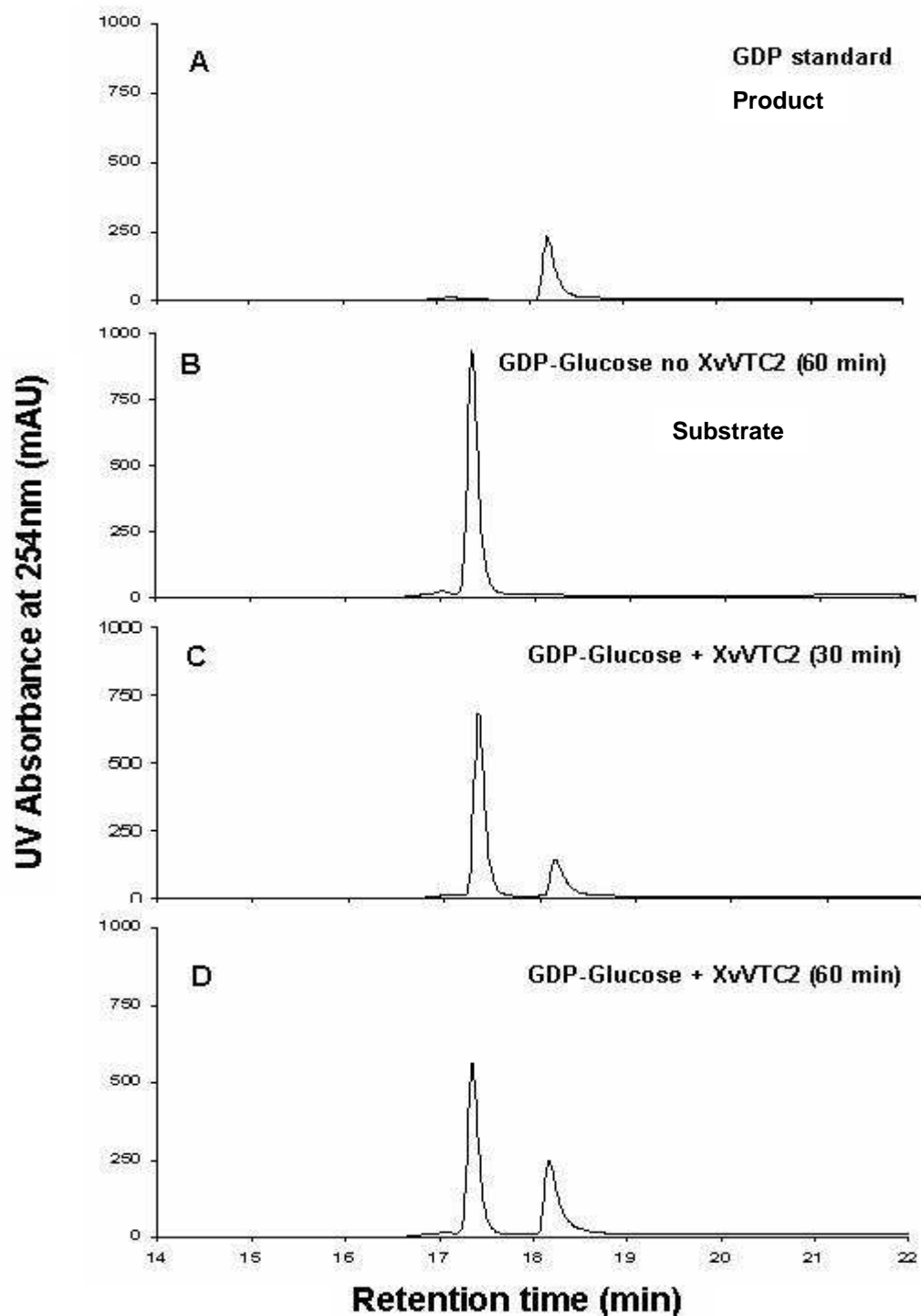


Figure 4.1: Reverse phase HPLC chromatograms showing phosphorylase activity of recombinant XvVTC2 protein. A, Reaction product standard (GDP elution 18.187 min); B, Negative control (Reaction substrate standard, GDP-D-glucose elution at 17.333 min); C, XvVTC2 ($0.26 \mu\text{g} \cdot \text{ml}^{-1}$) incubated with GDP-D-Glucose (1mM) at 26°C and in the presence of inorganic phosphate (5mM) GDP formation observed at 17.333min after 30 minutes; D, XvVTC2 ($0.26 \mu\text{g} \cdot \text{ml}^{-1}$) incubated with GDP-D-Glucose (1mM) at 26°C and in the presence of inorganic phosphate (5mM) GDP formation observed at 17.333min after 60 minutes.

It has been reported that VTC2 could have a guanyltransferase function, in which GMP is transferred from either GDP-L-galactose or GDP-D-glucose to a hexose-1-phosphate (Laing et al., 2007). This has not been tested in these experiments, but a phosphorylation function has been shown. Furthermore, studies by Linster et al., (2008) have shown that it is unlikely that transferase activity would occur in plants at the natural levels of the proposed guanyl acceptors. However it is likely that phosphorylase activity would occur at naturally occurring inorganic phosphate levels. This strongly suggests that phosphorylase activity of VTC2 is more likely than guanyltransferase activity. Thus it is reasonable to accept that this would be the likely mode of function of XvVTC2 as well.

The fact that XvVTC2 uses GDP-D-glucose as a substrate to produce D-glucose-1-phosphate raises an interesting proposition. Firstly it is known that the affinity for this substrate is almost equal to that of GDP-L-galactose (Laing et al., 2007; Linster et al., 2007; Linster et al., 2008). This would suggest that XvVTC2 might have an equally important function in other biochemical pathways involving GDP-D-glucose. The significance of the D-glucose-1-phosphate product is that it is a precursor to sucrose formation (Mueller et al., 2003; AraCyc, 2010).

As discussed in Chapter 1, sucrose is accumulated in response to desiccation in *X. viscosa*. This dual role of XvVTC2 in sucrose as well as ASC metabolism might be of significance, as in *X. viscosa* it provides a link between primary stress response which is ASC production, and the severe desiccation stress response which is sucrose accumulation. The three times higher affinity of VTC2 for D-glucose-1-phosphate, compared to L-galactose-1-phosphate, for the reverse reaction might indicate the importance of the conservation of this (GDP-D-glucose/D-glucose-1-phosphate) substrate affinity in the enzyme activity (Linster et al., 2007). This affinity for D-glucose-1-phosphate could, in the presence of excess D-glucose-1-phosphate, allow VTC2 to alter the flux in the sucrose production pathway by a feedback mechanism.

4.3.2 YFP localisation

The size (1278 bp) of the amplified fragment from the cDNA clone was the same as that obtained for protein expression primers (Figure 4.2 A). This indicates that the same product was amplified using the respective primers and that primer design was correct. Non-specific amplification was minimal and indicates optimal reaction conditions. Two clones were obtained that released the *XvVTC2* fragment (Figure 4.2 B, lanes 4 and 6). The release of the fragment is an indication that the restriction sites used for cloning were re-constituted properly in ligation (Figure 4.2 B) and suggests that the reading frame of the protein is correct. It is thus expected that fusion protein will be expressed with the YFP attached at the C-terminus of the *XvVTC2* protein (Figure 4.3).

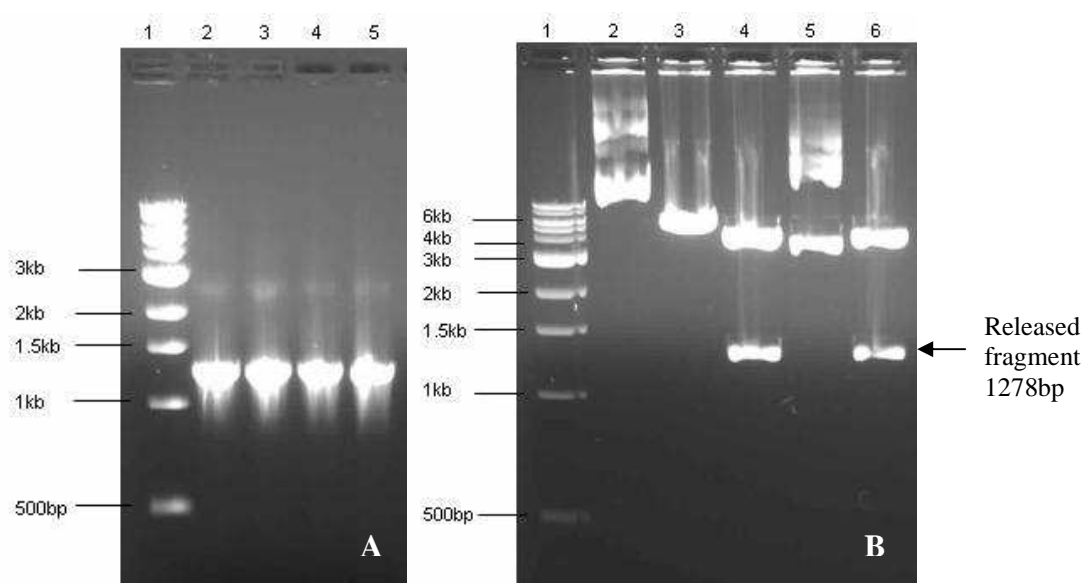


Figure 4.2: Ethidium bromide stained 1% w/v agarose gel showing in A) *XvVTC2* amplified PCR products from a cDNA clone, B) digested *XvVTC2* + pEYFP plasmid. In A) lane 1, New England Biolabs 1kb ladder, Lane 2, positive control using the VTC2expF and VTC2expR primers and a cDNA clone template; Lanes 3 – 5, PCR products obtained using the VTC2expF and VTC2yfpR primers from a cDNA clone template. In B) lane 1, New England Biolabs 1kb ladder, Lane 2, - undigested pEYFP vector, lane 3, negative control (pEYFP digested with *Bam*HI only); lanes 4 – 6, three different *XvVTC2* + pEYFP clones digested with *Bam*HI and *Kpn*I. The clones in lanes 4 and 5 show the release of the *XvVTC2* fragment, indicating the restriction site is reconstituted correctly on ligation

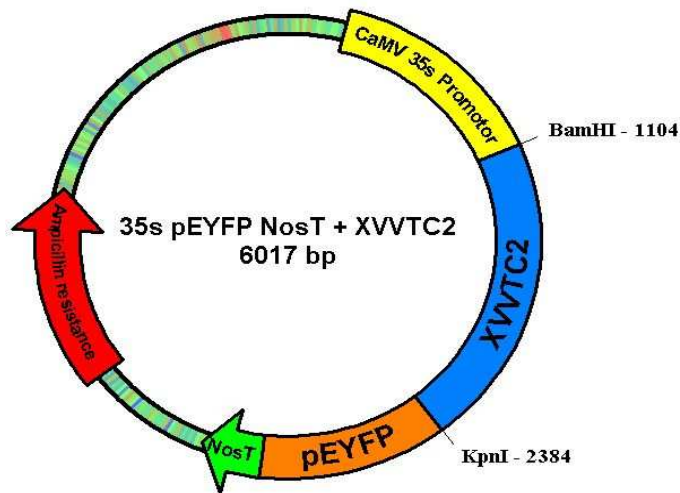


Figure 4.3: Recombinant plasmid map of 35S pEYFP NosT containing the *XvVTC2* gene. The plasmid map shows the CaMV 35s promotor (yellow) which controls the expression of the *XvVTC2*+pEYFP fusion protein. The *Bam*HI (1104) and *Kpn*I (2384) restriction sites are indicated as they were used to clone the *XvVTC2* (blue) fragment into the vector. The pEYFP coding region is indicated in orange downstream of the *XvVTC2* fragment. The NosT terminator (green) terminates the transcription of the fusion protein. The ampicillin resistance gene, used for antibiotic resistance selection, is indicated in red.

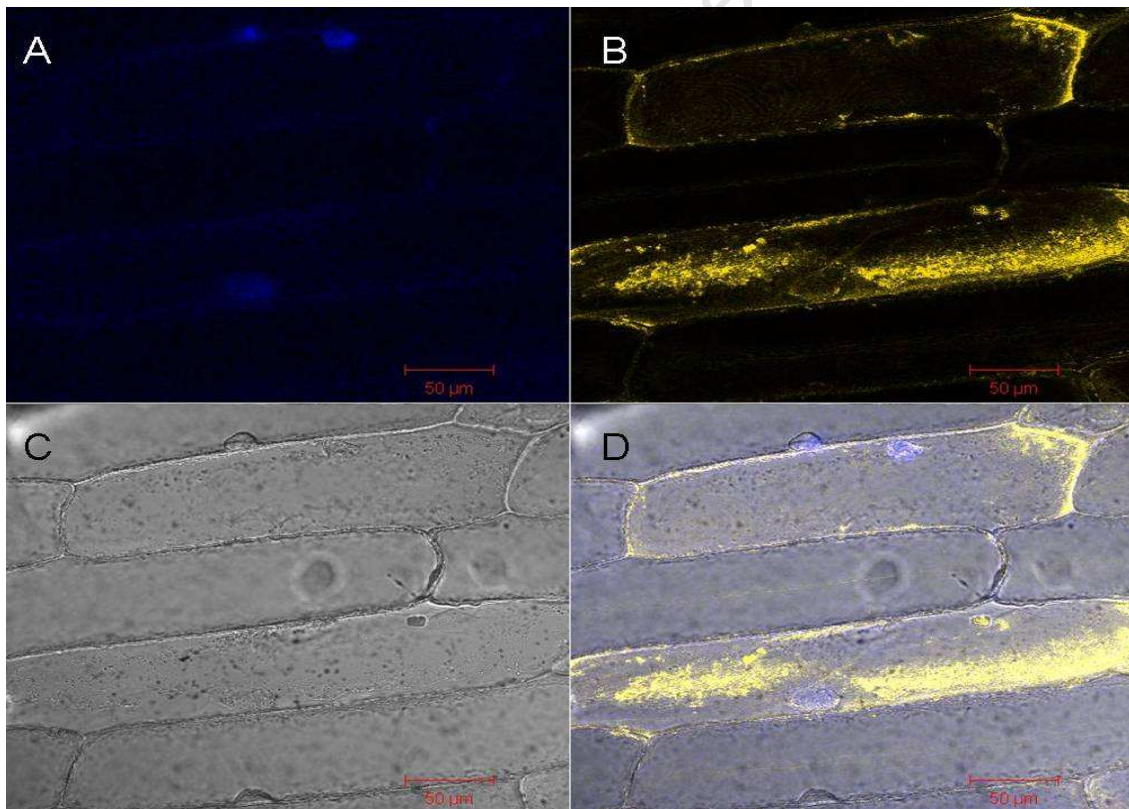


Figure 4.4: A series of images showing the expression of yellow fluorescent protein in transformed onion (*Allium cepa*) epidermal cells. The cells were bombarded with pEYFP plasmid coated gold particles. Frame A shows nuclei stained with Hoechst 33258 and cell walls stained with Aniline blue, Frame B shows yellow fluorescence of pEYFP protein, Frame C shows the cells in bright field and Frame D shows the composite image of A, B and C. The cells were incubated at 27°C for 24 hours after bombardment, stained and then viewed with a Zeiss LSM 510 Meta laser scanning confocal microscope.

Onion cells bombarded with the YFP control showed an even fluorescence in the cytoplasm of the cell (Figure 4.4, B and D). No particular pattern of fluorescence is observed, which indicates that the YFP protein does not localise specifically to any compartment within the cell. Some diffusion of the YFP protein into the nucleus is observed, which is expected as the YFP protein is smaller than the nucleus exclusion limit (Nigg, 1997; Gorlich, 1998). Transformed cells are distinguished from non-transformed cells by the presence of yellow fluorescence within them.

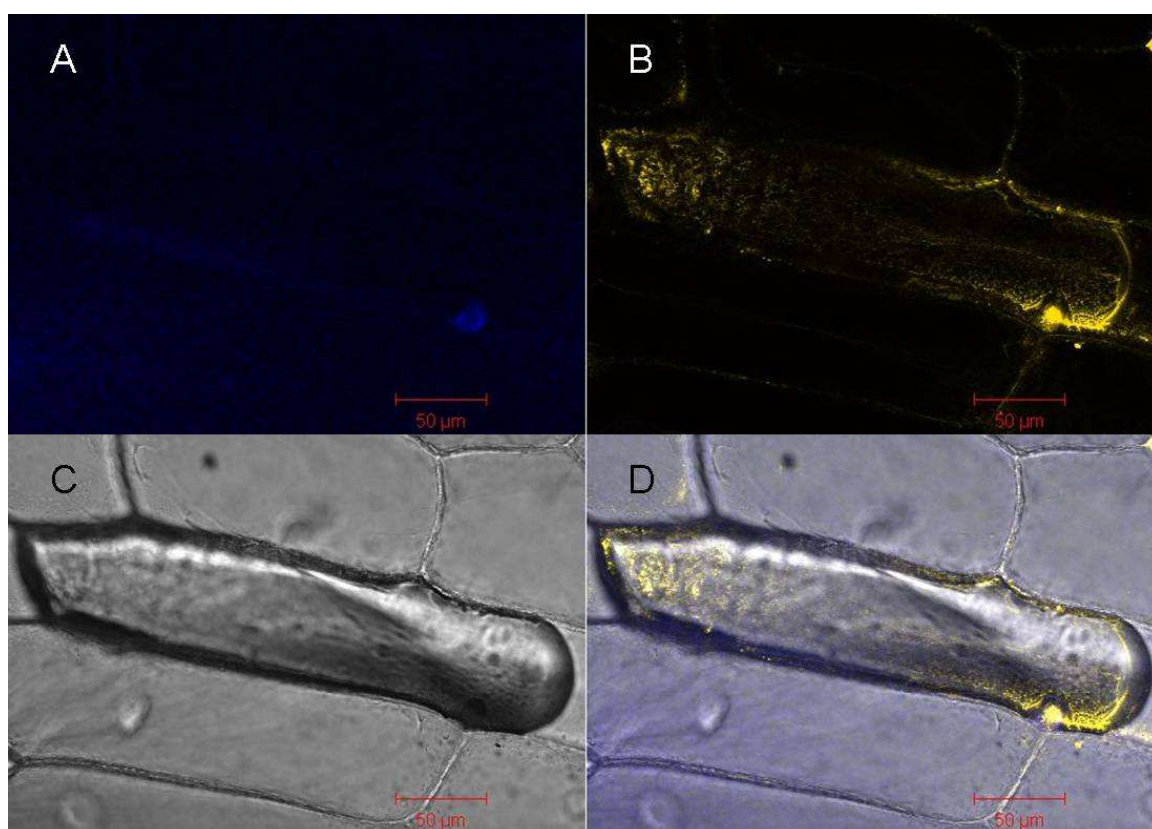


Figure 4.5: A series of images showing the expression of XvVTC2: pEYFP fusion protein in transformed onion (*Allium cepa*) epidermal cells. The cells were transformed by microparticle bombardment with XvVTC2: pEYFP plasmid coated gold particles. Frame A shows a nucleus stained with Hoechst 33258 stain and cell walls stained with Aniline blue, Frame B shows yellow fluorescence of the XvVTC2: pEYFP fusion protein, Frame C shows the cells in bright field and Frame D shows the composite image of A, B and C. The cells were incubated at 27°C for 24 hours after bombardment, stained and then viewed with a Zeiss LSM 510 Meta laser scanning confocal microscope.

The XvVTC2 protein is localised in the nucleus as well as cytoplasm of plant cells (Figure 4.5, B and D). The identification of two nuclear localisation signals (Chapter 2) indicated that the XvVTC2 protein could be localised in the nucleus. Furthermore it is known that the *A. thaliana* homolog (VTC2) is localised in the nucleus (Muller-Moule',

2008). The function of the protein in the nucleus has not yet been established. The size of the recombinant protein prohibits it from diffusing into the nucleus and has to be actively transported (Nigg, 1997; Gorlich, 1998; Muller-Moule', 2008). For the protein to be actively transported to the nucleus suggests that it plays a role there.

A possible role in the nucleus could involve the protein binding to the nucleotides GMP and GDP and thereby be involved in nucleotide cycling. This could have implications for gene regulation. Since it has been proposed that the regulatory step of the ASC biosynthesis pathway is at the VTC2 step, these localisation results might provide some evidence to that extent. However other substrate binding experiments will have to be conducted to study this hypothesis. Furthermore, creating mutant plants with mutations only in the nuclear localisation signals, and if possible without affecting the GDP-L-galactose phosphorylase activity, of the VTC2 gene might provide insight into the function of the protein in the nucleus. The results of this and the Müller-Moulé (2008) localisation study does suggest that VTC2 may be a multifunctional protein which has a role in ASC biosynthesis as well as possibly other roles in the nucleus that are still to be elucidated.

4.3.3 Western blot analysis

Other studies involving VTC2 homologs have focussed mainly on transcription profiling (Bulley et al., 2009; Ioannidi et al., 2009; Imai et al., 2009 b). However transcription of a gene does not necessarily mean its translation. This is even of greater importance in this study as water is a limiting factor and the mRNA might not be translated to form a protein. The lag between transcription and translation might be vital in the ability of the plant to survive the desiccation stress. If the lag is too great the plant stands the risk of oxidative damage.

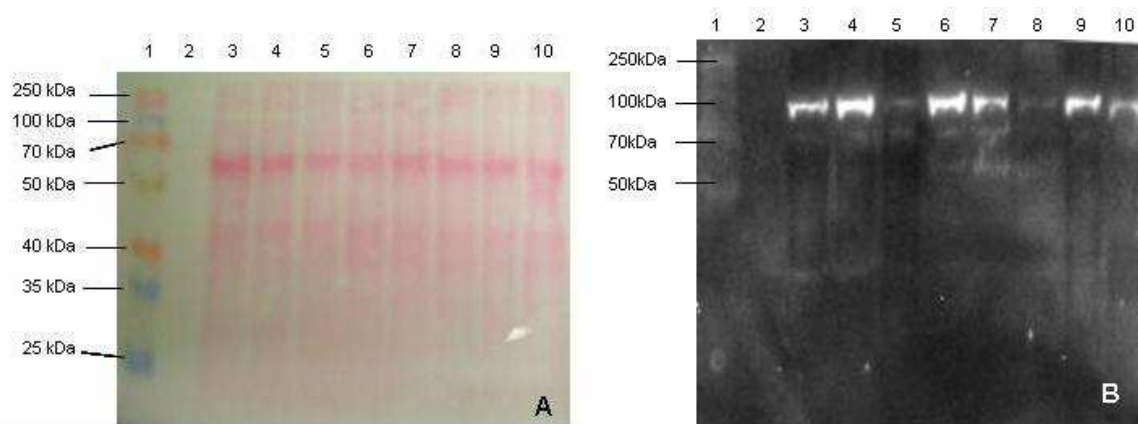


Figure 4.6: Ponceau S stained membrane (A) and western blot (B) of *X. viscosa* soluble leaf proteins extracted from plants during a dehydration experiment. The proteins were separated on a 12% SDS-PAGE. The ponceau S stained membrane shows equal loading of the gel and complete transfer of the protein to the membrane. The chemi-luminescent developed western blot shows the detection of XvVTC2 using polyclonal anti-XvVTC2 antibodies. The molecular weights indicated in B are extrapolated from A. Lane 1, Fermentas Spectra multicolour Broad range ladder (SM1841). Lane 2, blank. Lanes 3 – 7, samples taken during dehydration and lanes 8 -10 during rehydration at different relative water contents (RWC). The samples are; lane 3, 100% RWC, Lane 4, 76% RWC, Lane 5, 51% RWC, Lane 6, 21% RWC, Lane 7, 8% RWC, Lane 8, 31% RWC, Lane 9, 66% RWC and Lane 10, 79% RWC.

The protein expression profile showed an interesting pattern, which contrasts to that observed with the mRNA expression (Chapter 5). It should however be noted that the results discussed in this section are based on the results of only one experiment, with no replication. Thus the experiment would have to be repeated with replications to validate these results. The samples used for this study were obtained from biological repeat 3, and should be compared to that in Chapter 5. The relative protein level detected for 100% and 76% RWC is equal or higher when compared to the other sample points (Figure 4.6 B, lanes 3 and 4). The level then decreases at 51% RWC (Figure 4.6 B, lane 5) and increases again at 21% RWC (Figure 4.6 B, lane 6). The relative expression is then lower at the most severe desiccation point (8% RWC) (Figure 4.6 B, lane 7) and decreases further upon rehydration at 31% RWC (Figure 4.6 B, lane 8), before picking up again at 66% (Figure 4.6 B, lane 9) and decreasing again slightly at 79% RWC (Figure 4.6 B, lane 10). In the mRNA expression, the level at the first point is much lower and shows a sharp increase as dehydration progresses; upon rehydration the relative expression levels remain elevated and decreases slightly as rehydration progresses (Figures 5.3 & 5.4).

These differences can be attributed to delays between transcription and translation. The high levels of protein and low levels of mRNA in the initial samples can be attributed to no new transcription needed as the XvVTC2 protein levels present are sufficient. As the stress is applied the available protein might degrade, due to increased activity, and hence new transcription is needed, hence the sharp increase in transcript level and reduction in protein level at 51% RWC (Figures 5.4 and Figure 4.6 B, lane 5). The new transcripts are then translated to form an increase in protein level at 21% RWC to deal with the stress. As the desiccation progresses water becomes limiting for activity and the protein as well as mRNA transcript levels decrease slightly, but remain relatively high. Upon rehydration the available protein is used extensively and protein levels decrease. An increase in protein level is then again observed at 66% to 79% RWC during rehydration.

Another explanation as to why the qRT-PCR data and the western blotting do not correspond that there might be a rapid turnover of XvVTC2 protein. Other studies have suggested that there is an increase in the turnover rate of Nitrate reductase (NR) and the D1 protein of photosystem II in response to drought stress (Aro et al., 1993; Giardi et al., 1995; Ferrario-Méry et al., 1998). Due to the nature of the plant system under the stress condition, there might be need for the faster turnover of the XvVTC2 enzyme in order to produce sufficient ASC. The involvement of ASC in photosystem II as an electron donor in heat stressed plants does suggest that ASC plays a valuable role the maintenance of photosynthesis under stress conditions (Toth et al., 2009). ASC might play a similar role in early dehydration as well as during rehydration, when photosynthesis is active in the plant and the plant needs to gather all available resources to survive.

Other than the difference between protein level and transcript level, a difference between the size of the detected protein and the size expected was observed. The detected protein was tested for specificity to the recombinant expressed protein and showed great specificity and few non specific products (data not shown). The protein appears to be almost double in size to that of which is expected. Post translation modifications such as the possible phosphorylation of the protein (see chapter 2) could alter the protein's apparent molecular weight leading to it appearing larger in size. Another possibility is that the protein is forming a dimer. The protein was resuspended in ULB buffer and DTT was added, but this does not guarantee the breakdown of dimer bonds. Before

electrophoresis the resuspended protein was not heated (samples containing urea can not be heated because of carbamylation), which would have ensured the breaking of dimer bonds. The recombinant protein was heated before electrophoresis, which ensured the breaking of dimer bonds. Furthermore another related HIT-protein, ADP-glucose phosphorylase has been shown to function as a dimer (McCoy et al., 2006). To verify whether the protein does form a dimer the X-ray crystal structure would have to be determined.

Further protein expression studies will have to be done to verify this result. Other protein extraction methods could be attempted in which only protein is extracted and not RNA as used here. The resuspension buffer of the protein could be changed and the protein heated before electrophoresis to break any possible dimers that may form. The antibodies will also have to be tested and further optimised to show specificity only for XvVTC2. These modifications as well as testing under other conditions where the protein levels are known, as a control, would help validate the results obtained here.

4.4 Conclusions

This chapter dealt with the XvVTC2 protein characteristics in terms of biochemical function, cellular localisation and expression in response to desiccation. The reported GDP-glucose phosphorylase activity of other VTC2 homologs has been confirmed for XvVTC2 (Dowdle et al., 2007; Linster et al., 2007; Linster et al., 2008). For future studies the assay performed here can be taken further and the XvVTC2 enzyme kinetics determined. The enzyme will also have to be tested using GDP-L-galactose as a substrate, as this is the principal role in ASC biosynthesis. Expression of the recombinant protein to contain fewer tags, so that the protein more closely resembles its native state, would also be employed in such a study. The expression of mutant proteins in which certain sections are altered can be employed to determine specific binding sites. Various guanyl acceptors can be used in reaction to determine whether transferase activity exists and the extent to which it plays a role. This would shed some light on the existence of the proposed VTC2 cycle in which transferase activity is vital.

The localisation study confirmed what has been found by Muller Moulé (2008), in terms of nuclear localisation. It also confirms the prediction of nuclear localisation by the presence of the nuclear localisation signals as discussed in Chapter 2. The localisation of the protein would be better studied if transgenic lines expressing YFP:XvVTC2 fusion protein were developed. The function of the protein in the nucleus is also yet to be determined, with a role in nucleotide cycling proposed. Further experiments in which VTC2 mutants are transformed with a *VTC2* gene containing a mutation in the nuclear localisation signal could provide evidence as to the function of the nuclear localisation of the protein.

The western blot expression analysis provided some interesting results that on the surface do not correspond with what has been found in the qRT-PCR mRNA expression analysis. To validate the western blot expression analysis the experiment will have to be repeated with different protein extraction methods as has been suggested. Some explanations as to possible ways in which the protein expression lags behind the mRNA transcription have been provided. However without repeat protein expression experiments these explanations are merely speculation. An interesting observation in the western blot experiments was that it seems that the protein might function as a dimer. This has also been observed for a related protein, ADP-glucose phosphorylase (McCoy et al., 2006). Experiments similar to those characterising the structure and mechanism of the ADP-glucose phosphorylase could be employed to characterise XvVTC2 (McCoy et al., 2006).

Overall the experiments covered in this chapter have provided results to suggest the functional homology between XvVTC2 and VTC2 homologs from other plants. To confirm the function of XvVTC2 in the L-galactose pathway, GDP-L- galactose would have to be used as substrate in the biochemical assay. Some avenues for further study have been proposed. A key theme in these proposals is determining the structure and mechanism of the protein. This could provide evidence for the suspected bi-functionality of the enzyme.

5 Chapter 5: Water deficit Stress treatment and Quantitative Real-Time PCR analysis

University of Cape Town

5.1 Introduction

The expression profiling of ascorbate biosynthesis genes and more specifically *VTC2* has recently gained a lot of attention. Studies have been conducted in *A. thaliana*, tomato, peach, kiwifruit, acerola and apple (Badejo et al., 2008; Li et al., 2008; Muller-Moule', 2008; Bulley et al., 2009; Ioannidi et al., 2009; Li et al., 2009; Imai et al., 2009 b). These studies have mostly focussed on the gene expression during fruit development with only little mention given to expression during stress response.

This chapter deals with the preparation, stress treatments and sampling of the plants used for RNA extraction and protein extraction. Furthermore, quantification of the expression of *XvVTC2* in this stress response is analysed. The significance of this is that, to my knowledge, no study has reported the quantification of the expression levels of *VTC2* in response to severe drought or desiccation.

5.2 Materials and methods

5.2.1 Plant stress treatment

X. viscosa plants used in this study were clones generated by splitting a mother plant, that was grown from originally from seed (August 2003), into 5 clones of similar size. The clones were transferred to a long day, 16 hour light and 8 hour dark, 23°C growth room. The plants were acclimatised to the growth room conditions for approximately one year. Prior to stress treatment the dead leaf tips of the plants were trimmed. After the trimming of the tips the plants were left for 2 weeks prior to the start of the stress treatment. The three days prior to the start of stress treatment the plant were watered well.

Leaf samples were taken at approximately 10:00 am for each sample point in the dehydration treatment. Three leaf samples were taken from four of the plants for the first four sample points and thereafter four leaf samples per plant per sample point. The leaves were approximately the same size and each leaf was cut at the base. The leaves were split along the central vein. The part of the split leaves not containing the central vein was cut into smaller pieces, placed in individual foil envelopes and snap frozen using liquid nitrogen. The frozen leaf samples were then stored at -80°C until used for RNA and protein extraction. The part of the split leaves containing the vein was weighed whilst fresh and then placed at 72°C for 48 hours to dry. After drying the leaves were placed in a

desiccator for 15 minutes to cool down. The leaves were then weighed again and the relative water content (RWC) calculated.

The samples taken at the first sample point (representing the fully hydrated state) were used as the absolute water content (AWC). The water content of the leaves calculated after the first sample point were all calculated relative to that of the first sample point (AWC). The formula used for the calculation of the water content is: Water content (WC) = (Fresh weight – Dry weight)/ Dry weight. To get RWC for each sample point, the value obtained for abovementioned equation at that sample point (N) was divided by the value obtained for the first sample point (AWC) and multiplied by 100. The equation for this calculation is: % $RWC_N = (WC_N / AWC) \times 100$ (Farrant, 2009).

5.2.2 Quantitative Real-Time PCR analysis

For quantitative real-time (qRT) PCR analysis of gene expression several processes need to take place. The processes include; the isolation of RNA from the sample to be studied, the conversion of the RNA to cDNA, the running of the RT-PCR using the cDNA as template and the analysis of the RT-PCR data.

Prior to extraction all glassware, spatulas, pestles, mortars, microfuge tubes and tips were double autoclaved. RNA was extracted from the stored leaf samples collected during the desiccation treatment. The RNA was extracted using the BioBasic Tri-Reagent (Bio Basic, Canada). The leaf material was ground in liquid nitrogen using a pestle and mortar. Whilst grinding a small spatula tip of acid purified sand and PVPP were added to the sample. The material was not allowed to thaw and kept on ice to prevent RNA degradation. The half leaf that was ground was split into two separate microfuge tubes; one was stored at -80°C and the other used for extraction. Tri-Reagent (750µl) was added to the ground material, the tubes vortexed for five minutes and incubated at room temperature for five minutes. Thereafter 200µl of chloroform was added and the samples mixed by gentle inversion for 1 minute. The tubes were then incubated at room temperature for three minutes and thereafter centrifuged for 15 minutes at 12000g at 4°C. The aqueous phase was transferred to a fresh microfuge tube and the organic phase stored at -80°C for protein extraction. To the aqueous phase 500µl of isopropanol was added and the tubes incubated at room temperature for 10 minutes to allow for RNA precipitation. The RNA pellet was obtained by centrifugation for 10 minutes at 12000g at 4°C. The

supernatant was discarded and the RNA pellet washed in 1ml of ice-cold 75% ethanol. The RNA samples were centrifuged for 5 minutes at 6000g at 4°C. The pellet was allowed to air dry for 10 minutes and was resuspended in 100µl DEPC treated dH₂O at 55°C for 5 minutes.

After the initial extraction the RNA was DNase treated and further purified using a phenol-chloroform-isoamyl alcohol method. The extracted RNA was treated with DNaseI (Sigma, USA) to remove any DNA contamination in the RNA sample. The reaction mixture contained 44µl extracted RNA, 6µl 10x DNase buffer, 2µl DNaseI enzyme and 8µl DEPC treated dH₂O. The reaction mixture was incubated at room temperature for 30 minutes. An equal volume of Phenol (pH 4): Chloroform: Iso-amyl alcohol (25:24:1) was added and the sample mixed by inversion of the tube. The mixture was centrifuged for 10 minutes 12000g in a microcentrifuge at 4°C. The top aqueous layer was removed and placed in a fresh microfuge tube. To precipitate the RNA 8µl of 3M Sodium acetate (pH5.2) was added and the tube inverted. To this mixture 250µl absolute ethanol was added and the tube inverted. The sample was then again centrifuged at 12000g at 4°C for 20 minutes. The supernatant was discarded; the pellet air dried and resuspended in 50µl DEPC treated dH₂O.

To remove the phenol contaminants remaining in the sample a 1-Butanol-diethyl ether cleanup was done (Krebs et al., 2009). Water saturated 1-Butanol (500µl) was added to the DNase treated RNA sample, the sample was mixed by brief vortexing and the sample centrifuged at 10 000g for 30 seconds. The organic upper layer was carefully removed and discarded. Thereafter 500µl diethyl ether was added, the sample was mixed by brief vortexing and the sample centrifuged at 10 000g for 30 seconds. The upper organic layer was once again removed and discarded and the samples left open in the fumehood to ensure that all the diethyl ether evaporates. The purity and concentration was then evaluated by a Nanodrop 1000D spectrophotometer and by running the samples on agarose gels.

For cDNA conversion the Roche[®] Transcriptor first strand cDNA synthesis kit (Roche, USA) was used. The conversion reactions were set up as half reactions, but the other prescribed reaction conditions in the manual were followed. The reactions were set up using the anchored oligo (dT)₁₈ and random hexamer primers at a ratio of 1:24. Two half

reactions were performed on each RNA sample, and the products of the half reactions were pooled. For most of the samples 500ng of RNA was converted to cDNA per half reaction, thus in total for each sample 1µg of RNA was converted to cDNA. The lowest amount of RNA that was converted to cDNA was 195ng per half reaction. The cDNA was used in Real-Time PCR reactions to quantify the expression levels of *XvVTC2*.

The Real-Time-PCR reactions were set up as outlined in Appendix 2. The same setup was used for the *XvVTC2* as well as the 18s ribosomal RNA reference gene. The thermocycler used was the Rotor-gene[®] 6000 series, and the analysis was done using the software accompanying the machine.

Runs were done to setup standard curves for both the 18s as well the *XvVTC2* primers for all three biological repeats and the dehydration as well as rehydration part of the experiment. The cDNA template used for the standard curve runs were pooled samples of all the timepoints in either the dehydration or rehydration run. In the analysis all the runs were expressed as relative to the expression of the first (fully hydrated) sample. In the calculation of expression level the *XvVTC2* samples were normalised against the 18s reference gene for each specific sample. Relative quantification of the expression was done via two methods, the comparative quantification method (available with the Rotor-gene[®] 6000 software) and the REST method (Pfaffl, 2001). All statistics and graphs were drawn in Microsoft Excel 2003.

5.3 Results and Discussion

5.3.1 Plant stress treatment

There are many factors which influence the rate at which a plant dries. These factors include the size of the plant, soil moisture before drying, soil texture, temperature and light. To control many of these factors, the plants in this experiment were kept under the same temperature, light conditions, pot size, soil components, the plants were of similar size and all were fully watered at the start of the experiment. Even though these conditions were kept constant, natural variability was still observed in the dehydration and rehydration process (Figures 5.1). This variability was greatest in the beginning stages of the experiment and towards the end as the plants rehydrated. Large degrees of variation have been found in *X. humilis* and *C. wilmsii* in the early stages of dehydration as well (Farrant et al., 1999).

The quick recovery of the plant is common in resurrection plants and a very similar timecourse has been reported previously for *X. viscosa* (Gaff, 1977; Sherwin and Farrant, 1996). When compared with *C. wilmsii* and *M. flabellifolium*, the rate at which rehydration takes place is very similar in *X. viscosa*. However, even though the rate of water uptake is similar, *X. viscosa* takes longer to reach full metabolic activity due to its poikilochlorophyllic nature (Sherwin and Farrant, 1996). A hypothesis that could be made from this observation is, when compared to the other two plants, *X. viscosa* is more reliant on stored energy sources to rebuild its membranes and survive slightly longer without photosynthesis.

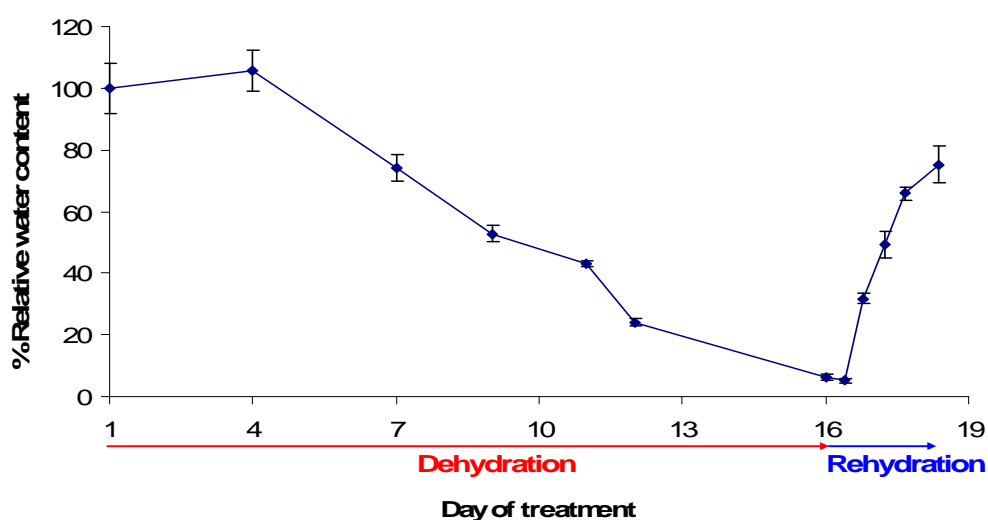


Figure 5.1: A graph showing the mean \pm SE (n=3) of the relative water content of *X. viscosa* plants. Leaf material was used to calculate the water content of the plants. Each sample point indicates the average of two technical repeat samples for three plants at that point. The dehydration sample points are indicated by the red line and the rehydration sample points are indicated by the blue line. The first day of sampling measurement was used as the full turgor measurement, the rehydration sample points are 10, 21, 30, 40 and 57 hours after watering. The relatively small error bars from the graph indicates that the plants dried at a similar rate.

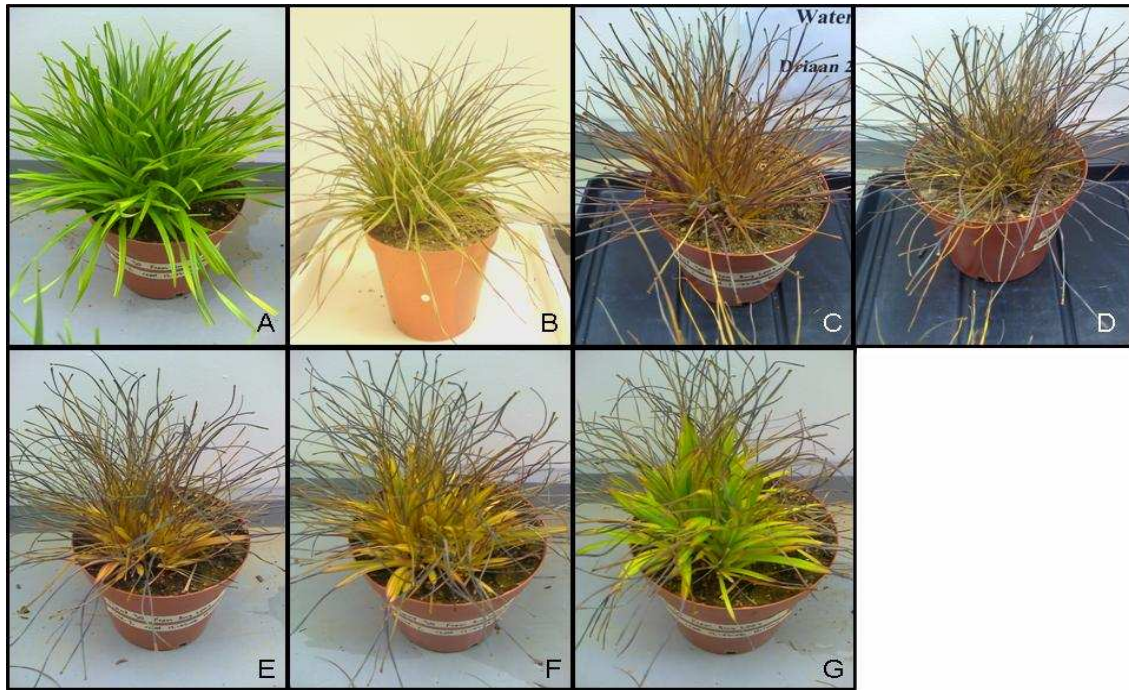


Figure 5.2: Images showing the drying and re-hydration of *Xerophyta viscosa* in a long day, 16h light and 23°C, growth room. A, fully hydrated plant (100% absolute water content, AWC). B, 70% RWC, C, 35% RWC, D, 7% RWC. Images E - G show a recovering plant at approximately 45%, 65% and 80% RWC respectively. All the images are of the same plant except image B which is a plant of similar size and age under the same stress treatment in the same growth room.

As dehydration progresses, the leaves change colour from a deep green to a yellow/brown colour and some leaves turn purple in colour (Figure 5.2). The brown yellow colour observed has been observed at approximately 35% RWC in other studies as well (Bhatt et al., 2009). The purple colour observed can be attributed to the production of anthocyanins and violaxanthin (Sherwin and Farrant, 1996; Sherwin and Farrant, 1998). The leaves dry from the ends down to the centre of the plant and fold in half along the midrib (Figure 5.2, B - D). Upon rehydration the leaves at first expand from the centre towards the ends (Figure 5.2, E - G). The leaves then start turning green again at approximately 80% RWC, which in this case is 57 hours after watering (Figure 5.2, G). From the reviewed literature presented in Chapter 1 as well as the above references the dehydration and rehydration cycle presented here is typical for *X. viscosa*.

5.3.2 Quantitative Real-Time PCR analysis

The expression of *XvVTC2* increases dramatically at approximately 50% RWC. The response is an initial 10 fold increase at 50% RWC and as the RWC decreases the expression level increases until a plateau of approximately 1000 fold is reached at 25% RWC (Figures 5.3 & 5.4). The expression levels start decreasing slowly as the plant is rehydrated, and if the experiment could have been prolonged for some time after achievement of full rehydration, it is expected that expression levels would have reached the same basal levels as before treatment. A similar trend is apparent across three biological replicates (Figures 5.3 & 5.4).

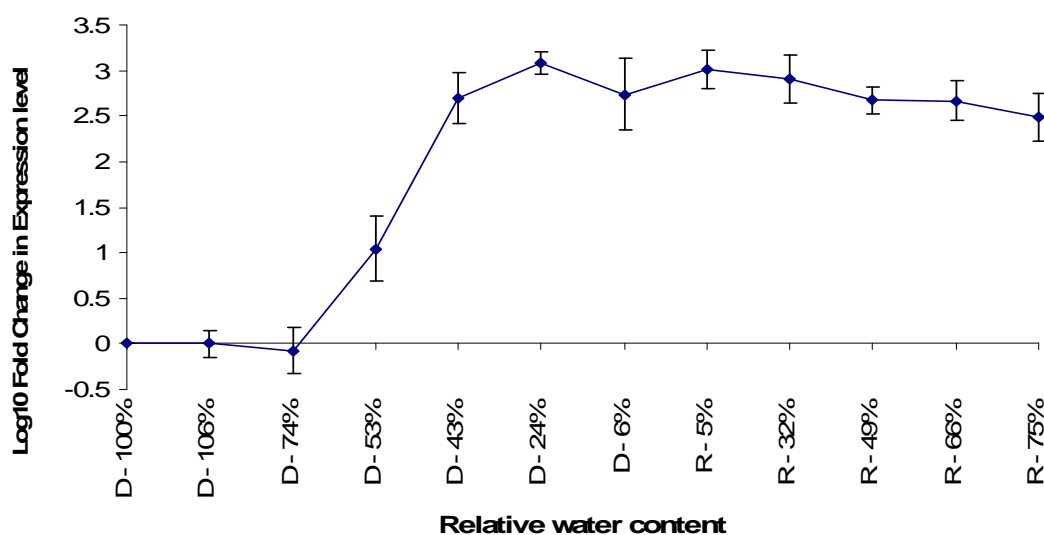


Figure 5.3: A graph showing the mean \pm SE (n=3) relative change mRNA expression level of *XvVTC2*, compared to 18s ribosomal RNA of *X. viscosa* plants under dehydration stress calculated by the comparative quantification method (Rotorgene 6000 software). The change in expression level (Y-axis) is indicated as a log10 fold change. The standard error of the mean is indicated by the error bars at the respective point of the graph. The mean relative water content of the plants is indicated on the X-axis as a percentage of absolute water content (full turgor). The respective D or R preceding the percentage water content indicates the dehydration (D) and rehydration (R) phases of the treatment.

Two different statistical methods were used to quantify the relative change in expression level of *XvVTC2*. These methods were; the comparative quantification method, provided as part of the Rotorgene 6000 software, as well as the Pfaffl REST method (Pfaffl, 2001). These methods gave different results when looked from an absolute value point of view (Figures 5.3 and Figures 5.4). The reaction curves can be viewed in appendix 8.

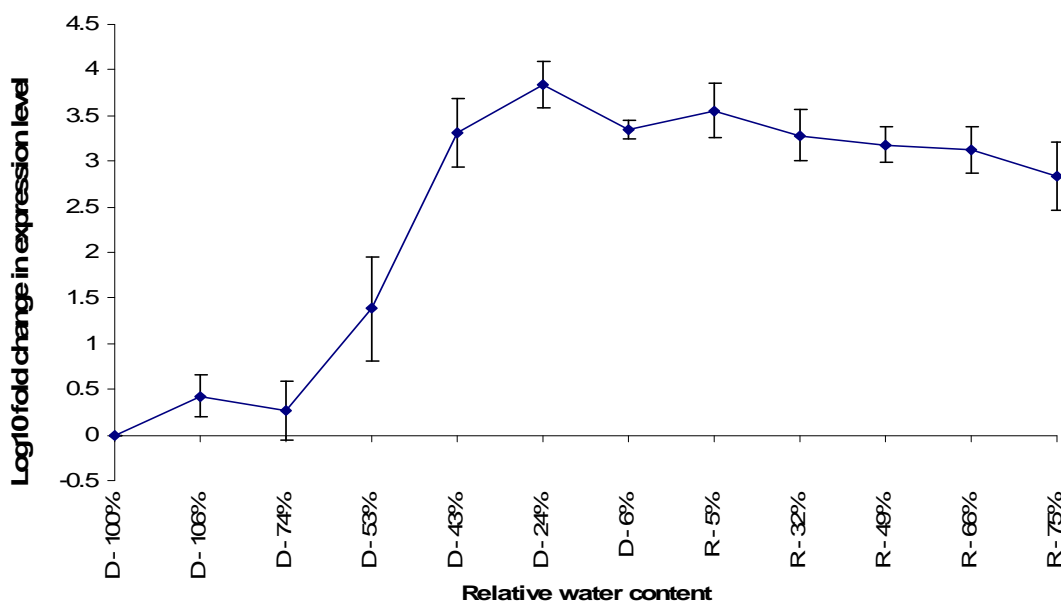


Figure 5.4: A graph showing the mean \pm SE (n=3) relative change mRNA expression level of *XvVTC2*, compared to 18S ribosomal RNA of *X. viscosa* plants under dehydration stress calculated by the Pfaffl REST method (Pfaffl, 2001). The change in expression level (Y-axis) is indicated as a log10 fold change. The standard error of the mean is indicated by the error bars at the respective point of the graph. The mean relative water content of the plants is indicated on the X-axis as a percentage of absolute water content (full turgor). The respective D or R preceding the percentage water content indicates the dehydration (D) and rehydration (R) phases of the treatment.

The differences in these methods is that the REST method requires standard curves, for the gene of interest (GOI) as well a reference gene, to be run at the start of the experiment which are then used to calculate the relative expression. This however means that the reaction efficiency between the standard curve run and the sample runs have to be the same. In these experiments the standard curve run could not be included with the sample run, due to the number of samples, and had to be run separately. Thus a difference in reaction efficiency between standard curve run and the sample runs would increase the error. A further drawback of this method is that if the same conditions are not present in future runs i.e. reagents differ, the results can be difficult to compare across experiments. However the method has been widely used and in these experiments the Pfaffl REST method shows the same trend as that of the comparative quantification method available with the Rotorgene 6000 software.

The comparative quantification method takes into account the reaction history of each reaction and does not use a standard curve. The software takes into account the take-off

point of the reaction, which is where the reaction leaves the linear background and the efficiency of each reaction is calculated. The formula uses the assay average amplification value, which is then used to calculate the relative expression. A disadvantage of this method is that it can only be used with the Rotorgene 6000 instrument, thus it would be difficult to do comparisons with results from other qRT-PCR instruments.

The more conservative estimate in relative expression is calculated using the Rotorgene comparative quantification method. Thus, by using the conservative estimate, from these results it can be reported that at least a 1000 fold increase in expression level of *XvVTC2* is observed in response to desiccation in the resurrection plant *X. viscosa*. However, from evidence highlighted in other studies, it is not uncommon for the *VTC2* gene in other plants to be upregulated by more than a thousand fold (Badejo et al., 2008).

The large increase in expression level during dehydration, if real, is of significance. However, this is not the first time that an expression level change of such magnitude has been reported for a *VTC2* homolog. In acerola (*Malphigia glabra*) the relative mRNA expression level also shows changes in excess of a thousand fold in fruit harvested at different time points post anthesis (Badejo et al., 2008). Furthermore, of all the ASC biosynthesis genes profiled the most significant change in expression is observed at the *VTC2* step of the pathway. The production of ASC in the plant is also correlated with the increase in expression level of the biosynthetic pathway genes. These facts indicate that the *VTC2* step of the pathway holds significance in terms of the regulation of ASC production.

Further evidence highlighting the importance of *VTC2* as a control point in the pathway, is found in the increase in ASC levels when *VTC2* is overexpressed in tobacco (*Nicotinia tabacum*) and *A. thaliana* (Bulley et al., 2009). The increase in ASC level is significant (4.2 fold) when just *VTC2* is overexpressed, however when both GME and *VTC2* are overexpressed the increase in ASC content is more than 8 fold. When just GME is overexpressed there is only a 1.2 fold increase in ASC content (Bulley et al., 2009). This shows that a major limiting factor of ASC biosynthesis is *VTC2* concentration and once that has been saturated, substrate availability becomes the limiting factor.

In *A. thaliana* there is also a stress induced increase in mRNA expression level of *VTC2*. Data from the Botany Array Resource shows that cold, osmotic, salt, UV-B and water deficit stress all lead to approximately a two fold increase in expression of *VTC2* (at4g26850) (Toufighi et al., 2005). The experimental design can be viewed in Appendix 7. This agrees with and provides context for the stress induced response observed in *X. viscosa*. The change in expression level might not be of the same magnitude, as the severity of the stress the plants were subjected to, were not of the same level either. It is important to note that the response to water deficit stress in the eFP browser is an early response and the expression level of *VTC2* is at normal levels when the stress is prolonged. The data available on the resource is data from *A. thaliana* experiments, a plant that cannot withstand desiccation. Furthermore, with the greatest response in *X. viscosa* being rather late, at approximately 50% RWC, it is not possible to compare the level of the stress response. Therefore, the only valid comparison that can be made is to take note of the presence of an increase in *VTC2* expression levels in response to stress in both plants. Of the hormones tested, the greatest increase in expression is in response to methyl jasmonate treatment. This data is validated by that fact that methyl jasmonate is known to be involved in stress response and more specifically the regulation of the ascorbate – glutathione cycle in stress response (Sasaki-Sekimoto et al., 2005). This mediation by jasmonates is believed to be vital to the coordinated response and provides resistance to environmental stresses (Wasternack and Parthier, 1997; Sasaki-Sekimoto et al., 2005).

Another family of hormones that increases the expression of *VTC2* is the brassinosteroids. These hormones are well known for their involvement in signal transduction pathways and involvement in stress response. The treatment of plants with brassinosteroids has shown to increase protection against many abiotic stresses (Clouse and Sasse, 1998). There is also an induction of antioxidant enzyme activity when plants are treated with these hormones (Nunez et al., 2004). Taking this evidence into account it is not inconceivable that *VTC2* production would be induced by the hormone. The relationship that brassinosteroids have with *VTC2*, ascorbate production and stress response is a possible point for further research that could shed some light on how plants cope with stress.

In *X. viscosa* in the response to desiccation, an initial increase in *XvVTC2* expression can be attributed to the increase in ROS as well as the need for ASC in its other roles related to stress response reviewed in Chapter 1. Once the absolute desiccated state is reached, approximately 6% RWC, the production of ASC is most probably reduced or even halted as the metabolism shuts down because of the lack of water. However, the mRNA level of *XvVTC2* still remains high and is presumably not degraded. It has been found in *C. wilmsii* that the plant does not rely on new transcription or translation during rehydration to recover from the desiccated state (Cooper and Farrant, 2002). When plants are rapidly dehydrated, they do however require new transcription and translation for recovery. In *X. humilis*, recovery of photosynthesis on rehydration also does not require transcription (this is happening during dehydration) but translation is required (Dace et al., 1998). Thus a similar mode of function can be at play for *XvVTC2* and probably other stress response genes in *X. viscosa*. There is also a need for ASC during recovery whilst the plant is returning to photosynthetic capacity. The photosynthetic machinery of resurrection plants is fully active even before complete rehydration (Sherwin and Farrant, 1996). Preserving the mRNA of *XvVTC2* allows the plant to rapidly respond to the need for ASC once water becomes available and metabolic functions, which produce ROS, are resumed.

The focus of this work is mainly related to expression of *XvVTC2* in response to water deficit stress. However it is important to note that several other studies have reported differential expression of *VTC2* homologs relating to other environmental cues, such as light levels and circadian rhythms (Dowdle et al., 2007; Yabuta et al., 2007). Dowdle et al., reported that when *A. thaliana* plants are transferred to high light level there is an approximately 5 fold increase in *VTC2* transcript levels and a 2 fold increase of *VTC5* transcript levels. The *VTC2* transcript data is also supported by data from Yabuta et al., (2007). There is also after several hours a 20 fold increase in GDP-L-galactose phosphorylase activity as well as an increase in the ASC pool size (Dowdle et al., 2007). Furthermore, it was reported that the other genes in the L-galactose pathway were not as responsive under high light as *VTC2*. As further evidence for the light regulation of *VTC2* transcript levels it has been found that the expression of the gene is dependant on the photosynthetic electron transport chain (Yabuta et al., 2007).

The regulation of *VTC2* by light would also suggest that circadian rhythms would play a role in gene regulation. When *A. thaliana* plants are dark and light treated for 24 hours respectively, the same pattern of *VTC2* expression has been observed as a plant that exposed to a regular light dark cycle over 24 hours (Dowdle et al., 2007). The absolute value of the expression level differs but the pattern remains constant which suggests that *VTC2* is controlled by the circadian clock.

5.4 Conclusions

The results presented here indicate that *XvVTC2* is significantly upregulated in response to desiccation in *X. viscosa*. The response is late and the levels are maintained during rehydration as well. The expression of *VTC2* homologs in other plants have shown to be upregulated in response several environmental stresses, developmental responses and light. These processes all require ASC as an antioxidant as ROS are produced. The involvement of ASC during several other responses, with particular reference to its role in the violaxanthin cycle and as electron donor during photosynthesis, could be of significance in how ASC could, in addition to ROS quenching, protect the plant and aid in recovery.

The high levels of *XvVTC2* mRNA also indicate that the RNA is not degraded during desiccation. This could allow the plant to respond immediately once water becomes available again. The increase of *VTC2* levels by jasmonic acid and brassinosteroids, both hormones that are associated with stress response signalling, indicate that these hormones play a role in the signalling cascade leading to ascorbate production (Appendix 7) (Toufighi et al., 2005). The fact that *VTC2* is upregulated by these hormones provides support for the argument that the *VTC2* is involved in the regulation of the flux through the L-galactose pathway.

6 Chapter 6: Overview and Conclusions

University of Cape Town

The aims of this dissertation were to characterise the *XvVTC2* gene in terms of sequence, expression in response to dehydration stress, cellular localisation and biochemical function. The results were used to propose possible modes of action of *XvVTC2* and how it might contribute to the ability of *X. viscosa* to withstand desiccation.

Sequence analysis revealed a high degree of similarity between *XvVTC2* and other *VTC2* homologs. The characteristic Hit-motif was present as well as other highly conserved regions within the protein. These regions include an N-myristoylation site, predicted nucleotide binding sites and a nuclear localisation signal. The function and significance of the N-myristoylation site, nucleotide binding sites and an additional nuclear localisation signal need to be determined experimentally. Several predicted phosphorylation sites might provide insights into the regions of the protein that are targeted for regulation.

Expression of the *XvVTC2* protein in *E. coli* required a considerable amount of optimisation. However, the protein was expressed and purified successfully. For future studies it would be valuable to optimise expression using a vector that adds fewer tags to the protein. An attempt can also be made to cleave the tags from the soluble recombinant protein after purification. The removal of the tags would provide a protein closer to its native state and would be of more value in structural, biochemical and kinetic studies.

Biochemical assays confirmed the GDP-D-glucose phosphorylase activity of the protein. By inference the protein is expected to exhibit GDP-L-galactose phosphorylase activity, and thereby its role in the ASC biosynthesis pathway. This activity could not be tested due to substrate availability issues. Only phosphorylase activity of the enzyme was tested and further studies would have to be conducted to investigate the possibility of guanyltransferase activity. Further assays will need to be done to determine the kinetics of the reactions presented.

Localisation studies indicated that the protein was localised to the nucleus and cytoplasm. This was predicted by the presence of nuclear localisation signals as well as a study by Muller-Moulé (2008) that showed the *A. thaliana* *VTC2* homolog was localised to the nucleus. The function of the protein in the nucleus is yet to be elucidated. It has been proposed that the protein might be involved in nucleotide cycling and could thereby affect

gene regulation. However further experiments where mutants are created in which the nuclear localisation signals are altered could provide further insight into the role of XvVTC2 in the nucleus. Nuclear localisation of the protein does suggest that the protein has other functions other than its phosphorylase activity en route to ASC biosynthesis.

Western blot analysis showed that the protein expression levels did not follow the same trend as the mRNA expression. This might indicate that XvVTC2 protein expression is to some extent regulated before translation at the mRNA level. The protein extraction and western blotting technique needs optimisation and further studies will need to be done to explain differences between protein and mRNA expression levels. The western blotting did however indicate that XvVTC2 might act as a dimer in its active form. However this needs to be confirmed by X-ray crystallography. Other possible expression analysis studies could also include various other stresses as well as hormone treatments.

Expression analysis showed that XvVTC2 is upregulated in response to desiccation in *X. viscosa*. Quantitative real-time PCR showed a significant increase, in excess of a thousand fold, in mRNA expression level at approximately 50% RWC. This is a relatively late response to desiccation and it proposed that the increase in expression is to supplement a depleted antioxidant defence system and thereby limit damage caused by ROS. The accumulation of XvVTC2 mRNA just before the virtually completely dry state could be in preparation for when water becomes available again. When water becomes available the plant would need ASC as antioxidant to quench ROS that are produced as the metabolic functions are resumed.

The significant increase in expression level of VTC2 has not been reported for a water stress related response in any other plant at either mRNA or protein level. This could be purely due to the nature of the resurrection plant studied here. Other, non resurrection plants do not possess the ability to survive under the conditions where the XvVTC2 gene is expressed. Therefore, it is predicted that regulatory mechanism in *X. viscosa* controlling XvVTC2 expression is different to that of plants used in other studies. The significance of this regulatory mechanism lies in that it is water deficit stress inducible. Further studies in which the promoter region of the XvVTC2 gene is isolated and tested in

other plants are underway. These studies are aimed to provide a water deficit stress inducible gene construct which can be used increase the drought tolerance of crop plants.

The improvement of drought tolerance of crop plants, via molecular techniques however should be treated with caution. A drought resistant crop plant does not necessarily mean the plant will have a high or even acceptable yield. It merely means that a plant subjected to drought will be able to survive the drought and depending on the stage of development might provide a yield advantage. This view is discussed by Serraj and Sinclair (2002) in terms of osmolyte accumulation in response to drought. A proposal from that study, which could be beneficial, is if root development is maintained so that the plants may reach deeper water sources in the soil. These views should not act as a deterrent but should be kept in mind when testing crops for increased drought tolerance under glasshouse or artificial conditions. An advantage of using *XvVTC2* is that, as discussed in Chapter 1, ASC plays a role in cell growth and root development. This combined with the other protective and signalling roles that ASC is involved in justifies further investigation into the potential of using *XvVTC2* in an attempt to confer drought tolerance to crop plants.

In conclusion, the goals set out at the start of the project have been reached and the results correspond with other studies conducted by Laing *et al.* (2007), Linster *et al.* (2007) and Muller-Moulé (2008). The results obtained in this project have increased the knowledge in terms of ASC regulation in response to desiccation in *X. viscosa*. Furthermore a platform for future studies involving the characterisation of *XvVTC2* and response to desiccation in *X. viscosa* has been created.

Appendix 1 – Oligos

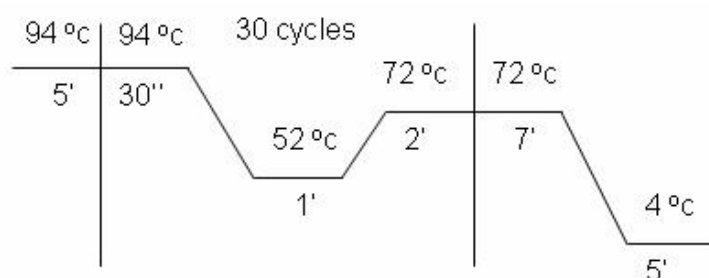
VTC2seqF:	5'-ggCTCTgCgTTgTgAATTg-3'
VTC2seqR1:	5'-TgCTTCTTgTAATgTTTAAgTTCCC-3'
VTC2seqR2:	5'-TCATTgTAaggACCAggCAg-3'
VTC2expF:	5'-CACggATCCgATgTTgAAgATTTggAgAgTgC-3'
VTC2expR:	5'-CgCgAgCTCgCCTggAggACTAgTCAACTC-3'
VTC2yfpR:	5'-TggTACCCgCTggAggACTAgTCAACTC-3'
VTC2rtF:	5'-CTgTATgggAgATAAgCggTCACATgg-3'
VTC2rtR:	5'-CCAgTggCCTCgAATATggATgCTTTC-3'
VTC2splnk2:	5'-gTgCCTgCCTTCgTTCAgTTgAgC-3'
VTC2int	5'-ggAggATCgAATgCgCAAaggAC-3'
VTC2splnk_R1:	5'-ggAAgACAgCATCCgCCgAgAC-3'
VTC2splnk_R2:	5'-gCAACCATCgTCgTCCATgAAgTTgg-3'
SplnkA:	5'-CgAATCgTAACCgTTCgTACgAgAATTC-3'
SplnkB:	5'-TCgTACgAgAATCgCTgTCCTCTCC-3'
Splnktop:	5'-CgAATCgTAACCgTTCgTACgAgAATTCgTACgAgAATC gCTgTCCTCTCCAACgAgCCAAgA-3'
SplnkXbaI	5'-CTAgTCTTggCTCgTTTTTTTTTgCAAAAA-3'
M13 forward	5'-gTAAAACgACggCCAgt-3'
M13 reverse	5'-CAggAAACAgCTATgAC-3'
pJet reverse	5'-AAgAACATCgATTTTCCATggCAg-3'
T7	5'-TAATACgACTCACTATAggg-3'

Appendix 2 – PCR Conditions

Standard PCR conditions:

Reaction conditions	
Stock Solution	Working concentration
10mM DNTPs	200 μ M
Buffer 10 X	1 X
10 μ M Forward Primer	400 nM
10 μ M Reverse Primer	400 nM
Polymerase (Taq)	1 unit
Target DNA (cDNA)	100 ng
MgCl ₂	1.5 mM

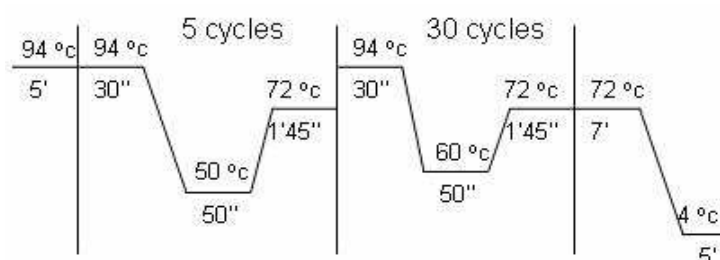
Cycling Conditions



PCR Conditions for Expression Primers:

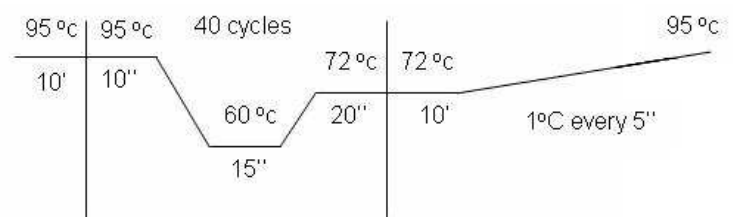
Reaction conditions	
Stock Solution	Working concentration
10mM DNTPs	200 μ M
Buffer 10 X	1 X
10 μ M Forward Primer	400 nM
10 μ M Reverse Primer	400 nM
Polymerase (Phusion High fidelity polymerase)	1 unit
Target DNA (cDNA)	25 ng
MgCl ₂	1.5 mM

Cycling Conditions



PCR conditions for qRT-PCR

Reaction conditions	
Stock Solution	Working concentration
Quantace sensi-mix	1 X
SYBR green	1 X
Primer mix	200 nM
Target DNA (cDNA)	1 μ l

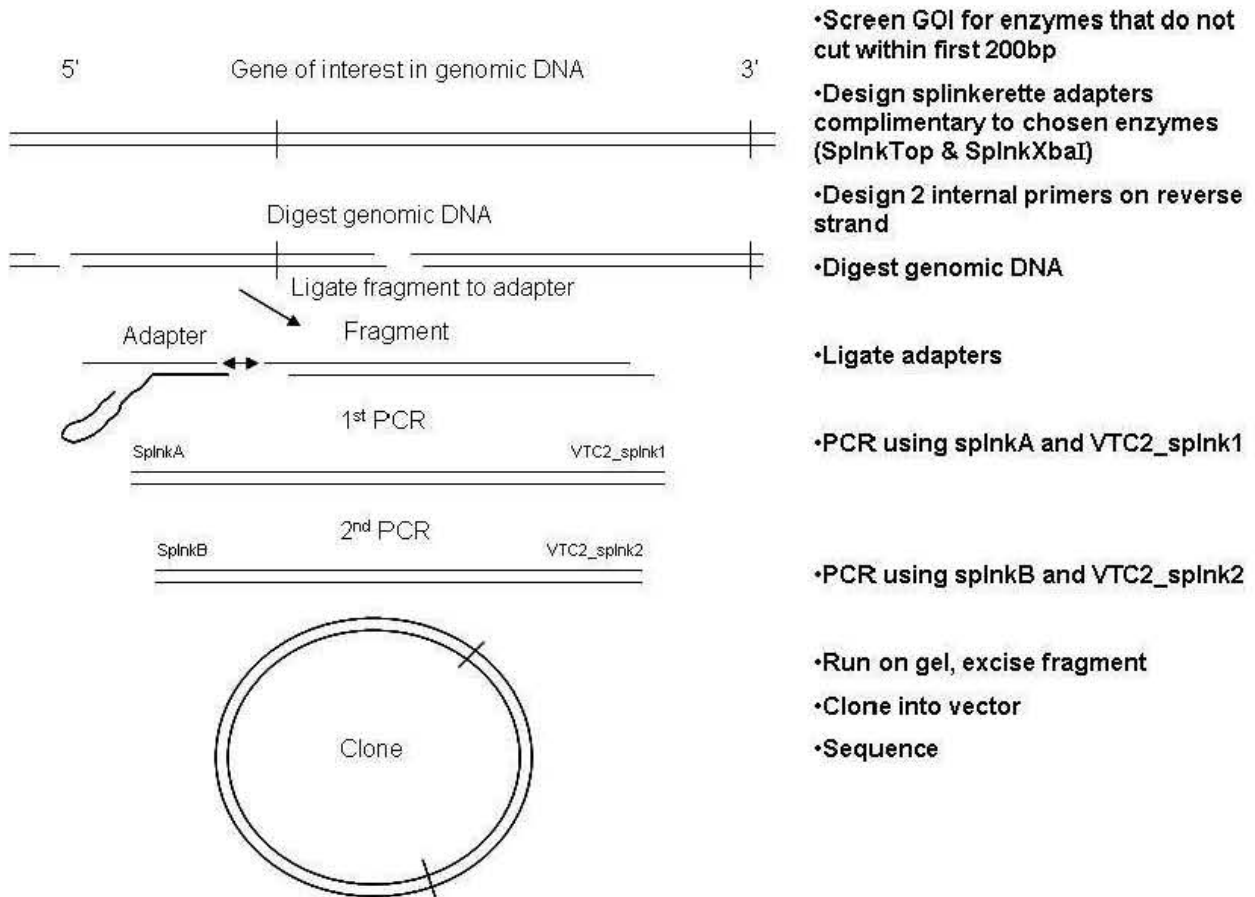


Appendix 3 – Transformation protocol

E. coli DH5 α competent cells were taken from -70°C and allowed to thaw on ice for 10 min. The ligation product was then added and the cell incubated on ice for a further 10 min. The cells were then heat shocked at 37°C for 4 min 55 sec then placed on ice for 2 min, after which 900 μ l LB media was added and the cells incubated in a shaker at 37°C for 90 min. The transformed cells were then plated on LB agar plates containing 100 μ g.ml⁻¹ ampicillin

University of Cape Town

Appendix 4 – Splinkerette flow diagram



Appendix 5 cDNA sequence

XVUTC2 Clone R1-2	NNNGGATTTTGAATTTGTGTAGAAAGATAATAGTTTC	AAAGATGTTGAAGAT	52
XVUTC2 Clone R1-3	NNCCGATTTTCGASATTTGTGTAGAAAGATAATAGTTTCTAAAGATGTTGAAGAT		54
XVUTC2 Clone R2-11	NCCAGATTTTCGASATCTGTGTAGAAAGATAATAGTTTCTAAAGATGTTGAAGAT		54
Consensus	n gattt ga at tgtgtagaaagata tagtttg aaagatgttgaagat		
XVUTC2 Clone R1-2	TTGGAGAGTGCCGACAT	TAGTTTCCAACCTTCATGGACGACGATGGT	106
XVUTC2 Clone R1-3	TTGGAGAGTGCCGACAT	TAGTTTCCAACCTTCATGGACGACGATGGT	108
XVUTC2 Clone R2-11	TTGGAGAGTGCCGACCTCTATTTTCCAACCTTCATGGACGACGATGGT	TGCGGCCG	109
Consensus	ttggagagtgcgcac t ta tttccaacttcattggacgacgatgg tgcggcgg		
XVUTC2 Clone R1-2	CAACTGTCTCGGCGGATGCTGTCTTCCAACCTCTAAAT	TGCCATTGTATGCCTTC	161
XVUTC2 Clone R1-3	CAACTGTCTCGGCGGATGCTGTCTTCCAACCTCTAAAT	TGCCATTGTATGCCTTC	163
XVUTC2 Clone R2-11	CAACTGTCTCGGCGGATGCTGTCTTCCAACCTCTAAAT	TGCCATTGTATGCCTTC	164
Consensus	caactgtctcggcggatgctgtcttccaacctctaaa tgccattgtatgccttc		
XVUTC2 Clone R1-2	AAACCTGATTTCGGGTCCTCTGTCTAGCACTGGGGATCTACCTTCAGACTTCTTCC		216
XVUTC2 Clone R1-3	AAACCTGATTTCGGGTCCTCTGTCTAGCACTGGGGATCTACCTTCAGACTTCTTCC		218
XVUTC2 Clone R2-11	AAACCTGATTTCGGGTCCTCTGTCTAGCACTGGGGATCTACCTTCAGACTTCTTCC		219
Consensus	aaacctgattcgggtcctcctgtctagcaactggggatctaccttcagacttcttc		
XVUTC2 Clone R1-2	TGCACACATTGCTTTTGGCAAGTGGGAGGATCGAATGCGCAAAGGACTGTTTCG		271
XVUTC2 Clone R1-3	TGCACACATTGCTTTTGGCAAGTGGGAGGATCGAATGCGCAAAGGACTGTTTCG		273
XVUTC2 Clone R2-11	TGCACACATTGCTTTTGGCAAGTGGGAGGATCGAATGCGCAAAGGACTGTTTCG		274
Consensus	tgacacattgtctt ttggcaagtgggaggatcgaatgcgcaaaggactgtttcg		
XVUTC2 Clone R1-2	ATACGATGTGACCACATGCG	AAACGAAGGTGATCCCGGGAAAGCATGGATTCAATT	326
XVUTC2 Clone R1-3	ATACGATGTGACCACATGCG	AAACGAAGGTGATCCCGGGAAAGCATGGATTCAATT	328
XVUTC2 Clone R2-11	ATACGATGTGACCACATGCG	AAACGAAGGTGATCCCGGGAAAGCATGGATTCAATT	329
Consensus	atacgatgtgaccacatgc aaacgaaggtgatcccgggaaagcatggattcatt		
XVUTC2 Clone R1-2	GCTCAACTGAACGAAGGCAGGCACCTTAAGAAAAGGCCTACTGAATTCAAGAGTTG		381
XVUTC2 Clone R1-3	GCTCAACTGAACGAAGGCAGGCACCTTAAGAAAAGGCCTACTGAATTCAAGAGTTG		383
XVUTC2 Clone R2-11	GCTCAACTGAACGAAGGCAGGCACCTTAAGAAAAGGCCTACTGAATTCAAGAGTTG		384
Consensus	gctcaactgaacgaaggcaggcaccttaagaaaaggcctactgaattcagagttg		
XVUTC2 Clone R1-2	ATCGGGTGCTTCAACCTTTCGATCCAGACAAGTTCAATTTACCAAGGTTGGACA		436
XVUTC2 Clone R1-3	ATCGGGTGCTTCAACCTTTCGATCCAGACAAGTTCAATTTACCAAGGTTGGACA		438
XVUTC2 Clone R2-11	ATCGGGTGCTTCAACCTTTCGATCCAGACAAGTTCAATTTACCAAGGTTGGACA		439
Consensus	atcgggtgcttcaacctttcgatccagacaagttcaatttccaagggttggaca		
XVUTC2 Clone R1-2	GGAGGAGGTTCTCTCCGCTTCGAGCCAGTGTGACAGCAAGTCAAACTTCTCC		491
XVUTC2 Clone R1-3	GGAGGAGGTTCTCTCCGCTTCGAGCCAGTGTGACAGCAAGTCAAACTTCTCC		493
XVUTC2 Clone R2-11	GGAGGAGGTTCTCTCTCCGCTTCGAGCCAGTGTGACAGCAAGTCAAACTTCTCC		494
Consensus	ggaggaggttctc tccgcttcgagccagtggtgacagcaagtcaaaacttctcc		
XVUTC2 Clone R1-2	GAGAGTGCGCCTATCGATTCAAATGACACCCCAAACGTCGTTGCAATCAATGTGA		546
XVUTC2 Clone R1-3	GAGAGTGCGCCTATCGATTCAAATGACACCCCAAACGTCGTTGCAATCAATGTGA		548
XVUTC2 Clone R2-11	GAGAGTGCGCCTATCGATTCAAATGACACCCCAAACGTCGTTGCAATCAATGTGA		549
Consensus	gagagtgcgcctatcgattcaaatgacaccccaaacgtcggtgcaatcaatgtga		
XVUTC2 Clone R1-2	GCCCAGTCGAGTACGGCCATGTCTCTTATTCCCCGTGTTTTGACTGTATACC		601
XVUTC2 Clone R1-3	GCCCAGTCGAGTACGGCCATGTCTCTTATTCCCCGTGTTTTGACTGTATACC		603
XVUTC2 Clone R2-11	GCCCAGTCGAGTACGGCCATGTCTCTTATTCCCCGTGTTTTGACTGTATACC		604
Consensus	gcccagtcgagtacggccatgtctcttattccccgtgttttgaactgtatacc		
XVUTC2 Clone R1-2	GCAAAGGATTGATCGAATGAGCTTTGAGCTTGCGGTTCGTATGGCTGCAGAGGCT		656
XVUTC2 Clone R1-3	GCAAAGGATTGATCGAATGAGCTTTGAGCTTGCGGTTCGTATGGCTGCAGAGGCT		658
XVUTC2 Clone R2-11	GCAAAGGATTGATCGAATGAGCTTTGAGCTTGCGGTTCGTATGGCTGCAGAGGCT		659
Consensus	gcaaaggattgatcgaatgagctttgagcttgcggttcgtatggctgcagaggct		

Appendix 5: Multiple sequence alignment of the sequences obtained from three colony PCR positive clones of *XvVTC2*. The first two lines indicate the sequences obtained from two *XvVTC2* clones using the VTC2seqF and VTC2seqR1 primers, the third line shows the sequences obtained from the clone using the VTC2seqF and VTC2seqR2 primers. The consensus sequence is shown in the fourth line. Full homology between bases is indicated in dark blue, homology between two of the bases is indicated in light blue and a white base shows no homology to any of the other aligned bases.

University of Cape Town

Appendix 6 – SDS Poly-acrylamide gel recipes

5% Stacking gel pre-mix	
dH2O	89.23 ml
1.5M Tris.HCl pH 6.8	9.6 ml
20% SDS	575 μ l
Total	99.4 ml

5% Stacking gel:		
	2 gels	4 gels
Pre-Mix	3.25 ml	6.5 ml
40% Acrylamide 19:1	525 μ l	1.5ml
10% APS	210 μ l	420 μ l
TEMED	5 μ l	10 μ l

12% Resolving gel pre-mix	
dH2O	129.3
1.5M Tris.HCl pH 8.8	8.76 ml
20% SDS	1.5 ml
Total	206.8 ml

12% Resolving gel:		
	2 gels	4 gels
Pre-Mix	6.8 ml	13.6 ml
40% Acrylamide 19:1	3 ml	6 ml
10% APS	200 μ l	400 μ l
TEMED	12 μ l	24 μ l

10% Ammonium persulfate (APS)	
Ammonium persulfate	1 g
dH2O up to	10 ml
Stable at 4oC for 2 weeks	

4 x SDS sample buffer	
Tris.HCl pH 6.8	1.66 ml
20% SDS	4 ml
DTT	0.62 g
Bromophenol blue	0.005 g
dH2O up to	10 ml

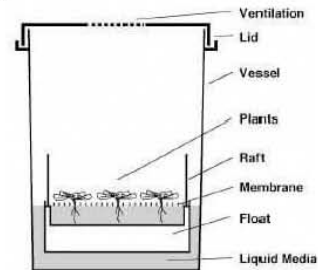
10 x SDS Electrophoresis Buffer	
Tris Base	30 g
Glycine	144 g
SDS	10 g
dH2O up to	1 L

Appendix 7 – eFP expression profiles of *VTC2* in *A. thaliana*

Abiotic stress

At4g26850 253922_at

Arabidopsis eFP Browser at bar.utoronto.ca
Winter et al., 2007. PLoS One 2(8): e718



- Plant material from 18 day old wild-type *Arabidopsis thaliana* plants of Columbia-0 ecotype was analyzed
- The seeds were sown on rafts in Magenta boxes containing MS-Agar-media. After 2 days in the cold room (4°C, dark), the boxes were transferred to a long day chamber. At day 11, the rafts were transferred in Magenta boxes containing MS-liquid-media.
- The plants were grown under long day conditions with 16/8 hrs light/dark, 24°C, 50% humidity and 150 $\mu\text{Einstein}/\text{cm}^2$ sec light intensity
- All measurements were taken in duplicates - the average of which is shown
- RNA was isolated and hybridized to the ATH1 GeneChip
- The data were normalized by GCOS normalization, TGT 100
- This study is part of the ATGenExpress project, funded by the DFG

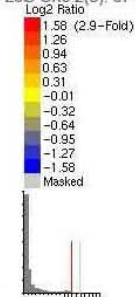
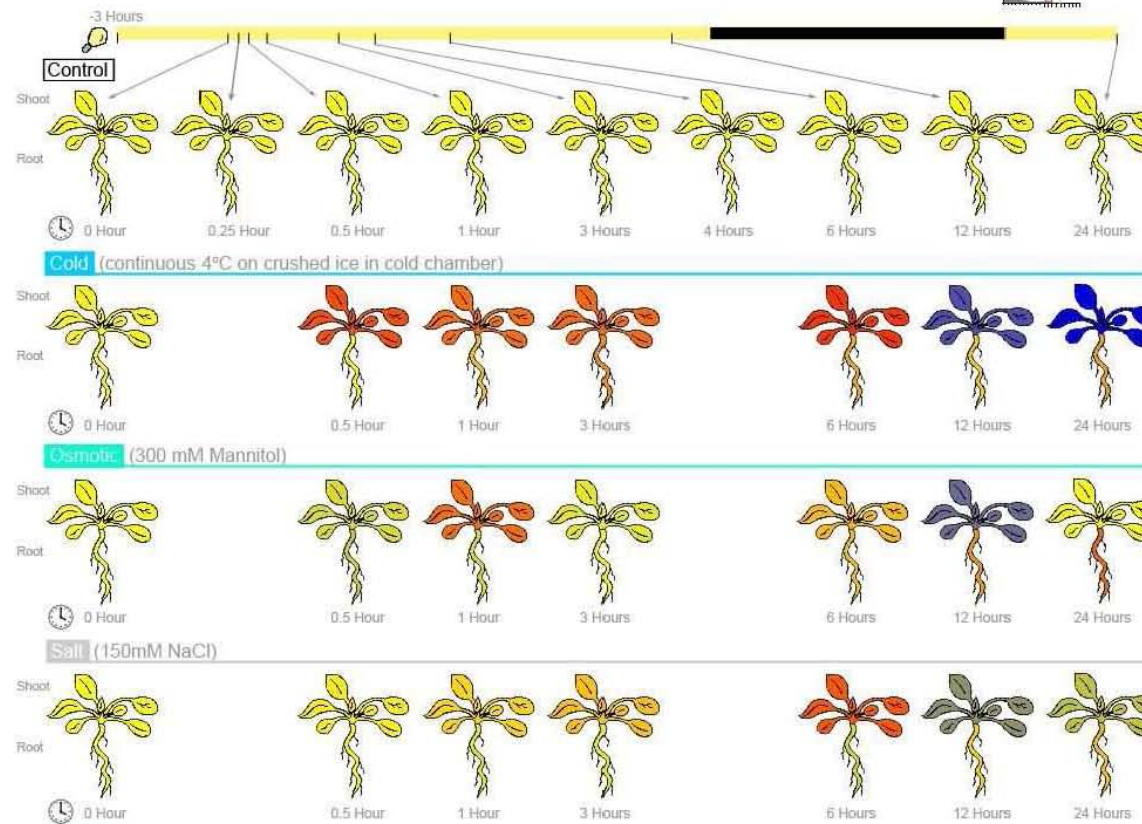
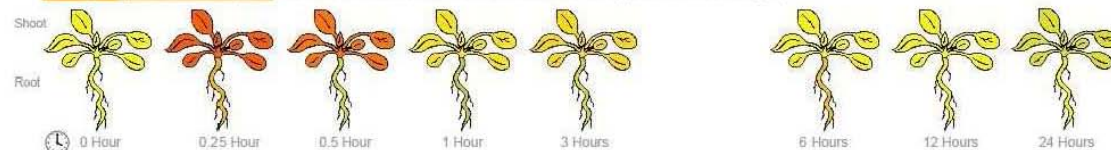


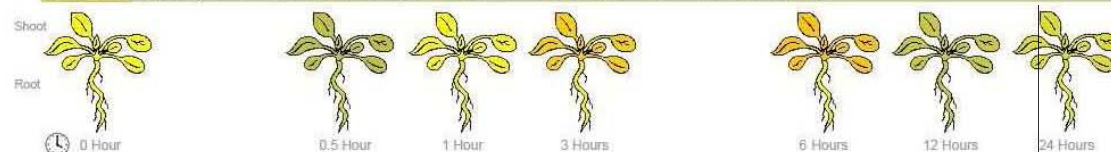
Figure and data from Kilian et al. (2007, Plant Journal 50:347-63)



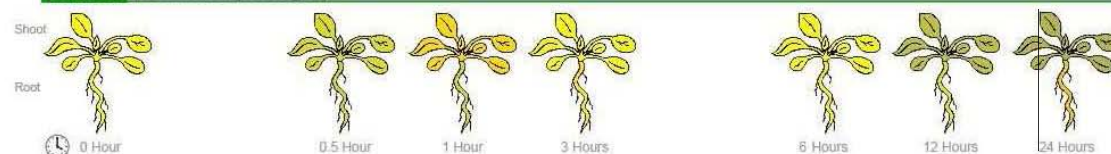
Drought (rafts were exposed to the air stream for 15 min with loss of app.10% fresh weight)



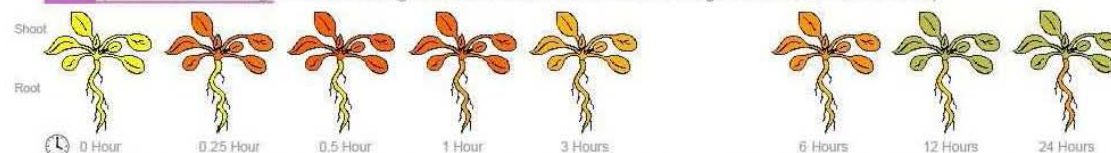
Genotoxic (bleomycin 1.5 ug/ml plus mitomycin C 22 ug/ml final concentration dissolved in water)



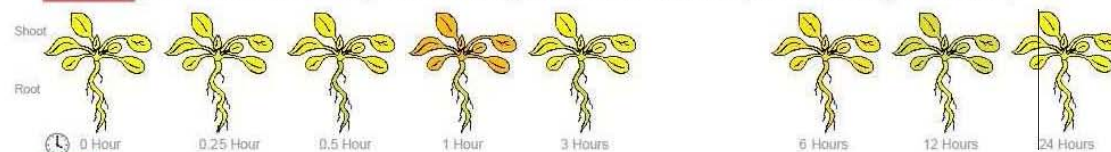
Oxidative (10 uM Methyl viologen)



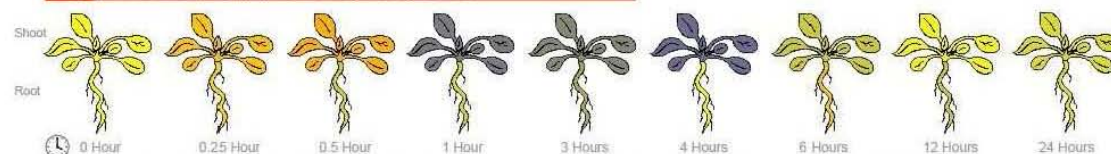
UV-B (15 minutes UV-B light field consisting of six fluorescent tubes filtered through transmission cutoff filters)



Wounding (punctuation of the leaves by 3 consecutive applications of a custom made pin-tool consisting of 16 needles)

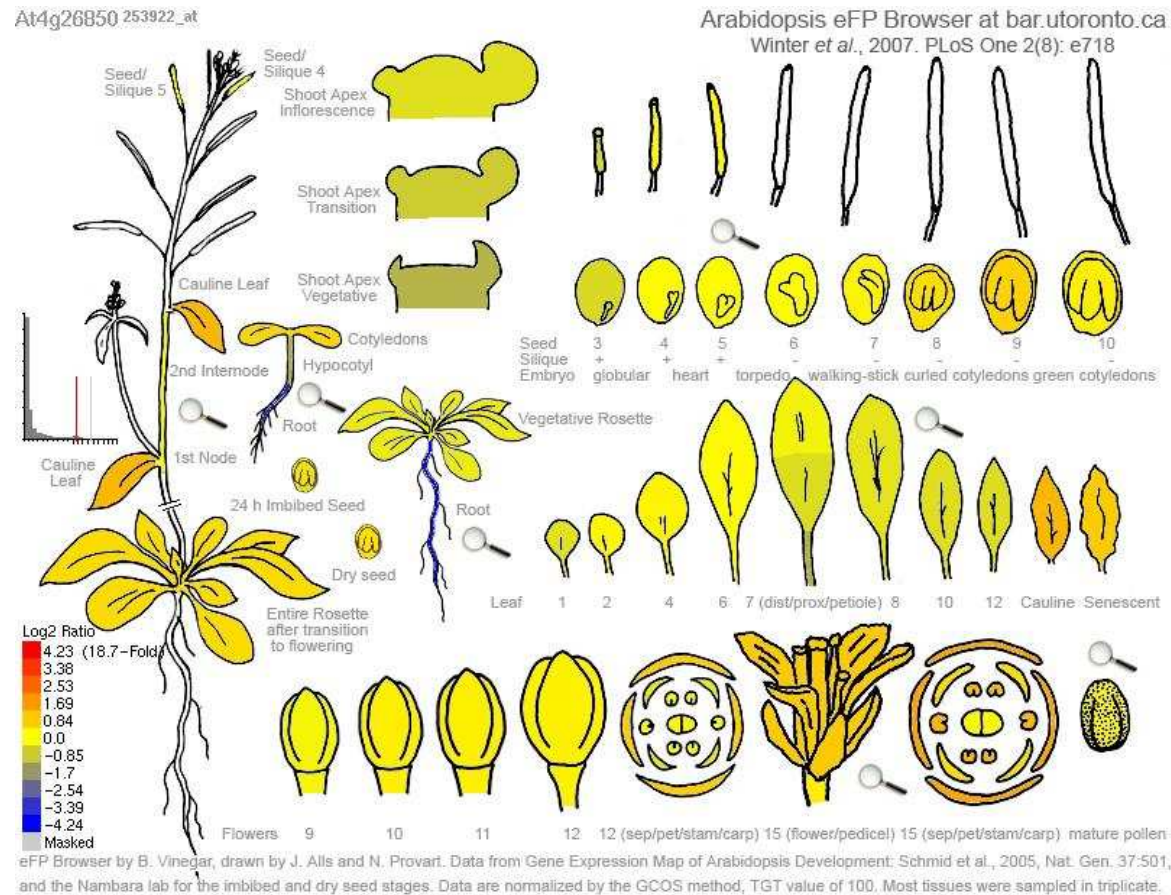


Heat (3 hours at 38°C followed by recovery at 25°C)



eFP Browser Stress Series by B. Vinegar and D. Winter, drawn by D. Winter. Data from AtGenExpress Abiotic Stress Series from Kilian et al. (2007, Plant J. 50:347-63)

Development



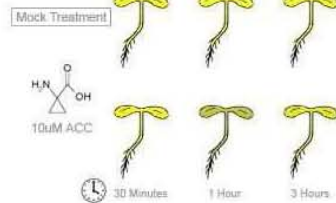
Hormone treatment

University of Cape Town

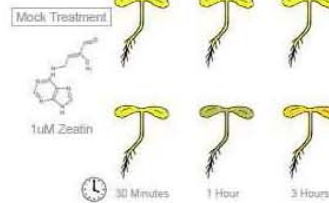
At4g26850 253922_at

□ = Control

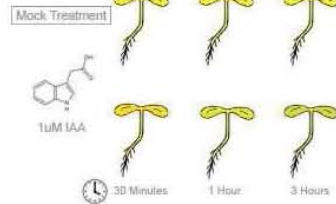
ACC



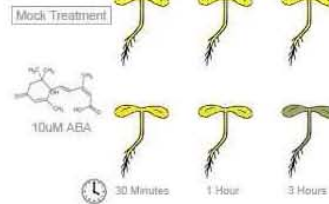
Zeatin



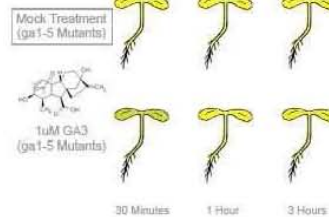
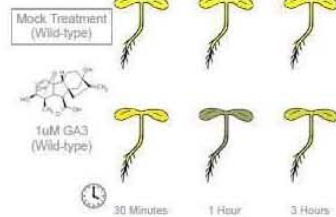
IAA



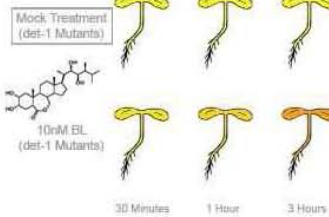
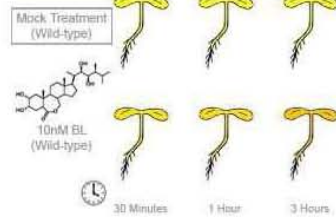
ABA



GA-3

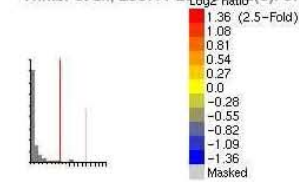


Brassinolide

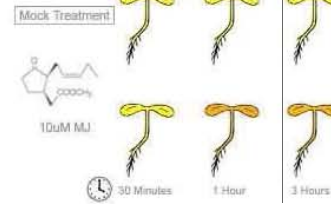


Arabidopsis eFP Browser at bar.utoronto.ca

Winter et al., 2007. *PLoS One* 2(8): e718



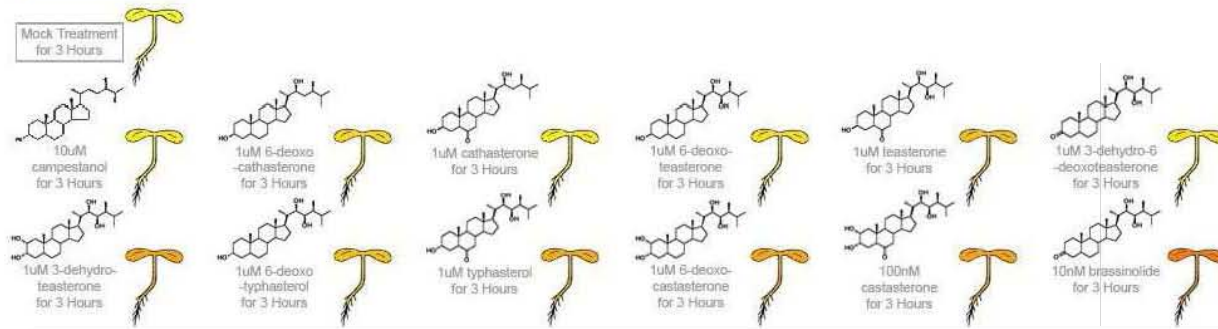
Methyl Jasmonate



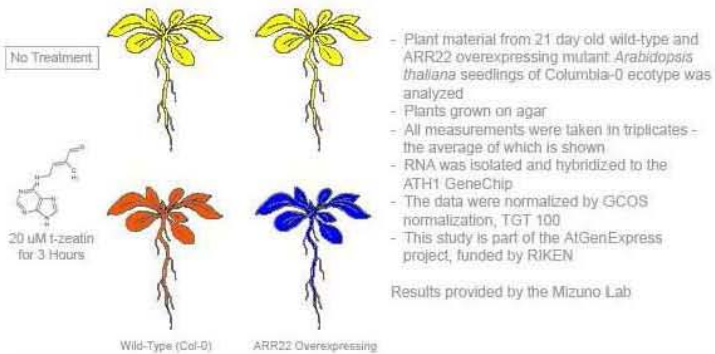
- Plant material from 7 day old wild-type or otherwise specified mutant *Arabidopsis thaliana* seedlings of Columbia-0 ecotype was analyzed
- Plants grown in liquid MS media under continuous light conditions at 23°C
- All measurements were taken in duplicates - the average of which is shown
- RNA was isolated and hybridized to the ATH1 GeneChip
- The data were normalized by GCOS normalization, TGT 100
- This study is part of the AtGenExpress project, funded by RIKEN

Results provided by the Shimada Lab

Brassinosteroids



Cytokinin



- Plant material from wild-type *Arabidopsis thaliana* seeds of Columbia-0 ecotype was analyzed
- Seeds observed under continuous light conditions at 22°C
- All measurements were taken in duplicates - the average of which is shown
- RNA was isolated and hybridized to the ATH1 GeneChip
- The data were normalized by GCOS normalization, TGT 100
- This study is part of the AtGenExpress project, funded by RIKEN

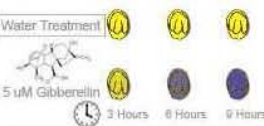
Results provided by the Nambara Lab

ABA during Seed Imbibition



Results provided by the Nambara Lab

Basic Hormones

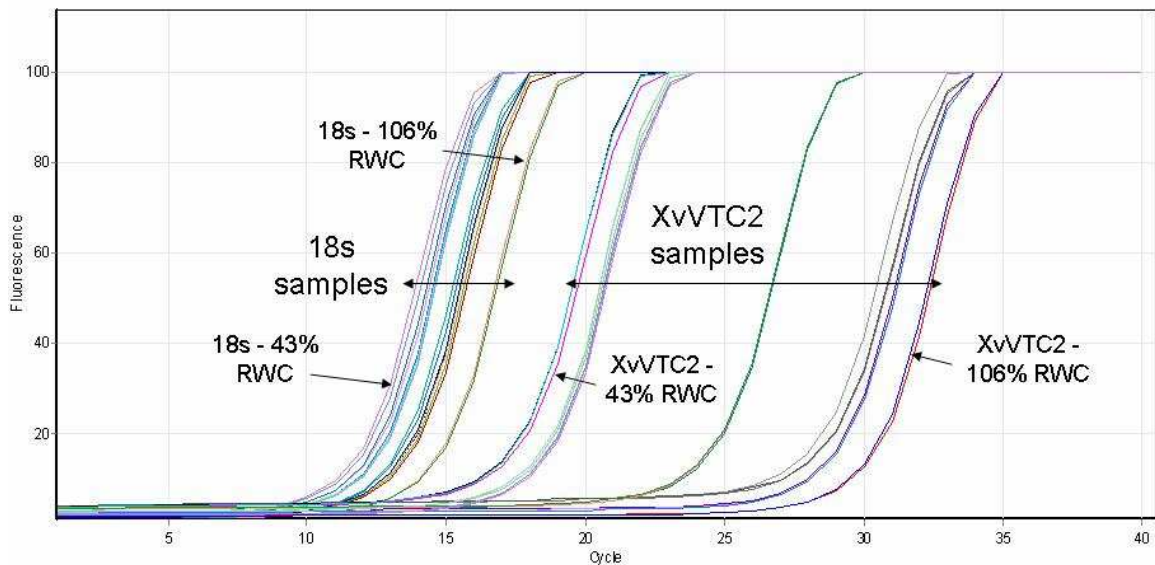


- Plant material from *ga1-3* mutant *Arabidopsis thaliana* seeds of Ler ecotype was analyzed
- Seeds observed under continuous light conditions at 22°C
- All measurements were taken in duplicates - the average of which is shown
- RNA was isolated and hybridized to the ATH1 GeneChip
- The data were normalized by GCOS normalization, TGT 100
- This study is part of the AtGenExpress project, funded by RIKEN

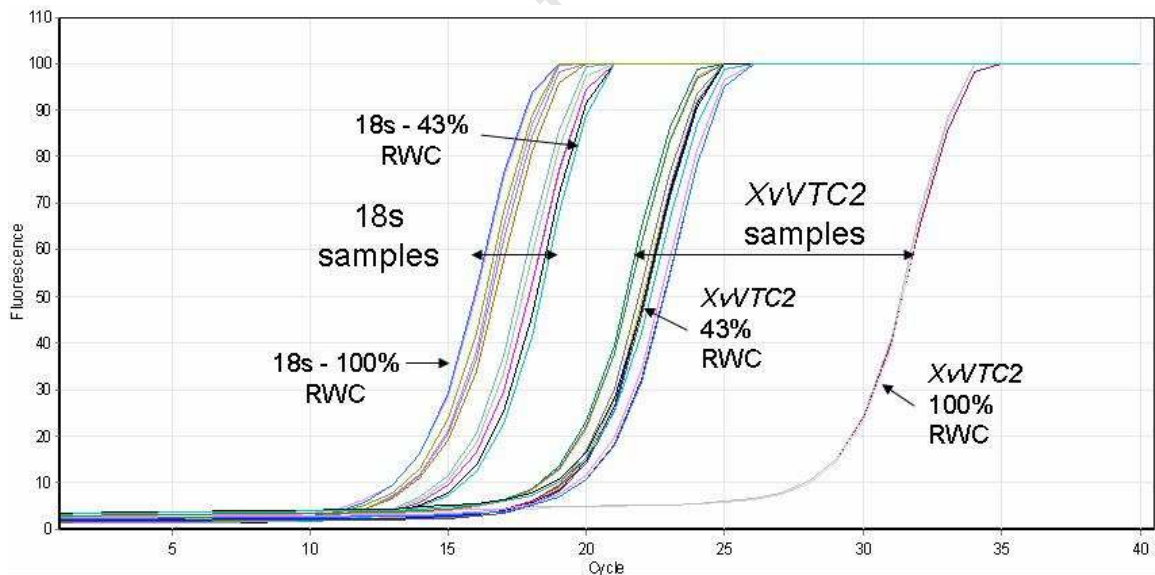
Results provided by the Yamaguchi Lab

eFP Browser Hormone Series by B. Vinegar and D. Winter. Data from AtGenExpress Hormone Series.

Appendix 8 – Real-time PCR runs

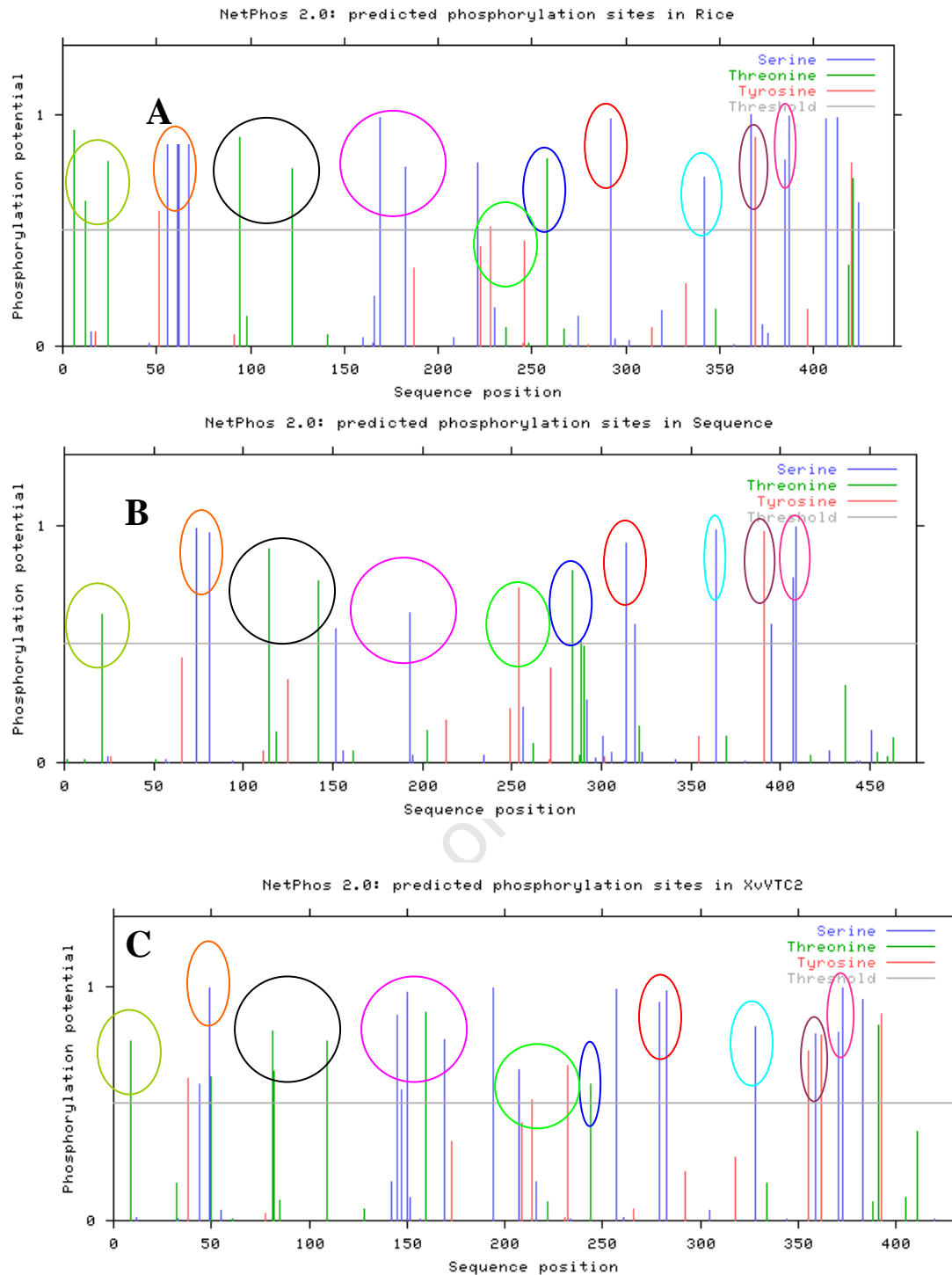


Real-time PCR amplification of 18s and XvVTC2 samples is response to dehydration of *X. viscosa* biological repeat 1.



Real-time PCR amplification of 18s and XvVTC2 samples in response to rehydration of *X. viscosa* biological repeat 1.

Appendix 9 – Phosphorylation site prediction graphs



Prediction of phosphorylation sites of the *Oryza sativa* (Rice) VTC2 (A), *Arabidopsis thaliana* VTC2 (B) and *Xerophyta viscosa* XvVTC2 (C) proteins by the Netphos 2.0 server (Blom et al., 1999). The threshold for predicted phosphorylation potential is at 0.5 and only where values are higher than the threshold, phosphorylation is predicted to happen. The vertical lines indicate serine (blue), threonine (green) and tyrosine (red) residues in their sequence position (x-axis) and the predicted phosphorylation potential of the residue (y-axis). Regions where predicted phosphorylation is conserved are indicated by coloured circles, where circles of the same colour indicate phosphorylation sites in the same region. These graphs show the similarity in trend of phosphorylation sites across the VTC2 homologs

References:

-
- Altschul SF, Madden TL, Schäffer AA, Zhang J, Zhang Z, Miller W, Lipman DJ** (1997) Gapped BLAST and PSI-BLAST: a new generation of protein database search programs. *Nucleic Acids Research* **25**: 3389 – 3402
- Apel K, Hirt H** (2004) REACTIVE OXYGEN SPECIES: Metabolism, Oxidative Stress, and Signal Transduction. *Annual Review of Plant Biology* **55**: 373 - 399
- AraCyc** (2010) Arabidopsis thaliana col Pathway: superpathway of sucrose and starch metabolism II (photosynthetic tissue). *In*, Vol 2010. Plant metabolic network
- Aro E-M, Virgin I, Andersson B** (1993) Photoinhibition of Photosystem II. Inactivation, protein damage and turnover *Biochimica et Biophysica Acta (BBA) - Bioenergetics* **1143**: 113 - 134
- Badejo AA, Fujikawa Y, Esaka M** (2008) Gene expression of ascorbic acid biosynthesis related enzymes of the Smirnoff-Wheeler pathway in acerola (*Malpighia glabra*). *Journal of Plant Physiology* doi:10.1016/j.jplph.2008.09.004
- Baker B** (2008) *XvVTC2* cDNA sequence. *In*. University of Cape Town, Cape Town
- Ballester A, Cervera M, Pena L** (2008) Evaluation of selection strategies alternative to *nptII* in genetic transformation of citrus. *Plant Cell Rep* **27**: 1005 – 1015
- Baneyx F** (1999) Recombinant proetin expression in *Eschericia coli*. *Current Opinion in Biotechnology* **10**: 411 - 421
- Barth C, Moeder W, Klessig DF, Conklin PL** (2004) The Timing of Senescence and Response to Pathogens Is Altered in the Ascorbate-Deficient Arabidopsis Mutant vitamin c-1. *Plant Physiology* **134**: 1784 – 1792
- Bartoli CG, Simontacchi M, Tambussi E, Beltrano J, Montaldi E, Puntarulo S** (1999) Drought and watering-dependant oxidative stress: effect on antioxidant contentin *Triticum aestivum* L. leaves. *Journal of Experimental Botany* **50**: 375 - 383
- Bartoli CG, Yu J, Gomez F, Fernandez L, McIntosh L, Foyer CH** (2006) Inter-relationships between light and respiration in the control of ascorbic acid synthesis and accumulation in *Arabidopsis thaliana* leaves. *Journal of Experimental Botany* **57**: 1621 – 1631
- Berjak P** (2006) Unifying perspectives of some mechanisms basic to desiccation tolerance across life forms. *Seed Science research* **16**: 1 - 15
- Bewley JD** (1995) Physiological aspects of desiccation tolerance - A retrospect. *International Journal Of Plant Science* **156**: 393 - 403
- Bhatt A, Naidoo Y, Gairola S, Nicholas A** (2009) Ultrastructural responses of the desiccation tolerant plants *Xerophyta viscosa* and *X. retinervis* to dehydration and rehydration. *Biologia plantarum* **53**: 373 - 377
- Blom N, Gammeltoft S, Brunak S** (1999) Sequence and Structure-based Prediction of Eukaryotic Protein Phosphorylation Sites. *Journal of Molecular Biology* **294**: 1351 - 1362
- Boutin JA** (1997) Myristoylation. *Cell. Signal.* **9**: 15 - 35
- Bradford MM** (1976) Rapid and Sensitive Method for the Quantitation of Microgram Quantities of Protein Utilizing the Principle of Protein-Dye Binding. *Analytical Biochemistry* **72**: 248 - 254

- Bryant G, Koster KL, Wolfe J** (2001) Membrane behaviour in seeds and other systems at low water content: the various effects of solutes. *Seed Science research* **11**: 17 - 25
- Bulley SM, Rassam M, Hoser D, Otto W, Schunemann N, Wright M, MacRae E, Gleave A, Laing W** (2009) Gene expression studies in kiwifruit and gene over-expression in *Arabidopsis* indicates that GDP-L-galactose guanyltransferase is a major control point of vitamin C biosynthesis. *Journal of Experimental Botany* **60**: 765 – 778
- Chalfie M, Tu Y, Euskirchen G, Ward WW, Prasher DC** (1994) Green Fluorescent Protein as a Marker for Gene Expression. *Science* **263**: 802 - 805
- Chen Z, Gallie DR** (2004) The Ascorbic Acid Redox State Controls Guard Cell Signaling and Stomatal Movement. *The Plant Cell* **16**: 1143 - 1162
- Chen Z, Young TE, Ling J, Chang S-C, Gallie DR** (2003) Increasing vitamin C content of plants through enhanced ascorbate recycling. *PNAS* **100**: 3525 - 3530
- Chopera DR** (2005) Molecular characterization of *XvINO1*, a myo-inositol 1-phosphate synthase gene from *Xerophyta viscosa*. University of Cape Town, Cape Town
- Chrispeels MJ, Sadava DE** (2003) *Plants, Genes and Crop Biotechnology*, Ed 2. Jones and Bartlett Publishers, Canada
- Clifford SC, Arndt SK, Corlett JE, Joshi S, Sankhla N, Popp M, Jones HG** (1998) The role of solute accumulation, osmotic adjustment and changes in cell wall elasticity in drought tolerance in *Ziziphus mauritiana* (Lamk.). *Journal of Experimental Botany* **49**: 967 - 977
- Clouse SD, Sasse JM** (1998) BRASSINOSTEROIDS: Essential Regulators of Plant Growth and Development. *Annu. Rev. Plant Physiol. Plant Mol. Biol.* **49**: 427 - 451
- Colville L, Smirnoff N** (2008) Antioxidant status, peroxidase activity, and PR protein transcript levels in ascorbate-deficient *Arabidopsis thaliana* vtc mutants. *Journal of Experimental Botany* **59**: 3857 – 3868
- Conklin PL, Barth C** (2004) Ascorbic acid, a familiar small molecule intertwined in the response of plants to ozone, pathogens, and the onset of senescence. *Plant, Cell and Environment* **27**: 959 – 970
- Conklin PL, Gatzek S, Wheeler GL, Dowdle J, Raymond MJ, Rolinski S, Isupov M, Littlechild JA, Smirnoff N** (2006) *Arabidopsis thaliana* VTC4 Encodes L-Galactose-1-P Phosphatase, a Plant Ascorbic Acid Biosynthetic Enzyme. *The Journal of Biological Chemistry* **281**: 15662 – 15670
- Conklin PL, Norris SR, Wheeler GL, Williams EH, Smirnoff N, Last RL** (1999) Genetic evidence for the role of GDP-mannose in plant ascorbic acid (vitamin C) biosynthesis. *PNAS* **96**: 4198 – 4203
- Conklin PL, Pallanca JE, Last RL, Smirnoff N** (1997) L-Ascorbic Acid Metabolism in the Ascorbate-Deficient *Arabidopsis* Mutant *vtc1*. *Plant Physiology* **115**: 1277 - 1285
- Conklin PL, Williams EH, Last RL** (1996) Environmental stress sensitivity of an ascorbic acid-deficient *Arabidopsis* mutant. *PNAS* **93**: 9970 - 9974
- Cooper K, Farrant JM** (2002) Recovery of the resurrection plant *Craterostigma wilmsii* from dessication: protection versus repair. *Journal of Experimental Botany* **53**: 1805 - 1813
- Córdoba-Pedregosa MdC, González-Reyes JA, Cañadillas MdS, Navas P, Córdoba F** (1996) Role of Apoplastic and Cell-Wall Peroxidases on the Stimulation of Root Elongation by Ascorbate. *Plant Physiology* **112**: 1119 - 1125

- Cordoba-Pedregosa MdC, Villalba JM, Cordoba F, Gonzalez-Reyes JA** (2007) Changes in Growth Pattern, Enzymatic Activities Related to Ascorbate Metabolism, and Hydrogen Peroxide in Onion Roots Growing Under Experimentally Increased Ascorbate Content. *Journal of Plant Growth Regulation* **26**: 341 – 350
- Crowe JH, Carpenter JF, Crowe LM** (1998) The role of vitrification in anhydrobiosis. *Annu. Rev. Physiol.* **60**: 73 – 103
- Dace H, Sherwin HW, Illing N, Farrant JM** (1998) Use of metabolic inhibitors to elucidate mechanisms of recovery from desiccation stress in the resurrection plant *Xerophyta humilis*. *Plant Growth Regulation* **24**: 171 – 177
- Dat J, Vandenabeele S, Vranova' E, Van Montagu M, Inze' D, Van Breusegem F** (2000) Dual action of the active oxygen species during plant stress responses. *Cellular and Molecular Life Sciences* **57**: 779 – 795
- Dauids F** (2009) Eliza method. *In* Research assistant Molecular and Cell Biology Department, University of Cape Town
- Day RN, Schaufe F** (2008) Fluorescent protein tools for studying protein dynamics in living cells: a review. *Journal of Biomedical optics* **13**: 031202-031201 - 031202-031206
- de Castro E, Sigrist CJA, Gattiker A, Bulliard V, Langendijk-Genevaux PS, Gasteiger E, Bairoch A, Hulo N** (2006) ScanProsite: detection of PROSITE signature matches and ProRule-associated functional and structural residues in proteins. *Nucleic Acids Research* **34**: W362 – W365
- Delledonne M, Zeier J, Marocco A, Lamb C** (2004) Signal interactions between nitric oxide and reactive oxygen intermediates in the plant hypersensitive disease resistance response. *PNAS* **98**: 13454 – 13459
- Devon RS, Porteous DJ, Brookes AJ** (1995) Splinkerettes - improved vectorettes for greater efficiency in PCR walknig. *Nucleic Acids Research* **23**: 1644 - 1645
- Dowdle J, Ishikawa T, Gatzek S, Rolinski S, Smirnoff N** (2007) Two genes in *Arabidopsis thaliana* encoding GDP-L-galactose phosphorylase are required for ascorbate biosynthesis and seedling viability. *The Plant Journal* **52**: 673 – 689
- Dyson MR, Shadbolt SP, Vincent KJ, Perera RL, McCafferty J** (2004) Production of soluble mammalian proteins in *Escherichia coli*: identification of protein features that correlate with successful expression. *BMC Biotechnology* **4**: doi:10.1186/1472-6750-1184-1132
- EMD Biosciences** (2005) pET system manual, Ed 11
- Endres S, Tenhaken R** (2009) Myoinositol Oxygenase Controls the Level of Myoinositol in *Arabidopsis*, But Does Not Increase Ascorbic Acid. *Plant Physiology* **149**: 1042 – 1049
- FAO** (2008 a) The State of food insecurity in the world 2008. Food and Agriculture Organization of the United Nations, Rome
- FAO** (2008 b) The state of food and agriculture - Biofuels: prospects, risks and opportunities. *In*. Food and Agriculture Organization of the United Nations, Rome
- Farrant JM** (2000) A comparison of mechanisms of desiccation tolerance among three angiosperm resurrection plant species. *Plant Ecology* **151**: 29 – 39
- Farrant JM** (2009) Calculating Relative Water Content in *Xeropyta viscosa*. *In*, Cape Town
- Farrant JM, Brandt W, Lindsey GG** (2007) An Overview of Mechanisms of Desiccation Tolerance in Selected Angiosperm Resurrection Plants. *Plant Stress* **1**: 72 - 84

- Farrant JM, Cooper K, Kruger LA, Sherwin HW** (1999) The Effect of Drying Rate on the Survival of Three Desiccation-tolerant Angiosperm Species. *Annals of Botany* **84**: 371 - 379
- Farrant JM, Lehner A, Cooper K, Wiswedel S** (2009) Desiccation tolerance in the vegetative tissues of the fern *Mohria caffrorum* is seasonally regulated. *The Plant Journal* **57**: 65 – 79
- Ferrario-Méry S, Valadier M-H, Foyer CH** (1998) Overexpression of Nitrate Reductase in Tobacco Delays Drought-Induced Decreases in Nitrate Reductase Activity and mRNA. *Plant Physiology* **117**: 293 - 302
- Foyer CH, Noctor G** (2005 a) Oxidant and antioxidant signalling in plants: a re-evaluation of the concept of oxidative stress in a physiological context. *Plant, Cell and Environment* **28**: 1056 – 1071
- Foyer CH, Noctor G** (2005 b) Redox Homeostasis and Antioxidant Signaling: A Metabolic Interface between Stress Perception and Physiological Responses. *The Plant Cell* **17**: 1866 - 1875
- Fry SC** (1998) Oxidative scission of plant cell wall polysaccharides by ascorbate-induced hydroxyl radicals. *Biochemistry Journal* **332**: 507 - 515
- Gaff DF** (1971) Desiccation-Tolerant Flowering Plants in Southern Africa. *Science* **174**: 1033 - 1034
- Gaff DF** (1977) Desiccation Tolerant Vascular Plants of Southern Africa. *Oecologia* **31**: 95 - 109
- Gatzek S, Wheeler GL, Smirnoff N** (2002) Antisense suppression of L-galactose dehydrogenase in *Arabidopsis thaliana* provides evidence for its role in ascorbate synthesis and reveals light modulated L-galactose synthesis. *The Plant Journal* **30**: 541 - 553
- Georgieva K, Roding A, Buchel C** (2009) Changes in some thylakoid membrane proteins and pigments upon desiccation of the resurrection plant *Haberlea rhodopensis*. *Journal of Plant Physiology* **166**: 1520 - 1528
- Giardi MT, Cona A, Geiken B, Kučera T, Masojídek J, Mattoo AK** (1995) Long-term drought stress induces structural and functional reorganization of photosystem II. *Planta* **199**: 118 - 125
- Gorlich D** (1998) Transport into and out of the cell nucleus. *The EMBO Journal* **17**: 2721 – 2727
- Hawkins T, Luban S, Kihara D** (2006) Enhanced automated function prediction using distantly related sequences and contextual association by PFP. *Protein Science* **15**: 1550 – 1556
- Hoeberichts FA, Vaeck E, Kiddle G, Coppens E, Cotte Bvd, Adamantidis A, Ormenese S, Foyer CH, Zabeau M, Inze´ D, Perilleux C, Breusegem FV, Vuylsteke M** (2008) A Temperature-sensitive Mutation in the *Arabidopsis thaliana* Phosphomannomutase Gene Disrupts Protein Glycosylation and Triggers Cell Death. *The Journal of Biological Chemistry* **283**: 5708 - 5718
- Hoekstra FA, Golovina EA, Buitink J** (2001) Mechanisms of plant desiccation tolerance. *Trends in Plant Science* **6**: 431 - 438
- Horemans N, Foyer CH, Potters G, Asard H** (2000) Ascorbate function and associated transport systems in plants. *Plant Physiol. Biochem.* **38**: 531 – 540
- Hulo N, Bairoch A, Bulliard V, Cerutti L, Cuche BA, de Castro E, Lachaize C, Langendijk-Genevaux PS, Sigrist CJA** (2007) The 20 years of PROSITE. *Nucleic Acids Research* doi:10.1093/nar/gkm977

- Imai T, Ban Y, Terakami S, Yamamoto T, Moriguchi T** (2009 b) L-Ascorbate biosynthesis in peach: cloning of six L-galactose pathway-related genes and their expression during peach fruit development. *Physiologia Plantarum* **136**: 139 – 149
- Imai T, Niwa M, Ban Y, Hirai M, Oba K, Moriguchi T** (2009 a) Importance of the L-galactonolactone pool for enhancing the ascorbate content revealed by L-galactonolactone dehydrogenase-overexpressing tobacco plants. *Plant Cell Tissue Org Cult* **96**: 105 – 112
- Ioannidi E, Kalamaki MS, Engineer C, Pateraki I, Alexandrou D, Mellidou I, Giovannonni J, Kanellis AK** (2009) Expression profiling of ascorbic acid-related genes during tomato fruit development and ripening and in response to stress conditions. *Journal of Experimental Botany* doi:10.1093/jxb/ern322
- Isherwood FA, Mapson LW** (1962) Ascorbic Acid Metabolism in Plants: Part II. Biosynthesis. *Annual Review Of Plant Physiology* **13**: 329 - 350
- Iyer K** (2009) gDNA Donor. *In* Research assistant Plant stress Laboratory University of Cape Town,
- Jahns P, Latowski D, Strzalka K** (2009) Mechanism and regulation of the violaxanthin cycle: The role of antenna proteins and membrane lipids. *Biochimica et Biophysica Acta* **1787**: 3 – 14
- Jubany-Marí T, Munné-Bosch S, Alegre L** (2010 a) Redox regulation of water stress responses in field-grown plants. Role of hydrogen peroxide and ascorbate. *Plant Physiol. Biochem.* **48**: 351 - 358
- Kiyaei A** (2008) cDNA Donor. *In*. Honours Student, Plant stress Laboratory University of Cape Town
- Kranner I, Beckett RP, Wornik S, Zorn M, Pfeifhofer HW** (2002) Revival of a resurrection plant correlates with its antioxidant status. *The Plant Journal* **31**: 13 - 24
- Krebs S, Fischaleck M, Blum H** (2009) A simple and loss-free method to remove TRIzol contaminations from minute RNA samples. *Analytical Biochemistry* **387**: 136 – 138
- Laing WA, Wright MA, Cooney J, Bulley SM** (2007) The missing step of the L-galactose pathway of ascorbate biosynthesis in plants, an L-galactose guanyltransferase, increases leaf ascorbate content. *PNAS* **104**: 9534 - 9539
- Lescot M, Dehais P, Thijs G, Marchal K, Moreau Y, Peer YVd, Rouze' P, Rombauts S** (2002) PlantCARE, a database of plant *cis*-acting regulatory elements and a portal to tools for *in-silico* analysis of promoter sequences. *Nucleic Acids Research* **30**: 325 - 327
- Li M-J, Ma F-W, Zhang M, Pu F** (2008) Distribution and metabolism of ascorbic acid in apple fruits (*Malus domestica* Borkh cv. Gala). *Plant Science* **174**: 606 - 612
- Li M, Ma F, Shang P, Zhang M, Hou C, Liang D** (2009) Influence of light on ascorbate formation and metabolism in apple fruits. *Planta* **230**: 39 – 51
- Linster CL, Adler LN, Webb K, Christensen KC, Brenner C, Clarke SG** (2008) A Second GDP-L-galactose Phosphorylase in *Arabidopsis* en Route to Vitamin C. *The Journal of Biological chemistry* **283**: 18483 - 18492
- Linster CL, Clarke SG** (2008) L-Ascorbate biosynthesis in higher plants: the role of VTC2. *Trends in Plant Science* **13**: 567 - 573
- Linster CL, Gomez TA, Christensen KC, Adler LN, Young BD, Brenner C, Clarke SG** (2007) *Arabidopsis* VTC2 Encodes a GDP-L-Galactose Phosphorylase, the Last Unknown Enzyme in the Smirnoff-Wheeler Pathway to Ascorbic Acid in Plants. *The Journal of Biological Chemistry* **282**: 18879 - 18885

- Lorence A, Chevone BI, Mendes P, Nessler CL** (2004) Myo-inositol oxygenase offers a possible entry point into plant ascorbate biosynthesis. *Plant Physiology* **134**: 1200 - 1205
- Majewska-Sawka A, Fernández MC, M'rani-Alaoui M, Münster A, Rodríguez-García MI** (2002) Cell wall reformation by pollen tube protoplasts of olive (*Olea europaea* L.): structural comparison with the pollen tube wall. *Sex Plant Reprod* **15**: 21 - 29
- Major LL, Wolucka BA, Naismith JH** (2005) Structure and Function of GDP-Mannose-3',5'-Epimerase: An Enzyme which Performs Three Chemical Reactions at the Same Active Site. *J. Am. Chem. Soc.* **127**: 18309 - 18320
- Maruta T, Yonemitsu M, Yabuta Y, Tamoi M, Ishikawa T, Shigeoka S** (2008) Arabidopsis Phosphomannose Isomerase 1, but Not Phosphomannose Isomerase 2, Is Essential for Ascorbic Acid Biosynthesis. *The Journal of Biological Chemistry* **283**: 28842 – 28851
- McCoy JG, Arabshahi A, Bitto E, Bingman CA, Ruzicka FJ, Frey PA, Jr** GNP (2006) Structure and Mechanism of an ADP-Glucose Phosphorylase from *Arabidopsis thaliana*. *Biochemistry* **45**: 3154 – 3162
- Millar AH, Mittova V, Kiddle G, Heazlewood JL, Bartoli CG, Theodoulou FL, Foyer CH** (2003) Control of Ascorbate Synthesis by Respiration and Its Implications for Stress Responses. *Plant Physiology* **133**: 443 – 447
- Miller G, Shulaev V, Mittler R** (2008) Reactive oxygen signaling and abiotic stress. *Physiologia Plantarum* doi: 10.1111/j.1399-3054.2008.01090.x
- Miller G, Suzuki N, Rizhsky L, Hegie A, Koussevitzky S, Mittler R** (2007) Double mutants deficient in cytosolic and thylakoid ascorbate peroxidase reveal a complex mode of interaction between reactive oxygen species, plant development, and response to abiotic stresses. *Plant Physiology* **144**: 1777 – 1785
- Mittler R, Vanderauwera S, Gollery M, Breusegem FV** (2004) Reactive oxygen gene network of plants. *Trends in Plant Science* **9**: 490 - 498
- Mohanty A, Luo A, DeBlasio S, Ling X, Yang Y, Tuthill DE, Williams KE, Hill D, Zadrozny T, Chan A, Sylvester AW, Jackson D** (2009) Advancing Cell Biology and Functional Genomics in Maize Using Fluorescent Protein-Tagged Lines. *Plant Physiology* **149**: 601 – 605
- Moore JP, Farrant JM, Driouich A** (2008 a) A role for pectin-associated arabinans in maintaining the flexibility of the plant cell wall during water deficit stress. *Plant Signalling & Behaviour* **3**: 102 - 104
- Moore JP, Lindsey G, Farrant JM, Brandt WF** (2007) An Overview of the Biology of the Desiccation-tolerant Resurrection Plant *Myrothamnus flabellifolia*. *Annals of Botany* **99**: 211 – 217
- Moore JP, Nguema-Ona E, Chevalier L, Lindsey GG, Brandt WF, Lerouge P, Farrant JM, Driouich A** (2006) Response of the Leaf Cell Wall to Desiccation in the Resurrection Plant *Myrothamnus flabellifolius*. *Plant Physiology* **141**: 651 – 662
- Moore JP, Tuan Le N, Brandt WF, Driouich A, Farrant JM** (2009) Towards a systems-based understanding of plant desiccation tolerance. *Trends in Plant Science* doi:10.1016/j.tplants.2008.11.007
- Moore JP, Vitré-Gibouin M, Farrant JM, Driouich A** (2008 b) Adaptations of higher plant cell walls to water loss: drought vs desiccation. *Physiologia Plantarum* **134**: 237 – 245

- Mowla SB, Thomson JA, Farrant JM, Mundree SG** (2002) A novel stress-inducible antioxidant enzyme identified from the resurrection plant *Xerophyta viscosa* Baker. *Planta* **215**: 716 – 726
- Mueller LA, Zhang P, Rhee SY** (2003) AraCyc: A Biochemical Pathway Database for Arabidopsis. *Plant Physiology* **132**: 453 – 460
- Muller-Moule P** (2008) An expression analysis of the ascorbate biosynthesis enzyme VTC2. *Plant Molecular Biology* DOI **10.1007/s11103-008-9350-4**
- Muller-Moule P, Havaux M, Niyogi KK** (2003) Zeaxanthin Deficiency Enhances the High Light Sensitivity of an Ascorbate-Deficient Mutant of Arabidopsis. *Plant Physiology* **133**: 748 - 760
- Mundree SG, Baker B, Mowla S, Peters S, Marais S, Willigen CV, Govender K, Maredza A, Muyanga S, Farrant JM, Thomson JA** (2002) Physiological and molecular insights into drought tolerance. *African Journal of Biotechnology* **1**: 28 - 38
- Nigg EA** (1997) Nucleocytoplasmic transport: signals, mechanisms and regulation. *Nature* **368**: 779 – 787
- Nunez M, Mazzafera P, Mazorra LM, Siquera WJ, Zullo MAT** (2004) Influence of brassinosteroid analogue on antioxidant enzymes in rice grown in culture medium with NaCl. *Biologia plantarum* **47**
- Pastori GM, Kiddle G, Antoniw J, Bernard S, Veljovic-Jovanovic S, Verrier PJ, Noctor G, Foyer CH** (2003) Leaf Vitamin C Contents Modulate Plant Defense Transcripts and Regulate Genes That Control Development through Hormone Signaling. *The Plant Cell* **15**: 939 - 951
- Peters S, Mundree SG, Thomson JA, Farrant JM, Keller F** (2007) Protection mechanisms in the resurrection plant *Xerophyta viscosa* (Baker): both sucrose and raffinose family oligosaccharides (RFOs) accumulate in leaves in response to water deficit. *Journal of Experimental Botany* **58**: 1947 – 1956
- Pfaffl MW** (2001) A new mathematical model for relative quantification in Real-Time RT-PCR. *Nucleic Acids Research* **29**: 2002 - 2007
- Pignocchi C, Fletcher JM, Wilkinson JE, Barnes JD, Foyer CH** (2003) The function of ascorbate oxidase in tobacco. *Plant Physiology* **132**: 1631 – 1641
- Qiagen** (2002) QIAexpress® Detection and Assay Handbook,
- Qiagen** (2005) QIAexpress® Ni-NTA Fast Start Handbook,
- Qian W, Yu C, Qin H, Liu X, Zhang A, Johansen IE, Wang D** (2007) Molecular and functional analysis of phosphomannomutase (PMM) from higher plants and genetic evidence for the involvement of PMM in ascorbic acid biosynthesis in Arabidopsis and Nicotiana benthamiana. *The Plant Journal* **49**: 399 - 413
- Ramagli LS, Rodriguez LV** (1985) Quantitation of microgram amounts of protein in two-dimensional polyacrylamide gel electrophoresis sample buffer. *Electrophoresis* **6**: 559 - 563
- Rybicki E** (1979) The serology of the Bromoviruses. University of Cape town, Cape Town
- Sanford J, Smith F, Russell J** (1993) Optimizing the biolistic process for different biological applications. *Methods enzymol* **217**: 483-509
- Sasaki-Sekimoto Y, Taki N, Obayashi T, Aono M, Matsumoto F, Nozomu Sakurai, Suzuki H, Hirai MY, Noji M, Saito K, Masuda T, Takamiya K-i, Shibata D, Ohta H** (2005) Coordinated activation of metabolic pathways for antioxidants and defence compounds by jasmonates and their roles in stress tolerance in Arabidopsis. *The Plant Journal* **44**: 653 - 668

- Scott A, Wyatt S, Tsou P, Robertson D, Allen N** (1999) Model system for plant cell biology: GFP imaging in living onion epidermal cells. *Biotechniques* **26**: 1125, 1128 -1132
- Serraj R, Sinclair TR** (2002) Osmolyte accumulation: can it really help increase crop yield under drought conditions? *Plant, Cell and Environment* **25**: 333 – 341
- Sherwin HW, Farrant JM** (1996) Differences in Rehydration of Three Desiccation-tolerant Angiosperm Species. *Annals of Botany* **78**: 703 - 710
- Sherwin HW, Farrant JM** (1998) Protection mechanisms against excess light in the resurrection plants *Craterostigma wilmsii* and *Xerophyta viscosa*. *Plant Growth Regulation* **24**: 203 – 210
- Sigrist CJA, Cerutti L, Hulo N, Gattiker A, Falquet L, Pagni M, Bairoch A, Bucher P** (2002) PROSITE: A documented database using patterns and profiles as motif descriptors. *Briefings in Bioinformatics* **3**: 265 – 274
- Smirnoff N** (1996) The Function and Metabolism of Ascorbic Acid in Plants. *Annals of Botany* **78**: 661 - 669
- Smirnoff N** (1998) Plant resistance to environmental stress. *Current Opinion in Biotechnology* **9**: 214 - 219
- Smirnoff N, Conklin PL, Loewus FL** (2001) Biosynthesis of Ascorbic Acid in Plants: A Renaissance. *Annu. Rev. Plant Physiol. Plant Mol. Biol.* **52**: 437 - 467
- Snustad DP, Simmons MJ** (2003) Principles of genetics, Ed 3. John Wiley & Sons
- Stover N** (2001) Splinkerette protocol. *In* nastover@uci.edu. UC Irvine
- Thakur JK, Malik MR, Bhatt V, Reddy MK, Sopory SK, Tyagi AK, Khurana JP** (2003) A POLYCOMB group gene of rice (*Oryza sativa* L. subspecies indica), OsIEZ1, codes for a nuclear-localized protein expressed preferentially in young seedlings and during reproductive development. *Gene* **314**: 1 - 13
- Thornton PK, Jones PG, Alagarwamy G, Andresen J, Herrero M** (2009) Adapting to climate change: Agricultural system and household impacts in East Africa. *Agricultural systems* doi:10.1016/j.agry.2009.09.003
- Torabinejad J, Donahue JL, Gunesequera BN, Allen-Daniels MJ, Gillaspay GE** (2009) VTC4 Is a Bifunctional Enzyme That Affects Myoinositol and Ascorbate Biosynthesis in Plants. *Plant Physiology* **150**: 951 – 961
- Toth SZ, Puthur JT, Nagy V, Garab G** (2009) Experimental Evidence for Ascorbate-Dependent Electron Transport in Leaves with Inactive Oxygen-Evolving Complexes. *Plant Physiology* **149**: 1568 – 1578
- Toth SZ, Puthur JT, Nagy V, Garab G** (2009) Experimental Evidence for Ascorbate-Dependent Electron Transport in Leaves with Inactive Oxygen-Evolving Complexes. *Plant Physiology* **149**: 1568–1578
- Toufighi K, Brady SM, Austin R, Ly E, Provart NJ** (2005) The Botany Array Resource: e-Northerns, Expression Angling, and promoter analyses. *The Plant Journal* **43**: 153 – 163
- Vicre M, Farrant JM, Driouich A** (2004 a) Insights into the cellular mechanisms of desiccation tolerance among angiosperm resurrection plant species. *Plant, Cell and Environment* **27**: 1329 – 1340
- Vicre M, Lerouxel O, Farrant J, Lerouge P, Driouich A** (2004 b) Composition and desiccation-induced alterations of the cell wall in the resurrection plant *Craterostigma wilmsii*. *Physiologia Plantarum* **120**: 229 – 239
- Wasternack C, Parthier B** (1997) Jasmonate-signalled plant gene expression. *Trends in Plant Science* **2**: 302 - 307
- Wheeler GL, Jones MA, Smirnoff N** (1998) The biosynthetic pathway of vitaminC in higher plants. *Nature* **393**: 365 - 369

- Wolucka BA, Montagu MV** (2007) The VTC2 cycle and the de novo biosynthesis pathways for vitamin C in plants: An opinion. *Phytochemistry* **68**: 2602 - 2613
- Wolucka BA, van Montagu M** (2003) GDP-Mannose 3,5-Epimerase forms GDP-L-gulose, a Putative Intermediate for the de Novo Biosynthesis of Vitamin C in Plants. *The Journal of Biological Chemistry* **278**: 47483 – 47490
- Yabuta Y, Mieda T, Rapolu M, Nakamura A, Motoki T, Maruta T, Yoshimura K, Ishikawa T, Shigeoka S** (2007) Light regulation of ascorbate biosynthesis is dependent on the photosynthetic electron transport chain but independent of sugars in Arabidopsis. *Journal of Experimental Botany* **58**: 2661 - 2671

University of Cape Town